

# **SOFT COMPUTING TECHNIQUES IN THE PREDICTION OF PERFORMANCE OF SEMICIRCULAR BREAKWATERS**

**Thesis**

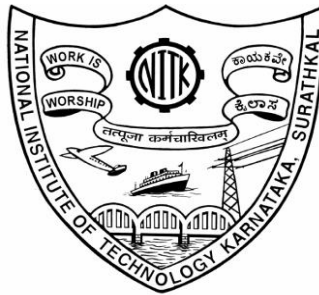
**Submitted in partial fulfilment of the requirements for the degree of**

**DOCTOR OF PHILOSOPHY**

by

**SUMAN KUNDAPURA**

(Reg. No: 155028 AM15F09)



**DEPARTMENT OF APPLIED MECHANICS AND HYDRAULICS  
NATIONAL INSTITUTE OF TECHNOLOGY KARNATAKA  
SURATHKAL, P.O. SRINIVASNAGAR-575 025  
MANGALURU, INDIA**

**DECEMBER 2019**

# **SOFT COMPUTING TECHNIQUES IN THE PREDICTION OF PERFORMANCE OF SEMICIRCULAR BREAKWATERS**

**Thesis**

**Submitted in partial fulfilment of the requirements for the degree of**

**DOCTOR OF PHILOSOPHY**

by

**SUMAN KUNDAPURA**  
(Reg. No: 155028 AM15F09)

Under the guidance of

**Prof. Subba Rao and Prof. Arkal Vittal Hegde**



**DEPARTMENT OF APPLIED MECHANICS AND HYDRAULICS  
NATIONAL INSTITUTE OF TECHNOLOGY KARNATAKA  
SURATHKAL, P.O. SRINIVASNAGAR-575 025  
MANGALURU, INDIA**

**DECEMBER 2019**

## **D E C L A R A T I O N**

*By the Ph.D. Research Scholar*

I hereby *declare* that the Research Thesis entitled “**Soft computing techniques in the prediction of performance of semicircular breakwaters,**” which is being submitted to the **National Institute of Technology Karnataka, Surathkal** in partial fulfilment of the requirements for the award of the Degree of **Doctor of Philosophy in Applied Mechanics and Hydraulics Department** is a *bonafide report of the research work* carried out by me. The material contained in this Research Thesis has not been submitted to any University or Institution for the award of any degree.

155025AM15F09, SUMAN KUNDAPURA

(Register Number, Name & Signature of the Research Scholar)

Department of Applied Mechanics and Hydraulics

Place: NITK-Surathkal

Date:

## CERTIFICATE

This is to *certify* that the Research Thesis entitled “**Soft computing techniques in the prediction of performance of semicircular breakwaters**” submitted by **Suman Kundapura**, Register Number: 155028 AM15F09, as the record of the research work carried out by her is *accepted as the Research Thesis submission* in partial fulfilment of the requirements for the award of degree of **Doctor of Philosophy**.

Prof. Subba Rao  
(Research Guide)

Prof. Arkal Vittal Hegde  
(Research Guide)

Prof. Amba Shetty  
(Chairman – DRPC)

DEPARTMENT OF APPLIED MECHANICS AND HYDRAULICS  
NATIONAL INSTITUTE OF TECHNOLOGY KARNATAKA, INDIA

## ACKNOWLEDGEMENT

To my guide, Prof. Arkal Vittal Hegde, who taught me to believe in myself, how to set goals, to work hard until it is achieved and to celebrate success. Sir, you are one of the most optimistic, knowledgeable yet simple personality I have ever met. I am blessed that you guided me. Thank you Sir! During my tough times when I was, and Prof. Hegde took voluntary retirement due to his health reasons, he handed over my research guidance to Prof. Subba Rao, who is a very knowledgeable, calm and composed person. I am blessed that he guided me towards submission. Thank you Sir!

I would like to express my gratitude to the Director, NITK, Surathkal, for permitting me to use the institutional resources. I am thankful to my RPAC, Dr. Annappa B., and Prof. Subba Rao who shaped my research towards publications and completion, with their useful inputs to my study and critical evaluation of my progress.

I thank all the faculty members of AMD who supported me and gave me a chance to persue a PhD in the Department. Thank you so much! Especially to Dwarakish Sir, our HOD when I started my PhD; who had insisted to publish a review paper of our research prior to the research proposal. I am thankful to him as this gave me a start to my publications.

I heartily thank my husband Hari and my in laws who supported me, by accepting my absence at home whenever I became busy with my research work, conference visits etc., I am grateful to the almighty for having my ever supporting parents, and not to miss my two little twinkling stars-my lovely daughters 'Tulsi' and 'Gauri'.

At the work place, on the go, I found many good friends. Amogh Mudbhatkal a perfect researcher, who was full of energy, always cleared my doubts, taught me how to research when I was totally unaware of the latest concepts. He was the driving force in the cabin, for me, for Vinay D.C. and my thambi Raja Pandi. Everytime Ramachandra Sir gave guest entry to the cabin the whole environment turned intellectual. Usha my buddy, who though younger to me gave good advices and supported me. Good were the days with their support. I am grateful to Sujay Raghavendra for his timely suggestions and clarifications in my work. Akshayji being a scholar under my guide gave me advice on the research mistakes one should not make. This list goes on as we research scholars and M. Tech students move on as a team in the department. I thank each and every one who has helped me in one or the other way.

I am also grateful to the department staff: Balu Anna, Anil, Pratima, Harish, Shashi, Shailesh, Jagadish Sir and Sitaram Sir for their unfailing support and assistance throughout the course of my Ph.D. and in the laboratory. A very special gratitude to everyone in the Administrative block and Accounts section for their cooperation.

Thanks for all your encouragement!

*Suman Kundapura*

## ABSTRACT

In the dynamic environment of the coast maintaining the harbor tranquility is possible only with the planning of proper protection structures. Breakwaters are one among the several coastal protection structures. Breakwaters could either run into the water linking to the shore or placed independently parallel to the shore. The former will lead to the accretion on up drift side and erosion on the down drift side of the structure but the latter provides shore protection without adversely affecting the longshore transport. Breakwaters attenuate the wave, slow the littoral drift and produces sediment deposition. To provide a basis for evaluating the effects of breakwater installation a comprehensive study on the hydrodynamic response of breakwaters needs to be investigated. Physical models could be used in the laboratory to assess the same however, it is expensive, laborious and time-consuming which involves many variables that affect the shape, strength, alignment, base stability and other phenomena. There are several empirical formulae but developed on limited data. Also, though numerical models are good option, it involves numerous assumptions not withstanding faster computing resources, most of which are time-consuming, tend to overestimate the hydraulic responses. The Computational Intelligence (CI) techniques can be made use to overcome some of these shortcomings. As they are capable of replicating the outcome of a numerical model with better accuracy.

Among the several breakwaters available, the emerged semicircular breakwater is found advantageous and also the study on this type of breakwater is limited. Hence the present study is taken up to predict the hydraulic responses like reflection coefficient, relative wave runup, stability parameter, of emerged seaside perforated semicircular breakwater using different soft computing techniques. The soft computing techniques used are Artificial neural network (ANN), Adaptive neuro-fuzzy inference system (ANFIS), Genetic algorithm based adaptive neuro fuzzy inference system (GA-ANFIS) and Particle swarm optimization based adaptive neuro fuzzy inference system (PSO-ANFIS).

The prediction is done using conventional data segregation method. Also, a methodology of segregating the lower ranges of wave height data, and not using it for training the network and then predicting the hydraulic responses purely for this segregated data is done successfully and it is named

as ‘below the range’ predictions. Similarly, a prediction for purely higher ranges of wave height data not used in training the network, has been carried out and it is named as ‘beyond the range’ prediction.

The study shows the possibility of prediction of the hydrodynamic characteristics like reflection coefficient, relative run-up parameter and stability parameter of the semicircular breakwater using the soft computing techniques for both dimensional as well as non-dimensional input parameters. In both the cases the predicted outputs the reflection coefficient, relative run-up parameter and stability parameter was good in the conventional data segregation case. Also, below the data range approach gave reasonably good results in both set of input parameters for the prediction of reflection coefficient. Whereas, in the case of beyond the data range predictions the results are good in the case of dimensional input parameters but not for non-dimensional input parameters in the prediction of reflection coefficient. The relative wave run-up parameter prediction for below and beyond the range predictions did not give satisfactory results for both set of input parameters. In the present study the stability parameter of emerged seaside perforated semicircular breakwater is predicted for a dataset of 389 data sets. The results found are good for both the set of input parameters in the case of conventional data segregation method. As the available dataset is only 389 data sets, the below the data range and beyond the data range approach was not done for stability parameter prediction.

From the performance of four different models in several cases considered, the prediction made by GA-ANFIS gave better results in maximum number of cases. The ANN also predicted the output parameter well, though it is an individual model. But, the disadvantage here is the number of neurons in the hidden layer is chosen based on trial and error method, depending on thumb rules. In the case of ANFIS method the FIS could be generated by grid partitioning, subtractive clustering or fuzzy c-means clustering. In the present study since the number of inputs in dimensional as well as non-dimensional case is more than 5 the grid partitioning method has not been employed as it suffers the curse of dimensionality. In such cases the subtractive clustering or fuzzy c-means clustering can be employed. In the study it is found that the prediction made by fuzzy c-means clustering-ANFIS gave better results in maximum number of cases of reflection coefficient prediction compared to subtractive clustering-ANFIS with dimensional input parameters. Hence for all the remaining cases FCM-ANFIS is employed. The performance of PSO-ANFIS model is not as good as GA-ANFIS in the different cases considered. Arriving at the optimal parameters of the hybrid model costs time.

However, these soft computing techniques can be adopted as an alternate technique to predict the hydraulic response of semicircular breakwaters by coastal engineers when similar site conditions are available.

**Keywords:** *semicircular breakwater, reflection coefficient, relative wave runup, stability parameter, artificial neural networks, adaptive neuro-fuzzy inference system, genetic algorithm, particle swarm optimization.*



## TABLE OF CONTENTS

<b>DESCRIPTION</b>	<b>PAGE NO.</b>
ABSTRACT	i
CONTENTS	iv
LIST OF FIGURES	ix
LIST OF TABLES	xii
NOMENCLATURE	xiv
ABBREVIATIONS	xv
<b>1 INTRODUCTION</b>	
1.1 GENERAL	1
1.2 BREAKWATERS	1
1.2.1 Types of breakwaters	2
1.3 SEMICIRCULAR BREAKWATERS	4
1.3.1 Advantages of semicircular breakwaters	6
1.3.2 Hydraulic response of semicircular breakwaters	7
1.4 SOFT COMPUTING TECHNIQUES	7
1.5 SCOPE OF THE WORK	9
1.6 ORGANISATION OF THE THESIS	10
<b>2 LITERATURE</b>	
2.1 LITERATURE ON SEMICIRCULAR BREAKWATERS	11
2.2 APPLICATION OF COMPUTATIONAL INTELLIGENCE IN BREAKWATERS	17
2.3 SUMMARY OF LITERATURE	28
2.4 PROBLEM IDENTIFICATION	30
2.5 RESEARCH OBJECTIVES	31
<b>3 MATERIALS AND METHODS</b>	
3.1 MATERIALS AND METHODS	33

3.1.1	Data used	33
3.1.2	Wave flume used	33
3.1.3	Normalization of the data and consistency check	36
3.2	METHODOLOGY FLOWCHART	40
3.3	PHYSICAL EXPLANATION OF PREDICTION VARIABLES OF SEMICIRCULAR BREAKWATERS UNDER STUDY	40
3.4	DEVELOPMENT OF ANN MODEL	45
3.5	DEVELOPMENT OF ADAPTIVE NEURO-FUZZY INFERENCE SYSTEMS (ANFIS) MODEL	47
3.5.1	Subtractive clustering	47
3.5.2	Fuzzy C-Means Clustering	48
3.5.3	ANFIS model (Adaptive neuro fuzzy inference systems)	50
3.6	PARTICLE SWARM OPTIMIZATION (PSO)	53
3.6.1	ANFIS training improved with PSO	54
3.6.2	Literature on PSO application	55
3.7	GENETIC ALGORITHM	57
3.7.1	Hybrid GA-ANFIS model	58
3.8	STATISTICAL PARAMETERS TO VALIDATE THE MODEL PERFORMANCE	60
<b>4</b>	<b>PREDICTION OF REFLECTION COEFFICIENT</b>	
4.1	REFLECTION COEFFICIENT	63
4.1.1	Data segregation for prediction of $K_r$	64
4.2	RESULTS AND DISCUSSION OF $K_r$ PREDICTION OF SEMICIRCULAR BREAKWATER USING DIFFERENT SOFT COMPUTING MODELS FOR DIMENSIONAL INPUT PARAMETERS	65
4.2.1	Reflection coefficient prediction performance of different soft computing models for the case of below the data range for dimensional input parameters	66

4.2.2	Reflection coefficient prediction performance of different soft computing models for the case of conventional below the data range for dimensional input parameters	69
4.2.3	Reflection coefficient prediction performance of different soft computing models for the case of beyond the data range for dimensional input parameters	72
4.2.4	Reflection coefficient prediction performance of different soft computing models for the case of conventional beyond the data range for dimensional input parameters	75
4.3	RESULTS AND DISCUSSION OF $K_r$ PREDICTION OF SEMICIRCULAR BREAKWATER USING DIFFERENT SOFT COMPUTING MODELS FOR NON-DIMENSIONAL INPUT PARAMETERS	78
4.3.1	Reflection coefficient prediction performance of different soft computing models for the case of below the data range for non-dimensional input parameters	78
4.3.2	Reflection coefficient prediction performance of different soft computing models for the case of conventional below data range for non-dimensional input parameters	83
4.3.3	Reflection coefficient prediction performance of different soft computing models for the case of beyond data range for non-dimensional input parameters	88
4.3.4	Reflection coefficient prediction performance of different soft computing models for the case of conventional beyond data range for non-dimensional input parameters	92
4.4	RESULTS AND DISCUSSION OF $K_r$ PREDICTION OF SEMICIRCULAR BREAKWATER USING DIFFERENT SOFT COMPUTING MODELS FOR 1274 GLOBAL DATA POINTS	96
4.4.1	Reflection coefficient prediction performance of different soft computing models using dimensional input parameters for global data of 1274 points	96

4.4.2	Reflection coefficient prediction performance of different soft computing models using non-dimensional input parameters for global data of 1274 points	101
4.5	CLOSURE	105
<b>5</b>	<b>PREDICTION OF RELATIVE WAVE RUN-UP PARAMETER</b>	
5.1	PREDICTION OF RELATIVE WAVE RUN-UP ( $R_u/H_i$ )	107
5.1.1	Data segregation for prediction of relative wave run-up ( $R_u/H_i$ )	107
5.2	RESULTS AND DISCUSSION OF $R_u/H_i$ PREDICTION OF SEMICIRCULAR BREAKWATER USING DIFFERENT SOFT COMPUTING MODELS FOR DIMENSIONAL INPUT PARAMETERS	108
5.3	RESULTS AND DISCUSSION OF $R_u/H_i$ PARAMETER PREDICTION OF SEMICIRCULAR BREAKWATER USING DIFFERENT SOFT COMPUTING MODELS FOR NON-DIMENSIONAL INPUT PARAMETERS	114
5.4	RESULTS AND DISCUSSION OF $R_u/H_i$ PREDICTION OF SEMICIRCULAR BREAKWATER USING DIFFERENT SOFT COMPUTING MODELS FOR DIMENSIONAL AND NON-DIMENSIONAL INPUT PARAMETERS FOR BELOW THE DATA RANGE PREDICTION	118
5.5	RESULTS AND DISCUSSION OF $R_u/H_i$ PREDICTION OF SEMICIRCULAR BREAKWATER USING DIFFERENT SOFT COMPUTING MODELS FOR DIMENSIONAL AND NON-DIMENSIONAL INPUT PARAMETERS FOR BEYOND THE DATA RANGE PREDICTION	119
5.6	CLOSURE	120
<b>6</b>	<b>PREDICTION OF STABILITY PARAMETER</b>	
6.1	STABILITY PARAMETER ( $W/\gamma H_i^2$ ) OF SEMICIRCULAR BREAKWATER	121
6.1.1	Data segregation for prediction of Stability parameter	122

6.2	RESULTS AND DISCUSSION OF $W/\gamma H_i^2$ PARAMETER PREDICTION OF SEMICIRCULAR BREAKWATER USING DIFFERENT SOFT COMPUTING MODELS FOR DIMENSIONAL INPUT PARAMETERS	122
6.3	RESULTS AND DISCUSSION OF $W/\gamma H_i^2$ PARAMETER PREDICTION OF SEMICIRCULAR BREAKWATER USING DIFFERENT SOFT COMPUTING MODELS FOR NON-DIMENSIONAL INPUT PARAMETERS	127
6.4	CLOSURE	131
<b>7</b>	<b>SUMMARY AND CONCLUSIONS</b>	
7.1	SUMMARY	133
7.2	CONCLUSIONS	133
7.3	CONTRIBUTIONS FROM THE STUDY	136
7.4	LIMITATIONS AND FUTURE SCOPE	136
	<b>REFERENCES</b>	137
	<b>PUBLICATIONS</b>	149
	<b>RESUME</b>	151

## LIST OF FIGURES

<b>Fig. No.</b>	<b>Figure caption</b>	<b>Page no.</b>
1.1	(a) Semicircular breakwater and (b) Typical detailing of semicircular	5
3.1	Experimental setup of wave flume	34
3.2	Data consistency of input parameters $H_i/gT^2$ , $d/gT^2$ , $h_s/d$ , $S/D$ , $R/H_i$ , $K_r$ , in the case of reflection coefficient prediction	37
3.3	Data consistency of input parameters $H_i/gT^2$ , $d/gT^2$ , $h_s/d$ , $S/D$ , $R/H_i$ , $R_0/H_i$ , in the case of relative wave run-up parameter prediction	38
3.4	Data consistency of input parameters $H_i/gT^2$ , $d/h_s$ , $S/D$ , $W/\gamma H_i^2$ , in the case of stability parameter prediction	39
3.5	Flowchart of Methodology	40
3.6	Variation of reflection coefficient with incident wave steepness and depth parameter for a constant $R/h_t$ of 0.92 for a perforated SBW model with $S/D$ ratio of 4	41
3.7	Influence of perforations on reflection coefficient for depth parameter of 0.01 to 0.015 and a constant $R/h_t$ of 0.92.	42
3.8	Variation of relative runup parameter with incident wave steepness and depth parameter for a constant $R/h_t$ of 0.92 for a perforated SBW model with $S/D$ ratio of 8	43
3.9	Influence of perforations on relative runup for depth parameter of 0.00572 to and a constant $R/h_t$ of 0.92	43
3.10	Variation of stability parameter with incident wave steepness and depth parameter for a constant $R/h_t$ of 0.92 for a perforated SBW model with $S/D$ ratio of 8	44
3.11	Influence of perforations on stability parameter with incident wave steepness	45
3.12	ANN structure of feedforward backpropagation network	47
3.13	Basic ANFIS structure	51

3.14	PSO-ANFIS simplified	55
3.15	PSO-ANFIS flowchart	56
3.16	GA-ANFIS model	59
4.1	Typical data segregation procedure for $K_r$ prediction of SBW	64
4.2	Scatter plot of predicted versus actual values of $K_r$ for different models for the case of below the range with dimensional input parameters	68
4.3	Comparison of predicted $K_r$ by ANN, ANFIS, GA-ANFIS, PSO-ANFIS models for the case of below the range with dimensional input parameters with observed $K_r$ values	68
4.4	Scatter plot of predicted versus actual values of $K_r$ for different models for the case of conventional below the range with dimensional input parameters	71
4.5	Comparison of predicted $K_r$ by ANN, ANFIS, GA-ANFIS, PSO-ANFIS models for the case of conventional below the range with dimensional input parameters with observed $K_r$ values	71
4.6	Scatter plot of predicted versus actual values of $K_r$ for different models for the case of beyond the range with dimensional input parameters	74
4.7	Comparison of predicted $K_r$ by ANN, ANFIS, GA-ANFIS, PSO-ANFIS models for the case of beyond the range with dimensional input parameters with observed $K_r$ values	74
4.8	Scatter plot of predicted versus actual values of $K_r$ for different models for the case of conventional beyond the range with dimensional input parameters	77
4.9	Comparison of predicted $K_r$ by ANN, ANFIS, GA-ANFIS, PSO-ANFIS models for the case of conventional beyond the range with dimensional input parameters with observed $K_r$ values	77
4.10	Scatter plot of predicted versus actual values of $K_r$ for different models for the case of below the range with non-dimensional input parameters	81
4.11	Comparison of predicted $K_r$ by ANN, ANFIS, GA-ANFIS, PSO-ANFIS models for the case of below the range with non-dimensional input parameters with observed $K_r$ values	82
4.12	Scatter plot of predicted versus actual values of $K_r$ for different models for the case of conventional below the range with non-dimensional input parameters	87

4.13	Comparison of $K_r$ prediction performance of ANN, FCM-ANFIS, SC-ANFIS models in case of conventional below the range with non-dimensional input parameters	87
4.14	Scatter plot of predicted versus actual values of $K_r$ for different models for the case of beyond the range with non-dimensional input parameters	90
4.15	Comparison of predicted $K_r$ by ANN, ANFIS, GA-ANFIS, PSO-ANFIS models for the case of beyond the range with non-dimensional input parameters with observed $K_r$ values	92
4.16	Scatter plot of predicted versus actual values of $K_r$ for different models for the case of conventional beyond the range with non-dimensional input parameters	94
4.17	Comparison of predicted $K_r$ by ANN, ANFIS, GA-ANFIS, PSO-ANFIS models for the case of conventional beyond the range with non-dimensional input parameters with observed $K_r$ values	96
4.18	Scatter plot of predicted versus actual values of $K_r$ for different models in case of 1274 global data points with dimensional input parameters	99
4.19	Comparison of predicted $K_r$ by ANN, ANFIS, GA-ANFIS, PSO-ANFIS models for the case of dimensional input parameters with observed $K_r$ values	99
4.20	Scatter plot of predicted versus actual values of $K_r$ for different models in case of 1274 global data points with non-dimensional input parameters	103
4.21	Comparison of predicted $K_r$ by ANN, ANFIS, GA-ANFIS, PSO-ANFIS models for the case of non-dimensional input parameters with observed $K_r$ values	103
5.1	Typical data segregation for $R_u/H_i$ prediction of SBW	107
5.2	Scatter plot of predicted versus actual values of $R_u/H_i$ for different models with dimensional input parameters	111
5.3	Comparison of predicted $R_u/H_i$ by ANN, ANFIS, GA-ANFIS, PSO-ANFIS models for the case of dimensional input parameters with observed values	111
5.4	Scatter plot of predicted versus actual values of $R_u/H_i$ for different models with non-dimensional input parameters	116
5.5	Comparison of predicted $R_u/H_i$ by ANN, ANFIS, GA-ANFIS, PSO-ANFIS models for the case of non-dimensional input parameters with observed values	118



6.1	Scatter plot of predicted versus actual values of $W/\gamma H_i^2$ parameter of different models for dimensional input parameters	126
6.2	Comparison of predicted $W/\gamma H_i^2$ by ANN, ANFIS, GA-ANFIS, PSO-ANFIS models for the case of dimensional input parameters with observed values	126
6.3	Scatter plot of predicted versus actual values of $W/\gamma H_i^2$ for different models with non-dimensional input parameters	128
6.4	Comparison of predicted $W/\gamma H_i^2$ by ANN, ANFIS, GA-ANFIS, PSO-ANFIS models for the case of non-dimensional input parameters with observed values	131

## LIST OF TABLES

Table No.	Table caption	Page no.
3.1	Experimental parameter ranges for $K_r$ prediction	34
3.2	Experimental parameter ranges for $R_0/H_i$ prediction	35
3.3	Experimental parameter ranges for $W/\gamma H_i^2$ prediction	35
4.1	Error metrics for different soft computing models for dimensional input parameters in the case of below the data range for predicting reflection coefficient	67
4.2	Error metrics for different soft computing models for dimensional input parameters in the case of conventional below the data range for predicting reflection coefficient	70
4.3	Error metrics for different soft computing models for dimensional input parameters in the case of beyond the data range for predicting reflection coefficient	73
4.4	Error metrics for different soft computing models for dimensional input parameters in the case of conventional beyond the data range for predicting reflection coefficient	76
4.5	Error metrics for different soft computing models for non-dimensional input parameters in the case of below the data range for predicting reflection coefficient	82
4.6	Error metrics for different soft computing models for non-dimensional input parameters in the case of conventional below the data range for predicting reflection coefficient	86
4.7	Error metrics for different soft computing models for non-dimensional input parameters in the case of beyond the data range for predicting reflection coefficient	91
4.8	Error metrics for different soft computing models for non-dimensional input parameters in the case of conventional beyond the data range for predicting reflection coefficient	95
4.9	Error metrics for different soft computing models for dimensional input parameters in the case of global data of 1274 points for predicting reflection coefficient	100
4.10	Error metrics for different soft computing models for non-dimensional input parameters in the case of global data of 1274 points for predicting reflection coefficient	104

5.1	Optimal parameters of different models for dimensional input parameters	112
5.2	Error metrics for different soft computing models for dimensional input parameters in the case of 750 data points for predicting relative wave run-up parameter	113
5.3	Optimal parameters of different models for non-dimensional input parameters	116
5.4	Error metrics for different soft computing models for non-dimensional input parameters in the case of 750 data points for predicting relative wave run-up parameter	117
6.1	Optimal parameters of different models for dimensional input parameters	124
6.2	Error metrics for different soft computing models for dimensional input parameters in the case of 389 data points for predicting stability parameter	125
6.3	Optimal parameters of different models for non-dimensional input parameters	129
6.4	Error metrics for different soft computing models for non-dimensional input parameters in the case of 389 data points for predicting stability parameter	130

## NOMENCLATURE

$H_i$	Incident wave height
$T$	Wave period
$S$	center to center spacing of perforations
$D$	Diameter of perforations
$R$	Radius of semicircular caisson
$d$	Water depth
$h_s$	Semicircular breakwater structure height
$K_r$	Reflection coefficient
$R_u/H_i$	Relative wave runup parameter
$W/\gamma H_i^2$	Stability parameter
$H_i/gT^2$	Incident wave steepness parameter
$d/gT^2$	Depth parameter
$S/D$	Ratio of spacing to diameter of perforations
$R/H_i$	Relative caisson radius
$h_s/d$	Relative structure height

## ABBREVIATIONS

ANN	Artificial Neural Network
ANFIS	Adaptive Neuro-Fuzzy Inference System
FCM	Fuzzy C-means Clustering
SC	Subtractive Clustering
FFBP	Feed-Forward Backpropagation Network
GA-ANFIS	Genetic Algorithm Based Adaptive Neuro Fuzzy Inference System
PSO- ANFIS	Particle Swarm Optimization- Adaptive Neuro Fuzzy Inference System
EPSBW	Emerged Seaside Perforated Semicircular Breakwater
CC	Correlation Coefficient
SWL	Sea Water level
MLP	Multi-Layer Perceptron
NN	Neural Network
PSO	Particle Swarm Optimization
RMSE	Root Mean Square Error
SI	Scatter Index
NSE	Nash Sutcliffe Efficiency
HIMMFPB	Horizontally Interlaced Multilayer Moored Floating Pipe Breakwater

# CHAPTER 1

## INTRODUCTION

### 1.1 GENERAL

The port and harbor tranquility is possible only with the planning of proper coastal protection structures. Breakwaters are one of the best coastal protection structures. They are built to dissipate the enormous energy of the sea waves. The design of such structures is of great importance as their installation involves huge investment. Reduction of the construction cost without compromising the structure stability is always the priority in any project. Also, the material used for the construction of the breakwaters could be different based on the availability of the materials and site conditions. It could be built with stones, rubble masonry or with their combination. The design life of a breakwater is usually 30-50 years for most rock structures. The breakwaters should be designed taking natural site characteristics into consideration as it has a direct impact on the shoreline. Sand accumulation behind the structure leads to the formation of a salient. Also, sand accumulating connects the breakwater to the shore forming a tombolo. The choice of the type of breakwater is site-specific and no single breakwater holds good under all site conditions.

### 1.2 BREAKWATERS

Breakwaters aim at protecting the coast or activities at the coastline. Breakwaters have varying impact on the shoreline based on their variants. In general, the several variants in the design of breakwater are:

- Emerged, submerged or floating
- Distance from shoreline and location relative to the surf zone
- Length and orientation
- Single or segmented
- Special shapes

Emerged breakwaters hinder the aesthetics of the beach but reduce the wave energy by wave by introducing run-up, breaking and partial reflection of incident waves. These

types of breakwaters dissipate more energy compared to the submerged type of breakwaters, where the crest of these breakwaters protrudes above the still water level. Submerged breakwaters attenuate lesser wave energy compared to emerged breakwaters. Submerged breakwaters offer multiple functions. By not interfering the aesthetics of the beach, it reduces the wave energy by partial reflection and partial transmission and also maintains the landward flow of water due to which there is water circulation. Floating breakwaters are basically floating barriers constructed where bed soil is not suitable for permanent structures. This type of breakwater is mobile, less expensive and is less damaging to commercial activities as well as the environmental processes. Floating breakwaters have a relatively higher maintenance cost, unable to withstand catastrophic storms.

In the design of detached offshore breakwater, its length should be optimal, neither too long nor too short such that the morphological response should be a smooth salient in the shoreline. If the length of any breakwater is too long then the changes in the flow pattern lead to the increase in current speeds towards the lee zone, near the breakwater heads. Unlike the longer breakwaters, shorter ones provide less shelter, lower eddy formation towards the lee zone, no high currents at the breakwater heads, and only slight changes in the general pattern of the longshore current. Breakwaters could be single or segmented depending on the requirement. Segmented breakwaters are most popularly in use as it provides better coastal protection. The curved breakwaters can be used for all type of coasts and as a replacement for traditional breakwaters. Different shapes of breakwaters are in use like semicircular breakwaters, quarter circular breakwaters, hemicylindrical breakwaters, rectangular breakwaters, porous pipe breakwaters, etc., There is a need to conduct more research on these different shapes of breakwaters to further implement these structures in the actual site.

### **1.2.1 Types of Breakwaters**

Breakwaters are basically classified as fixed and floating type. However, in recent decades, there are special types of breakwaters in use. The most feasible one is chosen for construction based on the prevailing environment and depending upon the required degree of shelter (Rajendra et al. 2017). The following are some of the types of breakwaters in use :

- Rubble mound breakwaters
- Vertical wall breakwaters
- Composite breakwaters
- Special type of breakwaters

Rubble mound breakwaters (RMB) are most widely used in places where natural stones are abundantly available. The RMB is constructed mainly to break the wave and vertical wall breakwaters to reflect the waves. The RMB is limited to shallow water environments from the technical and economical point of view. Modern-day constructions with concrete blocks could be used in deep waters as well. A large amount of literature is available in the case of rubble mound breakwaters as several researchers have explored this kind of structure for the stability of armor blocks and concluded that armor stability is a function of several factors. They concluded that armor stability depends on the depth of water, various characteristics wave, slope of the structure, armor unit weight, porosity and the total duration of the storm (Hudson, 1959; Brunn and Gunbak, 1976; Van der Meer and Pilarczyk, 1984; Gadre et al. 1985; Hegde and Samaga, 1996). Neelamani et al. (2002) studied the effect of a detached breakwater placed on the seaward side in front of an impermeable seawall. This significantly reduced the pressure, run-up, and rundown on the seawall. MuniReddy and Neelamani (2004) also studied the effect of a low crested rubble mound breakwater placed on the seaward side in front of the impermeable seawall and found reduction of pressure ratio with the increase in the relative height of the breakwater ( $h/d$ ). Several types of research on such a combination of low crested rubble mound structure in front of the seawall vertical or inclined are available in the literature.

Vertical wall breakwaters could be a simple vertical wall structure or composite structure with a rubble mound foundation. It could be low mound or high mound. However, the higher mound breakwater has a mound higher than the low water level and wave breaks on the mound. High mound composite breakwaters are unstable as the breaking waves induce impulsive pressure and scouring, due to which, low mound breakwaters are commonly used. Horizontally composite breakwaters have a vertical wall breakwater and concrete blocks in front of the breakwater to dissipate the wave energy which otherwise would damage the vertical wall. Rubble mound stabilizes the



foundation against wave force and reduces scouring of the upright section. Some special breakwaters are still in use though limited to special conditions. The curtain wall breakwater is used as secondary breakwaters to protect small craft harbors. Sheet pile or continuous pile vertical wall breakwaters are used to break small waves. A Horizontal plate breakwater can reflect and break waves. A floating breakwater is very useful as a breakwater in deep waters, but its effect is limited to relatively short waves. For the present study semicircular breakwater is taken up and the advantages of the semicircular breakwaters are discussed in the following section.

### **1.3 SEMICIRCULAR BREAKWATERS (SBW)**

The semicircular breakwater was first developed in Japan at the beginning of the nineties and was first adopted for the formation of the harbor in Miyazaki Port, Japan (Sasajima et al. 1994). The study of semicircular caisson breakwater was started by the Port and Harbour Research Institute of the Ministry of Transport of Japan, Coastal Development Institute of Technology and several other corporations in 1990. The semicircular breakwater is mainly a precast reinforced concrete structure having a semicircular shaped hollow caisson resting on a rubble mound as shown in (Fig. 1.1a). It is made of pre-stressed concrete and cast as different elements. Since the caisson is hollow its weight and the materials to be used are significantly less. It could be either emerged or submerged type, fully perforated or partially perforated. The Fig. 1.1b shows the emerged seaside perforated SBW, by employing this kind of breakwater the wave energy dissipation is done by creating turbulence inside the chamber thus reducing the pressure and force on the caisson. The spacing between the perforations depends on the diameter of perforation and the S/D ratio. The stability against sliding for SBW is good, since, the horizontal component of the wave force is smaller compared to the vertical component. In addition, the vertical component is applied downward the curved wall. The semicircular breakwater possesses a round top and, thus, offers more stability against the action of waves. Thus it also serves well as offshore detached breakwaters adopted for the protection of the coast against erosion. The SBW enhances the scenery compared to the conventional rubble mound breakwaters. The impermeable semicircular breakwaters are effective wave reflectors

and the permeable semicircular breakwaters are good energy dissipaters (Teh and Venugopal, 2013).

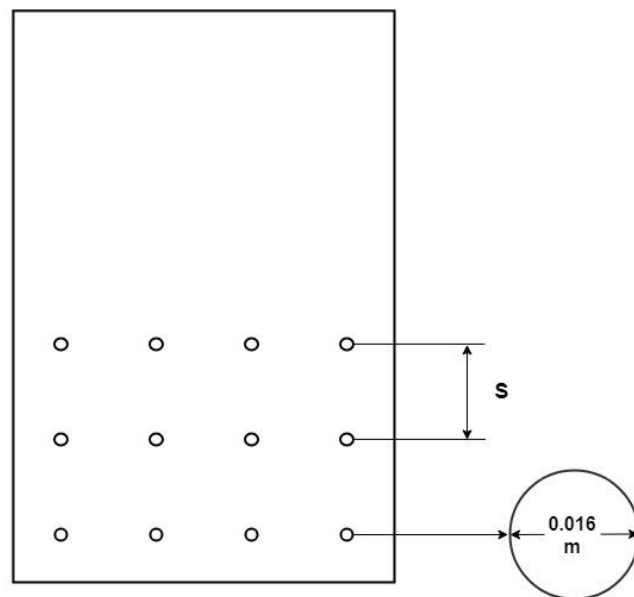
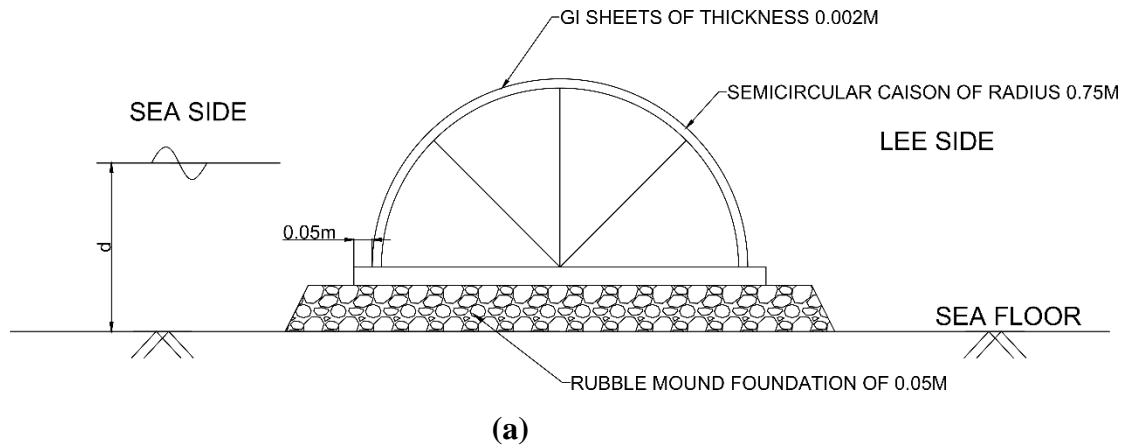


**Fig. 1.1 (a) Sectional view of Semicircular breakwater (b) Typical detailing of the semicircular breakwater**

### **1.3.1 Advantages of semicircular breakwaters**

Semicircular breakwaters (SBW) have many advantages over conventional breakwaters. These advantages make semicircular breakwaters more popular research topic for coastal engineers and scientists. Some of the advantages are mentioned below:

- High aesthetic value due to the arch type of construction.
- In case of relocation semicircular breakwaters can be easily dismantled and reassembled as it is the pre-stressed modular type of construction.
- It is a modular type construction which is relatively simple and no in-situ concrete work
- Reduction of construction material as the caisson of the semicircular breakwater is hollow and it does not require filling of materials as in the case of conventional rubble mound structures.
- The construction cost of a semicircular breakwater is about 20% lower than that of a conventional rubble mound structure (Xie, 2001).
- The dynamic force acting on the wall of SBW always passes through the center of the circle this will create a uniform sub-grade reaction. As the subgrade reaction per unit area is minimum applicability in soft foundations is possible (Tanimoto and Goda, 1992). Hence there is also no overturning moment induced by the wave pressure.
- Semicircular breakwater has high stability against sliding because the horizontal component of wave force causing sliding is considerably less than the vertical component (Yuan and Tao, 2003).
- Enhanced stability against overturning: SBW has high overturning stability because of its arch type shape (Graw et al., 1998). The stability can be increased further by making base slab perforated, which will reduce the uplift pressure (Sasajima et al. 1994).
- Applicability in a broad range of water depths: SBW was established to be an excellent coastal protection structure for a wider range of water depths (Tanimoto and Takashashi, 1994), especially when the seaside wall is perforated (Dhinakaran et al. 2011).

### **1.3.2 Hydraulic response of semicircular breakwaters**

Hydraulic response parameters of an emerged seaside perforated semicircular breakwater under study are reflection coefficient ( $K_r$ ), relative wave run-up ( $R_u$ ) and stability parameter ( $W/\gamma H_i^2$ ) which are the responses to the wave action on the structure. The study of the reflection coefficient is of importance as the incident and the reflected waves interact giving rise to standing waves/ clapotis in front of the coastal structure with occasional steep and unstable waves affecting the small boats. These waves may propagate into the harbor area leading to increased peak orbital velocities and may pave movement of beach material. Also, reflection increases littoral currents and local sediment transport under oblique waves. The study of the reflection coefficient is also important to keep the toe of the structure safe. The upward extreme level reached by each wave above the static water level is termed as wave run-up and determining this is important to fix the crest level of the structure in the design of the semicircular breakwater. Semicircular breakwater has high stability against sliding; however, the critical weight required to resist sliding needs to be found out in the design of the semicircular breakwater. This can be arrived at using the stability parameter ( $W/\gamma H_i^2$ ) of the semicircular breakwater.

In the present study, soft computing techniques such as ANN, ANFIS, GA-ANFIS, and PSO-ANFIS are used to predict the hydraulic responses of SBW. The data for this is collected from a two-dimensional monochromatic wave flume of Marine structures laboratory, NITK, Surathkal. The basic input parameters being the wave height, wave period, water depth, radius of the semicircular breakwater, center to center spacing of perforations, the diameter of the perforations and the structure height. Prediction is also done using a set of the non-dimensional parameter for the respective hydraulic response parameter.

### **1.4 SOFT COMPUTING TECHNIQUES**

Principal components of the soft computing techniques are evolutionary computing, machine learning, fuzzy logic, and Bayesian statistics, they could be applied independently or combined with other techniques to solve the complex problems. Soft computing techniques can resolve the non-linear problems with the expert knowledge

of cognition, recognition, understanding, learning to name a few in computing. Hybridization of soft computing techniques has great potential. However, individual techniques are also capable of good prediction. This hybrid system of soft computing techniques is growing rapidly with its many successful applications in the area of coastal engineering. The Computational Intelligence (CI) techniques could be made use of to overcome the shortcomings of past methods. Artificial Intelligence has emerged as one of the most revolutionary areas. An overview of applications of Artificial Intelligence in prediction and forecasting of different wave parameters associated with breakwaters are presented in the subsequent chapters. Computer networks can be trained to think for themselves and make intelligent decisions like human counterparts. There have been a significant number of research works, where the soft computing techniques are adopted to predict the wave run-up, wave transmission, reflection coefficient, stability and damage level of breakwaters (Dwarakish and Nithyapriya 2016).

Over the past decades, researchers have predicted the performance of various types of breakwaters using different soft computing techniques. Identifying the gaps in the literature the current research on semicircular breakwaters by the application of soft computing techniques to predict its hydrodynamic characteristics is carried out. Artificial intelligence (AI) could be an excellent option for prediction when the experimental study data is limited as experimentation is tedious and expensive. A need was also felt to develop the soft computing models to predict for ranges of wave height which are not involved in training the network so that we could predict the output variables for the ranges of wave heights for which experiments were not conducted. This is named as below and beyond the data range prediction. A comparison between the conventional method of prediction and below/beyond the data range prediction is done. The ANN, ANFIS, GA-ANFIS, PSO-ANFIS model prediction performances are compared with the experimental observations. Further, the robustness of the model is assessed by the error metrics like the Correlation coefficient, Root mean squared error, Scatter index, Nash Sutcliffe efficiency and Bias. This study could be useful to the coastal engineers in the prediction of the hydraulic responses of emerged seaside perforated semicircular breakwaters. The study also shows that for lower and higher

ranges of wave heights for which no physical model data is available the prediction of the hydraulic responses is possible.

### **1.5 SCOPE OF THE WORK**

The present research proposes to predict the hydraulic response of emerged seaside perforated non-overtopping semicircular breakwater using soft computing techniques for below and beyond the data ranges fed while training the network. The current research is an attempt to overcome the shortcomings of the past researches. In the literature, we find numerous models which are developed to predict the wave parameters for which the training data set involves all the ranges of data. Here, the model predicts for exclusively purely below and purely beyond the ranges of data used for training. If the conducted experiments are for certain wave height ranges then, by training the network, with these ranges we can predict the performance for lower ranges as well as the higher ranges of wave heights. Also, the conventional method of training and testing were done for a better understanding of the prediction performance.

## **1.6 ORGANISATION OF THE THESIS**

The thesis titled “**Soft computing techniques in the prediction of the performance of semicircular breakwaters,**” consists of the following chapters:

**Chapter 1** introduces the role of breakwaters in protecting the coast, the different types of breakwaters used in practice. It explains the advantages of semicircular breakwaters over other breakwaters. An introduction to soft computing techniques is also presented in this chapter.

An overview of research done on semicircular breakwaters and the current state of knowledge of the application of soft computing techniques in the field of coastal engineering is presented in **Chapter 2**

**Chapter 3** deals with materials and methods, the details of the experimental data used for the present study, the data consistency check, data normalization, methodology of soft computing models employed and their assessment statistics.

**Chapter 4** illustrates the wave reflection coefficient of emerged seaside perforated semicircular breakwaters, the data segregation in the current study and the prediction of wave reflection coefficient for below, beyond and conventional ranges of data segregation.

**Chapter 5** illustrates the relative wave run-up parameter of emerged seaside perforated semicircular breakwaters, the data segregation and the prediction of relative wave run-up parameter for below, beyond and conventional ranges of data segregation.

**Chapter 6** illustrates the stability parameter of emerged seaside perforated semicircular breakwaters, the data segregation and the prediction of the stability parameter for conventional ranges of data segregation.

The study conclusions arrived on the application of soft computing models to predict the hydraulic responses of emerged seaside perforated semicircular breakwaters is presented in **Chapter 7**

## **CHAPTER 2**

### **LITERATURE REVIEW**

This chapter attempts to critically review the research done on semicircular breakwaters and the current state of knowledge of the application of soft computing techniques in the field of coastal engineering particularly breakwaters.

#### **2.1 LITERATURE ON SEMICIRCULAR BREAKWATERS**

The Japan Institute of Port and Harbor Research developed the semi-circular breakwater (SBW) in the 1980s. Since then, research on these arch type breakwaters has been of interest. A first-ever 36 m long bottom seated semicircular caisson breakwater was constructed at Miyazaki Port, Kyushu Island, Japan from 1992 to 1993 (Sasajima et al. 1994; Aburatani et al. 1996). The structure built is 36 m long and made up of seaside perforated precast semi-circular caisson, with porosities of 25% and 10% for the seaside of the caisson and bottom slab respectively. Followed by this successful breakwater installation in Japan the countries like China and India have taken up similar studies. In 1997 China constructed a 527 m long SBW to protect the southern harbor side of the Tianjin port. In the year 2000, the largest SBW came into existence in the Yangtze River estuary in Shanghai, China with the length of the structure being 18 km (Xie, 2001; Graw et al. 1998).

By using Goda and Suzuki, 1976 caisson breakwater formula, Tanimoto and Takahashi (1994) recommended some empirical formulas to calculate the wave force on SBW. Sasajima et al. 1994 studied the world's first semicircular breakwater constructed at Miyazaki port in Japan. They measured the pressures and forces on the breakwater. The variation of the measured highest one-third wave pressure with respect to maximum wave force at different elevations along the seaward face were found to be less than the results of the modified theoretical formula of Goda and Suzuki 1976.

Yu et al. 1999 studied the hydraulic response of the semicircular breakwater when exposed to oblique irregular waves. They studied the wave force variation on a unit



length of SBW, wave steepness  $H_s/L_s$ , relative wave height  $H_s/d$ ,  $d'/H_s$  and the angle of incidence  $\theta_0$ . They suggested the empirical formula of the longitudinal distribution coefficient and the longitudinal load reduction factor. The study found that the horizontal wave force corresponding to wave trough value was more than the crest values.

Yuan and Tao, 2003 studied the wave forces on a semicircular breakwater (for three cases, i.e. submerged, alternately submerged, and emerged conditions by using a numerical model based on a hybrid method of boundary element method (BEM) and finite difference method (FDM). Wavemaker technology and the non-reflected open boundary were adopted. Five sets of experimental data of different diameters and shapes of SBW has been used to calibrate and verify the numerical model the numerical results matched very well with the experimental data. They derived a simplified formula for calculating the total wave forces on the breakwaters from the numerical results suitable for submerged, alternately submerged, and emerged conditions.

By using Goda and Suzuki (1976) caisson breakwater formula, Tanimoto and Takahashi (1994) recommended some empirical formulas to calculate the wave force on SBW. Sasajima et al. (1994) studied the world's first semicircular breakwater constructed at Miyazaki port in Japan. they measured the pressures and forces on the breakwater. the variation of the measured highest one-third wave pressure with respect to maximum wave force at different elevations along the seaward face were found to be less than the results of the modified theoretical formula of Goda and Suzuki (1976).

SriKrishnapriya et al. (2000) in their results on the variation of the dynamic pressures on an impermeable semicircular breakwater revealed that it compared well with the two-dimensional finite element model of Sundar et al. (2001). They found that their measured values were less than those of the modified formulation of Goda and Suzuki (1976), particularly when nearer to the SWL, and conclusions were similar to that of Sundar and Raghu (1997). Further, the dimensionless pressures were found to reduce with increase in the scattering parameter,  $ka$ , where,  $ka$  is the wave number and 'a' is

the radius of the semicircular caisson. In addition, the pressures were reported to be less for higher  $h_w/h_t$ , where,  $h_t$  is the total height of the model, that is, the height of the rubble mound plus the height of the semicircular caisson. Sundar and Ragu (1997) conducted experiments on a solid type SBW subjected to random waves. He studied the wave runup, wave reflection, and dynamic pressures. The reflection coefficient ( $K_r$ ) for the SBW model ranges from 0.6-0.95 over a wave steepness range of 0.2 to 0.095. The results indicate that the SBW is quite effective in reflecting the incident wave energy. The pressure spectrum at still water level (SWL) results in lesser energy compared to that of immediately below the SWL, which is due to the intermittence effect. The pressure spectra were found to decrease towards the sea bed. The zero<sup>th</sup> spectral moment at a location ( $z/d = -0.10$ ), immediately below the SWL, was nearly 60 to 75% greater than that exerted at the SWL. The shape of the pressure spectra is slightly broader than the corresponding wave spectrum. The shoreward peak pressures follow a Raleigh distribution. The study also reveals that the variations are similar to those of the corresponding wave spectra. The variation of the zero<sup>th</sup> spectral moment of the run-up with a variation of the zero<sup>th</sup> spectral moment of wave elevation ( $m_0$ ) $\eta$  along with the line of best fit reveals that the energy under the run-up spectra increases with increase in energy in the incident wave spectrum. They observed that the trend in variation of the relationship of statistical averages of run-up was similar to that obtained for pressures.

Dhinakaran et al. (2002) compared the dynamic pressures and forces exerted on impermeable and seaside perforated semicircular breakwaters (SBW model with 7 and 11% perforations) due to regular waves. They observed that for higher  $h_w/h_t$  (water depth/total height of breakwater), the reflection coefficient ( $K_r$ ) and the dimensionless pressure is less. As the water depth increases the vertical force is almost twice the horizontal force. They found that the seaside perforated SBW dissipates more energy due to the provision of perforations and is subjected to lower hydrodynamic pressures and forces and reflects a lower amount of energy. The estimation of wave reflection coefficient using empirical formulae and numerical models can be undertaken to integrate the complexity of coastal processes. Several empirical formulae and

numerical models to predict  $K_r$  for a wide range of coastal structures have been listed out by Zanuttigh and Van der Meer (2008) concluding that these methods are time-consuming and leading to probable overestimation of wave reflection.

Nishanth (2008) carried out experiments to find the hydrodynamic performance characteristics of emerged seaside perforated and non-perforated semicircular breakwaters. The results showed that the non-dimensional wave run-down ( $R_d/H_i$ ) and wave run-up ( $R_u/H_i$ ) increases with the increase in incident wave steepness ( $H_i/gT^2$ ) and depth parameter ( $d/gT^2$ ). Ganesh (2009) conducted studies on seaside perforated model of semicircular breakwaters with S/D ratios of 2 and 6 for varying wave heights, periods in different water depths. Similarly, he studied the performance of both side perforated model of semicircular breakwaters with different S/D ratios of 2, 4, 6 and 8. The results of the study showed that as the percentage of perforations increased or the S/D ratio decreased, the value of the reflection coefficient, relative runup and relative rundown decreased, but the value of the transmission coefficient increased. The conclusions of Vishal Kumar (2010) were the same as that of Ganesh (2009) for perforated models with different S/D ratios.

Dhinakaran et al. (2009) studied how the perforations, water depth and rubble mound height of an SBW affect the non-breaking wave transformations. The experimental study of an SBW model for three different perforation ratios with 7%, 11%, and 17% was selected to study the variation of reflection, transmission, runup characteristics and dimensionless horizontal and vertical forces as a function of relative water depth. They compared the obtained results with semicircular breakwater model results of Sri Krishnapriya et al. (2000) and Dhinakaran et al. (2002, 2008). They found that the model with perforation percentage of 11% on the seaside and fully perforated type gives an optimum performance regarding energy dissipation and transmission. The increase in the percentage of perforations from 0 to 11 decreases the reflection coefficient and from 11 to 17% the reflection coefficient increases. Usually, with longer wave periods, the distance run by the waves over the curved surface is larger, hence more energy is dissipated and less reflection. In case SBW with 11%

perforations, the energy dissipation is irrespective of wave period. In the case of SBW with 17% perforations, waves of smaller period waves as well as longer period waves dissipate lesser energy because of its perforation size compared with models up to 11% perforations. The total height of the model recommended being about 1.25 times the water depth and height of the rubble mound which is 0.29 times the total height of the model. These values if adopted in the field gives a better performance of SBW. For all the considered perforation case, the dimensionless vertical force is very much higher than the dimensionless horizontal force. The vertical force acts on the semicircular caisson, adding stability to the breakwater. The long period waves exerted more force on the caisson compared to short period waves. The increase in water depth highly influences the wave force by increasing the force on the caisson. Thus the variations of force and pressure directly influence the stability of SBW, i.e. the minimum weight required to ensure that the stability of SBW increases with an increase in force and pressure. The comparison of transmission coefficient indicates that, for submerged condition, SBW transmits lesser energy than conventional rubble mound breakwater, whereas for surface piercing condition  $K_t$  value is on the higher side for SBW (till 11 percentage perforation) than rubble mound breakwater and is within the upper bound. The effect of perforations and the effect of rubble mound height on hydrodynamic characteristics of seaside perforated SBW models are more significant compared to the effect of water depth. The increase in rubble mound height resulted in a significant reduction in reflection and transmission coefficients and run-ups for  $h_r/h_t$  values from 0.18 to 0.29 and it is less significant for further increase in  $h_r/h_t$  to 0.36. The transmitted wave height on the seaside exceeds 50 percent of incident wave height in case of SBW17 almost in all the  $h_w/h_t$  ratios tested and concluded that SBW17 will affect the tranquility condition on the shoreward direction. Dimensionless run-up decreases with an increase in water depth and perforation and in case of higher water depth, there is no much reduction in values observed among the different cases of seaside and fully perforated SBW.

Hegde et al. (2010) conducted the study on a semicircular breakwater in a two-dimensional wave flume subjected to regular waves which shows that the relative run-

up and run-down decreases by the increase of perforations in the breakwater. With the increase in wave steepness the relative wave run-up increases and the relative wave run-down decreases. Also, with the increase in depth parameter the relative wave run-up and wave run-down increases. The energy loss coefficient including transmission and reflection coefficients were studied by Kudumula and Mutukuru (2013) for a semicircular low-crested breakwater. A comparison of the wave force characteristics on the impermeable vertical seawall with a combination of low crested rubble mound breakwater and a semicircular low crested breakwater was done. The wave forces on the vertical wall were less for semicircular low-crested breakwater for zero submergences in all the cases considered in the study. The waves impinging on an emerged seaside perforated SBW partly gets reflected seaward, and the rest enters through the perforations dissipating the energy. The seaward reflected waves may compromise structure stability by scouring the structure toe further causing a problem in its foundation (Zanuttigh et al. 2013). Hegde and Naseeb (2014), evaluated the wave transmission of semicircular breakwaters for different radii and for various submergence ratios. The study found a decrease in wave transmission as the incident wave steepness increased for all the considered submergence ratios. The lower reflection coefficient is desirable to keep the structure safe (Hodaei et al. 2016). A detailed review on different laboratory methods of wave reflection coefficient estimation of coastal structures are listed in the review of (Varghese et al. 2016) and suggests the usage of Isaacson three probe method to study monochromatic waves in the laboratory Isaacson, 1991. However, the scope to estimate the wave reflection coefficient for partially perforated caissons still exists.

Sreejith (2016) found the stability of emerged SBW models to resist sliding by determining the critical weight required. He evaluated the hydrodynamic performance by finding the wave run-up and wave reflection characteristics of the model. He also conducted a study on emerged non-perforated SBW model and seaside perforated SBW models of diameter to spacing ratios of 8, 4 and 2. He found that as the perforation increases stability parameter decreases. The percentage of reduction of stability parameter at least gets doubled by doubling the percentage of perforations from the

S/D ratio of 8 to 4. With the increase in incident wave steepness for all ranges of depth parameters for all SBW models Stability parameter ( $W/\gamma H_i^2$ ) and Relative wave runup parameter ( $R_w/H_i$ ) was found to decrease whereas the Reflection coefficient ( $K_r$ ) was found to increase. As the depth parameter increased for constant incident wave steepness the relative runup decreased, the reflection coefficient was found to decrease, and the stability parameter increased for all SBW models. He obtained a nomogram which could be used successfully for finding the critical weight required for stability against sliding for an emerged SBW.

Gope et al. (2016) studied the flow over the semicircular breakwater and examined the variations of properties like temperature, flow properties using Computational Fluid Dynamics taking into account the viscosity factor. They concluded that FLUENT software simulated well for semi-circular breakwater and GAMBIT performs geometrical modeling with high accuracy and is better than conducting the physical model study. Hegde et al. (2015) conducted an experimental study to understand the variation of the non-dimensional stability parameter with incident wave steepness for different values of dimensionless depth parameter and a nomogram was developed for computing the sliding stability of the breakwater. Hegde et al. (2018) studied the sliding stability of seaside perforated semicircular breakwater of 0.6 m radius and S/D ratio of 8 and 4. He found that as an incident wave steepness and perforation increases the dimensionless stability parameter exponentially decreases. As the depth parameter increased, the critical weight required for the stability against sliding of semicircular breakwaters also increased. The study of the influence of incident wave steepness and influence of perforations on the wave reflection and run up was performed. Reflection coefficient was found to be decreasing with the increase in perforation. Run up parameter was found to be decreasing with increase in  $H_i/gT^2$  and S/D ratio.

## **2.2 APPLICATION OF COMPUTATIONAL INTELLIGENCE IN BREAKWATERS**

The design of armor layer units of breakwater depends on the anticipated damage ratio. Prediction of the damage ratio of the breakwater is possible using the ANN model.

Artificial Intelligence simulations can efficiently interpolate the experimental data sets for a variety of combinations of wave height, wave period, wave steepness and slope angle. Damage ratio estimation for breakwater design uses the inputs like mean wave period, wave steepness, significant wave height, and the breakwater slope. Though ANN models can efficiently model the non-linear relationships between inputs and outputs, fuzzy logic better estimated the damage ratio as it closely mimics the environment. The damage ratio was modeled as a function of wave height, wave period, wave steepness and breakwater slope instead of generating a typical regression equation (Yagci et al. 2005).

The stability number forecasting of the conventional rubble mound structures by fuzzy logic approach is more accurate, as it deals with the uncertainties not accounted for by empirical formulae. The input parameters to the developed FL model are permeability of structure, the slope angle of the breakwater, a number of waves, surf similarity parameter, and damage level to predict the stability number. Along with these parameters in Van der Meer's equations the non-dimensional parameter, i.e., depth to significant height ratio ( $d/H_s$ ), at the structure toe is also used to take into account the effect of foreshore breaking waves. The fuzzy logic model developed is the most superior model in prediction of stability number for conventional rubble mound breakwater design, followed by Van der Meer's approach and Mase et al.'s ANN model, respectively (Erdik 2009).

Stability number of armor block is a vital issue while designing rubble mound breakwaters. The prediction of Stability number of armor block can be accurately done using model trees. Model trees are easier to use, and they represent understandable mathematical rules. Here the conventional governing parameters were used as input variables, and the predicted stability numbers of breakwater armor outperformed the previous empirical and soft computing methods. Model trees produce easy and significant formulas (Etemad-Shahidi and Bonakdar, 2009).

The maximum wave runup on breakwaters for determining the crest level of

breakwaters through traditional regression-based empirical model approaches involves several assumptions such as linearity, normality, variance constancy, etc. Whereas, ANN predicts the maximum wave runup accurately overcoming the drawback of the conventional empirical model and suffice as a modern approach towards  $R_{u2\%}/H_s$  prediction to determine the crest level of coastal structures accurately. Here many three layer feed-forward type of ANN is used and the model with four inputs, five neurons in hidden layer with only one output, yields the best result out of all developed models. The accuracy of the developed model is evaluated with the empirical model based on regression of Van der Meer and Stam (1992) and found that the ANN outperformed regression model in  $R_{u2\%}/H_s$  prediction (Erdik et al. 2009).

Artificial Intelligence (AI) models can be developed for the preliminary design of rubble mound breakwaters. However, the final design necessitates examining other failure modes because the coastal structure safety is highly variable. The fuzzy systems and fuzzy neural networks are found more advantages in the prediction of stability number of rubble mound breakwaters as it incorporates fuzzy logic as expert systems relative to hybrid neural networks (Balas et al. 2010).

Kirkgöz and Aköz (2005) observed that a breaking wave has highest impact force on a vertical wall when the wave breaks on a vertical wall with a near vertical front face at the instant of impact is called “perfect breaking.” The accurate prediction of these impact forces on coastal structures is dependent on the configurations of wave breaking. They employed artificial neural networks (ANN) to predict the geometrical properties like the breaker crest height,  $h_b$ , breaker height,  $H_b$ , and water depth in front of the wall,  $d_w$ , of perfect breaking waves on the vertical wall of composite-type breakwaters. The study found that ANN prediction can be done more accurately by artificial neural networks compared to linear and multi-linear regressions

Adaptive Neuro-Fuzzy Inference System (ANFIS) outperformed the artificial neural networks model in the prediction of the wave transmission coefficient of horizontally interlaced multilayer moored floating pipe breakwater (HIMMFPB). In this work, the



input variables that influence the  $K_t$  of HIMMFPB such as  $S/D$ ,  $W/L$ ,  $H_i/d$  and  $H_i/L$  were considered, and six ANFIS models were constructed. They developed four ANFIS models with  $W/L$ ,  $H_i/d$ ,  $H_i/L$  and  $K_t$  as input data with a first-order Sugeno model containing 27 rules and three generalized bell membership functions. The ANFIS5 model was developed including  $S/D$  ratio also as the input parameter with the structure using the first-order Sugeno model containing 81 rules and three generalized bell membership functions. The ANFIS6 model is similar to ANFIS5 model but does not consider  $H_i/L$  as the input parameter. With Principal Component Analysis (PCA) the most influencing parameter is found to be  $S/D$  and  $W/L$  whereas, the least influencing parameter was found to be  $H_i/L$ . Parameter variation study for ANFIS5 and ANFIS6 model were conducted. The various ANFIS model study concludes that  $S/D$  has a significant influence and  $H_i/L$  has no significant influence in the prediction of  $K_t$  of HIMMFPB. The study concludes that the ANFIS can serve as another approach to study the wave-structure interactions of HIMMFPB (Mandal et al. 2009; Patil et al. 2011).

Prediction of normalized scour depth at the head of the vertical wall breakwater using artificial neural networks (ANN) outperformed the existing empirical formulae. They found that ANN predicts well for dimensional input parameters compared to the non-dimensional input parameters. For the network with dimensional parameters, the inputs to the ANN network were the width of the breakwater head ( $B$ ), the wave angle of attack ( $\Phi$ ), wave period ( $T$ ), maximum current velocity ( $U_m$ ) and the network output was non-dimensional scour depth ( $S/B$ ). Implementing a forward perception three layers network with back propagation the prediction of scour depth around breakwaters were performed. Similarly, for a network with non-dimensional parameters, the network was trained with the dimensionless parameters of Reynolds number ( $Re$ ), Shields number ( $\theta$ ) and Keulegan-Carpenter number ( $KC$ ). Reynolds number  $Re = U_m B / \nu$ , where,  $U_m$  is the maximum current velocity,  $B$  is the width of the breakwater head  $\nu$  is the kinematic viscosity. Shields number,  $\theta = \tau_o / (\gamma_s - \gamma) d$  in which  $\tau_o$  is the shear stress,  $\gamma_s$  is the sediment unit weight,  $\gamma$  is the water unit weight,  $d$  is the sediment particle diameter. Keulegan-Carpenter number,  $KC = U_m T / B$ , and sediment Reynolds number ( $Re$ ). Based on a trial and error method the number of hidden layer neurons was taken

as three. A sensitivity analysis shows that the Keulegan - Carpenter number is the most influencing parameter in the scour process (Jabbari and Talebi, 2011).

An ANN model was developed to predict the reflection coefficient. The input parameters influencing the reflection coefficient were crest freeboard  $R_c$ , crest width  $B$ , seaward angle  $\alpha$ , the significant incident wave height  $H_i$  and peak period  $T_p$  or peak wavelength  $L_p$ . They considered three dimensionless parameters for the study as model inputs i.e., Iribarren number  $I_r$ , relative crest freeboard  $R_c/H_i$  and relative crest width  $k_p B$ , with  $k_p$  as wave number associated to the peak wavelength. The optimum architecture was arrived by evaluating the performance of each architecture. The results obtained from 400 different ANN models with ten different architectures were trained, tested and validated finally choosing the best architecture. They concluded that this model could be regarded as a virtual laboratory, replacing physical model tests in a conventional laboratory in determining the reflection coefficient (Castro et al. 2016).

The M5' model tree prediction of wave runup on rock slopes using Van der Meer experimental data was found to be better than the Van der Meer and Stam formula, Kingston and Murphy (1996) formula and Erdik and Savci's TS Fuzzy method (Etemad-Shahidi and Bonakdar 2009). Jafari and Etemad-shahidi (2012) using the M5' model tree successfully predicted the overtopping rate at rubble mound structures using a small CLASH database.

To predict the wave transmission of horizontally interlaced multilayer moored floating pipe breakwater (HIMMFPB) they developed a hybrid Genetic Algorithm tuned Support Vector Machine Regression (GA-SVMR). Interfacing the MATLAB SVM toolbox with a genetic algorithm, a better generalization of GA-SVMR model was achieved by optimizing the SVM and kernel parameters simultaneously. Six GA-SVMR models were developed using different kernel functions (with linear, polynomial, RBF, erbf, spline and b-spline kernels) for training. The first step is for GA to generate the initial population to identify optimum factors of kernel functions and SVMs. Next step is to perform an SVM process using the assigned value of the factors in the chromosomes and calculate the individual chromosome performance using

fitness function for GAs. Optimal parameters are selected if the calculated fitness value satisfies the terminal condition in GAs, if not apply the genetic operators to produce a new generation of the population. After which again perform the training process with the calculation of the fitness value. Repeat the process until a stopping condition is satisfied. With the completion in genetic search, chromosomes that show the best performance in the last population were selected as optimal SVMs and kernel parameters. These optimized parameters were tested with the test data. The GA-SVMR model with b-spline kernel function performed better than other five kernel functions for the given set of data. Also, it outperformed his earlier developed ANN and ANFIS models. Thus GA-SVMR could be taken as another approach to study the prediction performance of HIMMFPB (Patil et al. 2012).

Koç and Balas (2012) predicted the stability number of rubble mound breakwaters using FNN in the framework of multilayer feed-forward supervised neural networks with AND and OR fuzzy neurons optimizing its parameters with gradient descent algorithm. As the accuracy of the prediction was not appreciable, there was a need for improvement. An improvement over Balas fuzzy neural networks in the prediction of stability number of rubble mound breakwaters by structural and parametric optimization using HGA-FNN (hybrid genetic algorithm-based fuzzy neural network) was established for better stability assessments. Here two models were developed one the standard GA-FNN (genetic algorithm-based fuzzy neural network) and the other is HGA-FNN (hybrid genetic algorithm-based fuzzy neural network). The HGA-FNN is having an advantage over GA-FNN as it involves a local search method, with the hill climbing method used in the current study. In the case of both the models the training, validation and testing was done for the same data involving five inputs they are the permeability coefficient ( $P$ ), the damage level ( $S$ ), the number of waves ( $N$ ), the slope of the breakwater ( $\cot \theta$ ), and the surf similarity parameter ( $\epsilon_m$ ), to predict the only output the stability number ( $N_s$ ). The results show that the predictive performance of the HGA-FNN model is better than that of the GA-FNN model since it effectively combines local and global optimization. HGA-FNN has better prediction potential as it combines local and global search methods for stability assessments of rubble mound

breakwaters by simultaneously optimizing structures and weights.

Garrido and Medina 2012 developed a semi-empirical model based on a potential flow theoretical model which was modified with specific, empirical formulas to obtain a much better agreement with the experimental tests. Pruned neural network models with evolutionary strategies were used to identify the nonlinear relationships between the structural and wave attack parameters and the Jarlan-type breakwater reflectivity. The developed model was valid for regular as well as random waves on single and double-chamber Jarlan-type breakwaters estimating the reflection coefficient with an RMSE less than 10% with respect to observed values.

Wave reflection coefficient prediction by using ANN for a wide database with structures of straight and non-straight slopes, seawalls, caissons, and circular caissons, Acquareefs, and structures under wave attacks. The developed ANN model was trained by 13 non-dimensional input elements chosen based on a sensitivity test of ANN performance considering the extended input dataset (including wave and structure characteristics) and 40 hidden neurons. Uncertainty of predictions through the technique of bootstrap sampling is found to have the same error distributions as the ones obtained from the non-bootstrap sampling. The results show that the model has good stability. Prediction of wave reflection coefficient from coastal and harbor structures for a wide variety of wave conditions, structure geometry, and structure type is possible using Artificial Neural Networks (Zanuttigh et al. 2013).

The estimation of damage of breakwater armor blocks can be better by considering tidal level variation. The study revealed that the expected damage increased with the increase in the tidal level when compared with a constant tidal level. Here a shallow water wave height prediction artificial neural network (ANN) model was developed using offshore wave height and estimated the breakwater damage incorporating tidal level variation near shore. This reduced the total analysis time in estimating the breakwater damage of armor blocks and also allows it to apply a random simulation method such as Monte Carlo simulation (MCS) to estimate the damage using deep sea wave distribution. The

ANN predicted waves were compared with that from a wave transformation analysis. The study shows that by assuming tidal level constant at HWL, the damage of breakwater armor blocks is overestimated hence the tidal level variation should be incorporated (Kim et al. 2014).

MATLAB-based regression is used to determine the wave transmission coefficient of a quarter-circular breakwater (QBW). Here the wave transmission coefficient ( $K_t$ ) is established as a dependent variable on the independent non-dimensional parameters  $H_i/d$  (relative wave height),  $H_i/gT^2$  (incident wave steepness parameter), and  $h_c/H_i$  (relative freeboard). The relation established between the two using a MATLAB-based regression and the accuracy was assessed on some statistical parameters. Noise removal of the collected experimental data performed for accurate prediction of the ANN model, where the data with more than  $\pm 15\%$  in MSE and relative error were removed. The refined set of data were further subjected to regression in MATLAB, and a new model is obtained for the wave transmission coefficient ( $K_t$ ) whose accuracy improved significantly. The author further applied ANN for the same problem. The predominant input variables influencing the performance and stability of quarter-circular breakwaters (QBW) are  $H_i/d$  (relative wave height),  $H_i/gT^2$  (incident wave steepness parameter), and  $h_c/H_i$  (relative freeboard), while the transmission coefficient  $K_t$  is considered as the output variable to train the ANN. Using the Levenberg–Marquardt method of backpropagation, an ANN model is developed to predict the  $K_t$  of QBW. The predicted wave transmission coefficient using ANN was found to be better than that of MATLAB-based multiple regression. The study concludes ANN was a better approach in the prediction of wave transmission (Goyal et al. 2014; Goyal et al. 2015).

Nikoo et al. (2014) arrived at the optimum of double-layer perforated-wall breakwaters (DLPW) based on data-driven simulation modeling, multi-objective optimization, and game theory. The DLPW breakwaters are employed to achieve a reduction in wave reflection and maximize the wave transmission to acceptable limits. Using the experimental data of DLPW, two ANFIS models were developed to predict the performance of DLPW breakwater and it is further linked with NSGA-II multi-

objective optimization model to arrive at the optimum dimensions of DLPW breakwater.

ANN models can predict the reflection coefficient ( $K_r$ ) of the emerged perforated quarter circular breakwater (EPQCB) for beyond the range data of the wave period ( $T$ ) used for training. Here the prediction of reflection coefficient ( $K_r$ ) for two modes of data was done, i.e., dimensional as well as non-dimensional. The input parameters used in the case of dimensional mode are water depth ( $d$ ), wave height ( $H$ ), structure height ( $h_s$ ), spacing ( $S$ ), Diameter ( $D$ ) and radius ( $R$ ). The input parameters used in the case of non-dimensional input parameters are wave steepness  $H_i/gT^2$ , depth parameter  $d/gT^2$ , spacing-perforation ratio  $S/D$ , relative wave run-up  $R/H_i$  and relative water depth  $h_s/d$ . The results show that the prediction of reflection coefficient ( $K_r$ ) of emerged perforated quarter circular breakwater using ANN with dimensional input parameters gave better accuracy than the non-dimensional input parameters (Raju et al. 2015).

The damage level prediction of non-reshaped berm breakwaters was done successfully using GA-SVM models which improved the performance of SVM models (Narayana et al. 2014). Soft computing techniques are an alternative to physical and mathematical model study to determine the damage level of a non-reshaped berm breakwater which is complex and non-linear. In the damage analysis input parameters that influence the damage level ( $S$ ) of non-reshaped berm breakwater are used as inputs, such as wave steepness ( $H/L_o$ ), surf similarity, relative berm position by water depth ( $h_B/d$ ), armor stone weight ( $W_{50}/W_{50max}$ ), relative berm width ( $B/L_o$ ), and relative berm location ( $h_B/L_o$ ). The proposed model optimizes SVMs and kernel parameters simultaneously and predicts damage level. The PSO-SVM model with polynomial kernel function predicted better than the other SVM models (Harish et al. 2015).

The armor stone weight required for a particular site condition for a particular wave height range is determined based on the stability number which will indicate how stable the armor stone is. To estimate this stability number, it is important to know the relation between the stability number and other parameters which are related to waves and

structure. Hence using Principal component analysis, a variable selection method, the influence of variables unused in the previous studies were considered, and research was carried out. Here a hybrid model of ANN with PCA is developed for estimating the stability number of rock armor using the experimental datasets of Van der Meer (1988). The experimental data had 11 input parameters of which grouping six as Group 1 with well-distributed values and the remaining five as another group, i.e., Group 2 which varies amongst only a few values. Transforming Group 1 parameters into six PC's using PCA, all the parameters were trained to ANN. The sixth PC obtained here had zero percent of the total variance. But the results obtained by including all PC's were better compared to that by excluding the sixth PC. Finally, six PC's of Group 1 and five parameters directly from Group 2 as the input variables, trained to ANN model. This hybrid ANN with PCA model outperformed the previous empirical and ANN models (Lee et al. 2015).

The construction of a berm breakwater and further allowing it to reshape subjecting to storms to achieve a stable profile rather than constructing a reshaped berm breakwater directly is found more economical as it requires smaller size armor stones. However, the study of the stability of such breakwaters is important. The input variables are wave height, wave period, water depth, berm width, berm position from the sea bed, the slope of the breakwater, the nominal dimension of armor unit and storm duration. Whereas, the output variable was the failure of the breakwater regarding berm recession. The dimensionless parameters obtained by performing a dimensional analysis on these variables are stability Number  $H/\Delta D$ , wave steepness  $H/gT^2$ , storm duration  $N$ , relative berm position  $h_b/d$ , relative berm width  $B/d$ , number of primary layers  $N$ , breakwater slope  $\cot\alpha$  and relative berm recession  $R_{ec}/D_{n50}$ . A Principal Component Regression (PCR) was performed using Xlstat® software with all the seven input parameters of which stability Number  $H/\Delta D$ , wave steepness  $H/gT^2$ , relative berm position  $h_b/d$  and relative berm width  $B/d$  had high factor loadings above 0.6. Subjecting these four parameters to a PCR analysis, the loadings of all the four parameters were found to be greater than 0.70 and found to be important. Even with the reduction of three parameters, the decrease in  $R^2$  and RMSE was insignificant. The reason for the

elimination of these parameters is because the variation of storm duration and number of primary layers was not high and breakwater slope was a constant which did not vary the output significantly. Principal Component Regression (PCR) analysis is a very effective tool in reducing the number of input parameters. The damage level of Reshaped berm breakwater can be well estimated by knowing the most influencing input variables on the output (Janardhan et al. 2015).

Stability assessment of a rubble-mound breakwater has been attempted here by applying Genetic programming (GP) models to explore the explicit relationship between the stability number of armor blocks and influencing variables. He developed four GP models called GPM1, GPM2, GPM3, and GPM4. The GPM1 and GPM2 models were developed using the training subsets Type 1 (579 data sets) and Type 2 (62 data sets) respectively, of Van Der Meer experiments with function F1. Similarly, GPM3 and GPM4 models were developed using the training subsets Type 1 (579 data sets) and Type 2 (62 data sets) respectively, of Van Der Meer experiments with function F2. The F2 function had more function operators compared to F1. Comparing the measured stability numbers of Van der Meer (1988) with the predictions done by the four GP models, GPM3 and GPM4 models produced lower values of SI, MAPE, and RMSE with respect to GPM1 and GPM2 models. Genetic programming (GP), the method found to have better prediction performance compared to the Van der Meer's stability equations of rubble-mound breakwaters. Genetic programming can capture complex real-world relationships effectively with a limit on the parse tree size to control the bloating of GP (Koç et al. 2016).

Ghasemi et al. 2016 evaluated the wave transmission coefficient ( $K_t$ ) for floating breakwaters (FBs) of  $\pi$ -type. FBs are designed to reduce wave energy hence  $K_t$  is an important aspect of the design. A new hybrid artificial neural network (ANN) model developed for predicting  $K_t$  of  $\pi$ -type FB, combines particle swarm optimization (PSO) and Levenberg-Marquardt (LM) for learning of ANN. Experimental data sets were obtained for  $\pi$ -type FB from a wave basin of the University of a Coruña, Spain. The performance of the proposed model in comparison with the efficiency of the existing



formulas cited in the literature is high.

Pourzangbar et al. 2017b predicted the maximum scour depth at breakwaters due to non-breaking waves using Genetic Programming (GP) and Artificial Neural Networks (ANNs). The study shows that GP outperformed ANN and also the existing formulas to predict the scour depth. They found that the reflection coefficient largely influenced scour depth. Similar prediction using M5' model and the SVR models of maximum scour depth at breakwaters due to non-breaking waves were predicted well by M5' model compared to the SVR model.

Kuntoji et al. (2018) predicted the wave transmission over a submerged reef of the tandem breakwater using soft computing techniques like PSO-ANN and PSO-SVM. They found that the PSO-SVM tool outperforms PSO-ANN in predicting wave transmission.

### **2.3 SUMMARY OF LITERATURE**

With the several advantages over conventional breakwaters, the semicircular breakwater is an area of interest for research. The study of performance characteristics of a semicircular breakwater is essential before deploying the structure in the sea. From the detailed literature review, it is found that not many studies were done on emerged semicircular breakwaters. The harbor tranquility can be maintained and terminal efficiency can be improved by reducing the wave reflection from the breakwater. The wave reflection coefficient is a key aspect in the assessment of breakwater and very few studies have been reported on the estimation of wave reflection performance of caisson structures like semicircular breakwaters. There is no fair amount of research in accurately estimating the  $K_r$  of these breakwaters. Although the physical model studies are reliable not many studies have been carried out on emerged seaside perforated semicircular breakwaters.

Wave run-up is one of the most important physical process which is studied to design the breakwater height and crest level of semicircular breakwaters or as an indicator of

possible overtopping or wave transmission (Arunjith et al., 2013; Shankar and Jayaratne, 2003). It mainly depends on the structure shape, roughness, porosity, depth of water at the structure toe, bottom slope in front of the structure and incident wave characteristics (US Army Corps of Engineers, 2002). The run-up is an important factor to be considered for the stability of the structure as run-up level influences the inflow of water into the structure and the elevation of water level within the structure core causing differential hydrostatic pressures. There is no sufficient literature regarding the wave run-up estimation of the emerged seaside perforated semicircular breakwater.

As the pressure on a semicircular wall acts towards the center of the circle, these breakwaters generally have smaller horizontal force, lesser overturning moment and minimum soil subgrade reaction resulting in better stability and lesser cost in comparison with vertical breakwaters. However, it is important to find the sliding stability of semicircular breakwaters. Not many experimental studies nor any prediction techniques is found in this regard in the literature for the emerged seaside perforated semicircular breakwater.

The literature on the efficiency of prediction of hydraulic response of different coastal structures using different soft computing techniques is quite promising, in spite of the data complexity, incompleteness, and incoherence. The application of techniques like ANN, ANFIS, GA, PSO, SVM, etc., individually or combined to various coastal engineering problems is found in the literature. To name a few the optimization of breakwater dimensions using the response of the structure, prediction of stability number, prediction of damage ratio, prediction of relative runup, prediction of reflection coefficient for different types of breakwaters is found in the literature. However, no study focusses on prediction when an insufficient quantity of data is available (i.e., when data is not available for all ranges of wave height). Any physical and numerical model studies of these structures are complex, expensive and time-consuming. Hence, there is a need for further research to arrive at an alternative to overcome the shortcomings of past research. These soft computing techniques can be adopted as an alternate technique to predict the hydraulic response of semicircular breakwaters by coastal engineers when similar site conditions are available. In this regard the current study is taken up.

## **2.4 PROBLEM IDENTIFICATION**

Selection of a particular type of breakwater depends on various factors like environmental aspects, utilization, construction cost, layout, available construction materials, maintenance cost involved, etc. However, among the various types of breakwaters, semicircular breakwaters are becoming popular these days, because of its numerous advantages like better aesthetics, low construction cost, the requirement of lesser construction material, its applicability to soft foundations and a broad range of water depths, high stability against sliding and overturning. Hence, research on SBW is gaining momentum of late. The scaled down physical model studies of the semicircular breakwater could be carried out in wave flumes or basins in order to know the prototype performance characteristics under different wave conditions. However, physical modeling of SBW is expensive, time-consuming and demands a lot of efforts. In order to overcome this problem and achieve greater accuracy, a better scale may be adopted, but this process is enormously expensive. Numerical models could be used to evaluate the performance of the same, but the limitation here is complex hydrodynamics of fluid-structure interaction, which is rather difficult to be modeled in a numerical model. Hence, researchers have applied Artificial Intelligence to assess the hydrodynamic performance of breakwaters, however, they cannot replace the physical models as they are data-driven. These soft computing models developed for breakwaters are specific to the site and it can be employed when experimental data is available for similar site conditions where a new semicircular breakwater is to be designed. Only a limited study is found in the literature in the area of SBW, the present work aims to apply soft computing techniques in the prediction of hydraulic response, particularly of the emerged seaside perforated semicircular breakwater.

Many times, there is a need to predict the performance of semicircular breakwater for parameters, beyond the range of training data set used for soft computing predictions. This is because of the higher expenditure involved in the physical modeling of the semicircular breakwater for larger wave parameters, like greater wave heights, large water depths, large radii of the breakwater, etc. Similarly, in the case of very small wave height, smaller water depths and small radii values. An attempt has been made in

the present work to predict the performance of semicircular breakwater for below and beyond the range of data used for soft computing model techniques. All of the data used in the present work is obtained from physical model experiments conducted in a monochromatic wave flume at the Marine Structures Laboratory of the Department of Applied Mechanics and Hydraulics, NITK, Surathkal (Nishanth 2008; Sooraj 2009; Vishal 2010; Sreejith 2015 and Surakshitha, 2017).

## **2.5 RESEARCH OBJECTIVES**

Based on the research gaps mentioned above, the following objectives are framed:

1. To predict the wave reflection coefficient ( $K_r$ ) of emerged seaside perforated non-overtopping semicircular breakwater by conventional, below and beyond the data range approach for dimensional as well as non-dimensional input parameters using ANN, ANFIS, GA-ANFIS, and PSO-ANFIS.
2. To predict the relative wave runup parameter ( $R_u/H_i$ ) of emerged seaside perforated non-overtopping semicircular breakwater by conventional, below and beyond the data range approach for dimensional as well as non-dimensional input parameters using ANN, ANFIS, GA-ANFIS, and PSO-ANFIS.
3. To predict the stability parameter ( $W/\gamma H_i^2$ ) of emerged seaside perforated non-overtopping semicircular breakwater by conventional approach for dimensional as well as non-dimensional input parameters using ANN, ANFIS, GA-ANFIS, and PSO-ANFIS.



## **CHAPTER 3**

### **MATERIALS AND METHODS**

This chapter presents the experimental setup from which the data is acquired and the details of soft computing techniques.

### **3.1 MATERIALS AND METHODS**

#### **3.1.1 Data used**

As mentioned earlier the experimental data is collected from physical model experiments on emerged perforated semicircular breakwater (EPSBW) carried out using the monochromatic wave flume in the Marine Structures Laboratory of the Department of Applied Mechanics and Hydraulics, NITK, Surathkal. The experimental setup used in the laboratory is as shown in Fig. 3.1. The wave climate of Mangaluru coast as given by Dattatri and KREC study team (1994) were considered for selecting the input wave parameters. The largest single wave recorded off the Mangaluru coast was found to be 5.4 m. The predominant wave period during the monsoon season is 9 to 10 s, while longer period waves are experienced in the fair weather season. In the non-monsoon months (October to May), the maximum wave heights are less than 1m in height. The tides at Mangalore are semi-diurnal type. The tidal range in the area is about 1.68 m. Hence, in the present investigations, wave heights in the range of 1.0 m to 5.4 m and wave periods in the range of 6 to 12 s are considered for modeling. Incident wave heights used in the flume varied from 3 to 20 cm, wave periods ranged from 1.4 s to 2.5 s, water depths used were 35 cm, 40 cm, 45 cm, and 50 cm and the model scale was 1:30.

#### **3.1.2 Wave flume used**

The basic dimensions of wave flume used are length 50 m, width 0.71 m and depth 1.1 m. About 15 m length of the flume is provided with glass panels on one side. It has a 6.3 m long, 1.5 m wide and 1.4 m deep chamber at one end where the bottom hinged flap generates waves. The flap is controlled by an induction motor of 11 KW, 1450 rpm. This motor is regulated by an inverter drive, with the frequency of 0-50 Hz and rotating with a speed range of 0-155 rpm. This facility can generate regular waves of heights 0.08 m to 0.24 m and of periods 0.8 s to 4 s. A series of vertical asbestos sheets are spaced at

about 10 cm distance from each other and kept parallel to the length of the flume to dissipate the generated waves by damping the disturbance caused by successive reflection and to smoothen them. The calibrations of the wave flume and probes were done prior to conducting the experiments.

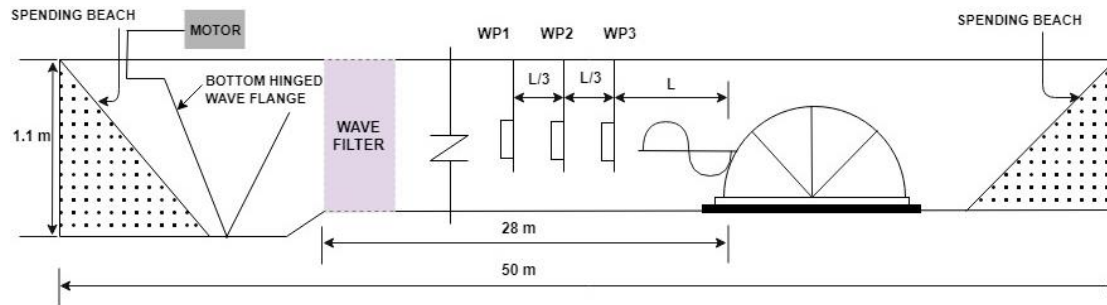


Fig. 3.1 Experimental Setup of wave flume (Not to scale)

The data for the current study is obtained from the experiments conducted in a monochromatic wave flume at the Marine structures laboratory, NITK, Surathkal. The experimental parameter ranges for prediction of reflection coefficient ( $K_r$ ) is as shown in the Table 3.1. Table 3.2 shows the experimental parameter ranges for prediction of relative wave run-up parameter ( $R_u/H_i$ ) and Table 3.3 shows the experimental parameter ranges for prediction of stability parameter ( $W/\gamma H_i^2$ ).

**Table 3.1 Experimental parameter ranges for  $K_r$  prediction**

<b>Input parameters</b>	<b>Data Range</b>
Incident wave height, $H_i$ (m)	0.06 -0.18
Wave period, $T$ (s)	1.2– 2.6
Depth of water, $d$ (m)	0.35, 0.40, 0.45, 0.50
Radius of the semicircular caisson, $R$ (m)	0.45, 0.60
Perforation spacing, $S$ (m)	0.032, 0.048, 0.064, 0.096, 0.128,
Perforation diameter, $D$ (m)	0.012, 0.016
<b>Structure-specific parameters</b>	
SBW structure height $h_s$ (m)	0.502, 0.652, 0.730

**Table 3.2 Experimental parameter ranges for  $R_w/H_i$  prediction**

<b>Input parameters</b>	<b>Data Range</b>
Incident wave height, $H_i$ (m)	0.06 -0.18
Wave period, $T$ (s)	1.2– 2.6
Depth of water, $d$ (m)	0.35, 0.40, 0.45, 0.50
Radius of the semicircular caisson, $R$ (m)	0.45, 0.60, 0.75
Perforation spacing, $S$ (m)	0.032, 0.048, 0.064, 0.096, 0.128,
Perforation diameter, $D$ (m)	0.012, 0.016
<b>Structure-specific parameters</b>	
SBW structure height $h_s$ (m)	0.502, 0.652, 0.730, 0.802

**Table 3.3 Experimental parameter ranges for prediction of  $W/\gamma H_i^2$** 

<b>Input parameters</b>	<b>Data Range</b>
Incident wave height, $H_i$ (m)	0.06 -0.18
Wave period, $T$ (s)	1.4– 2.6
Depth of water, $d$ (m)	0.35, 0.45
Radius of the semicircular caisson, $R$ (m)	0.45, 0.60, 0.75
Perforation spacing, $S$ (m)	0.032, 0.064, 0.128,
Perforation diameter, $D$ (m)	0.016
<b>Structure-specific parameters</b>	
SBW structure height $h_s$ (m)	0.502, 0.652, 0.802



### 3.1.3 Normalization of the data and consistency check

The wave parameters obtained from the experiments are normalized to (0, 1). The normalization is done by using Equation 3.1 before feeding to the network. This is done to bring all the input variables in a common range so that the network gets trained without being hindered by the effect of very high or very low values. However, in the current study, the variation of the ranges of the input and target values are not large.

$$Z_i = \frac{x_i - \min(x_i)}{\max(x_i) - \min(x_i)} \quad (3.1)$$

Where,

$Z_i$  - is the normalized data for the  $i^{\text{th}}$  variable between 0 to 1,

$x_i$ - is the data point  $i^{\text{th}}$  variable,

$\max(x_i)$ - is the maximum amongst all the data points of  $i^{\text{th}}$  variable,

$\min(x_i)$ - is the minimum amongst all the data points of  $i^{\text{th}}$  variable.

The consistency of the data is as shown in Fig. 3.2, Fig 3.2 and Fig. 3.3

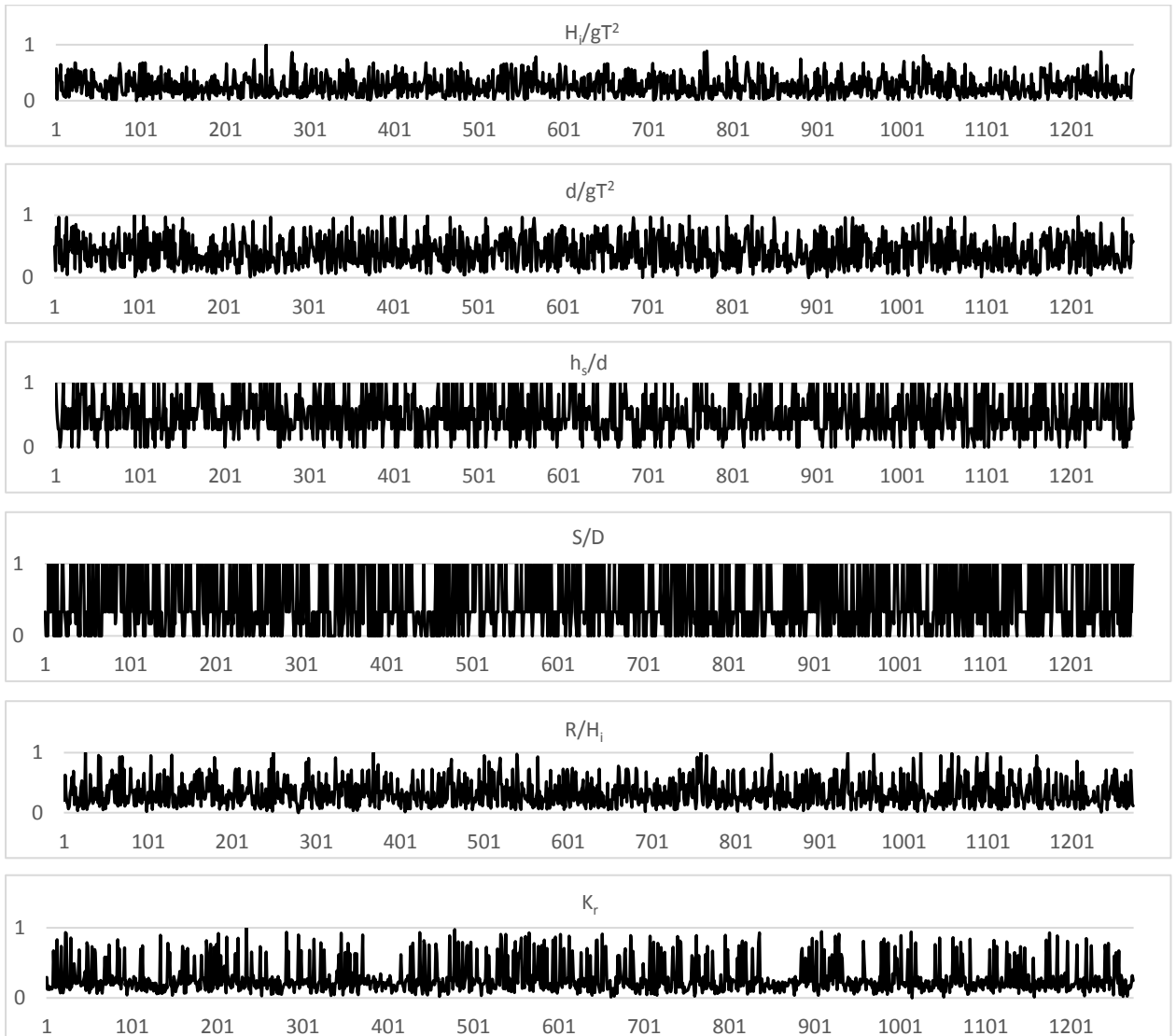


**Fig. 3.2 Data consistency of input parameters  $H_i/gT^2$ ,  $d/gT^2$ ,  $h_s/d$ ,  $S/D$ ,  $R/H_i$ ,  $K_r$ , in the case of reflection coefficient prediction**

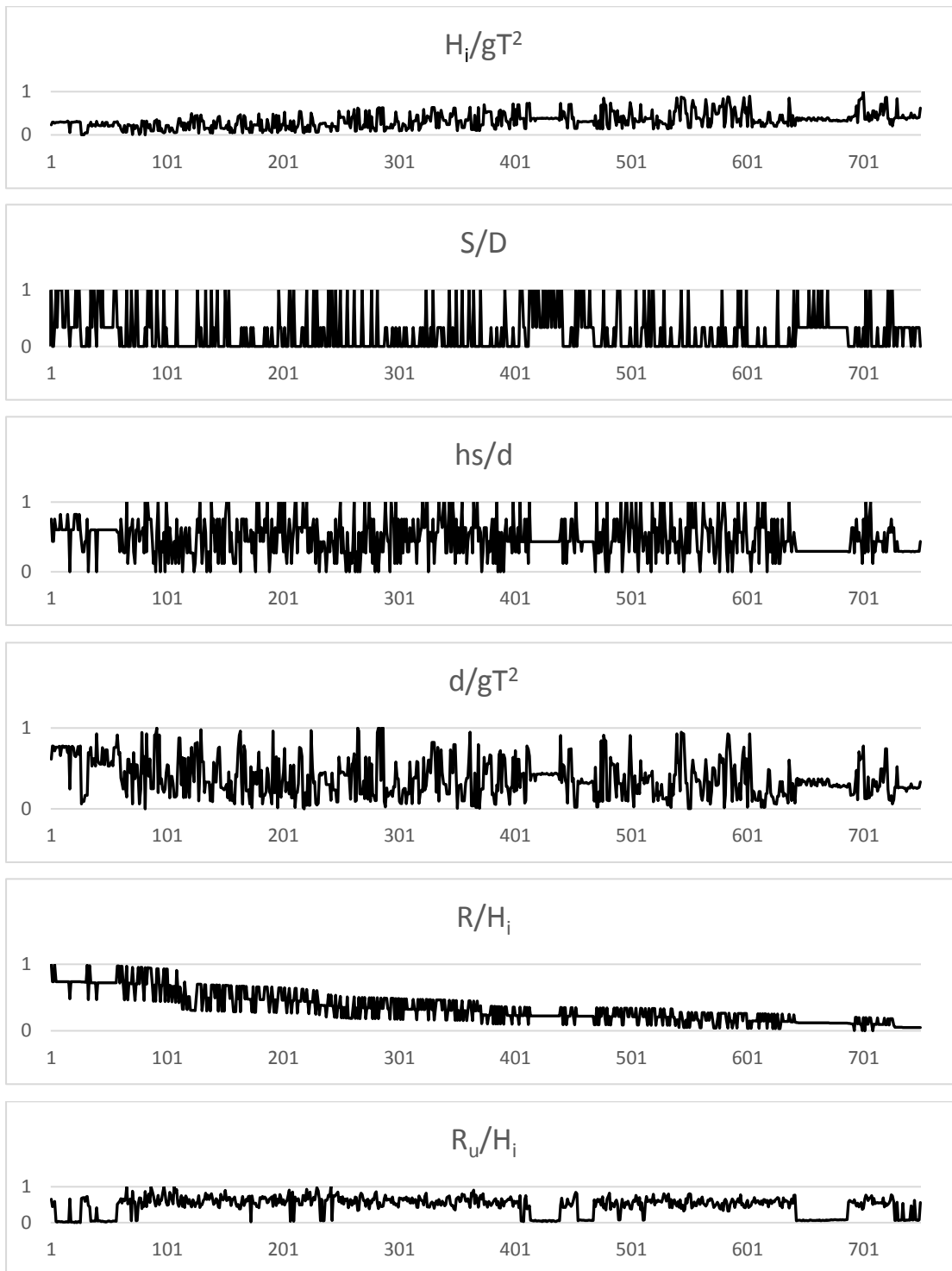


**Fig. 3.3 Data consistency of input parameters  $H_i/gT^2$ ,  $d/gT^2$ ,  $h_s/d$ ,  $S/D$ ,  $R/H_i$ ,  $R_u/H_i$ , in the case of relative wave run-up parameter prediction**

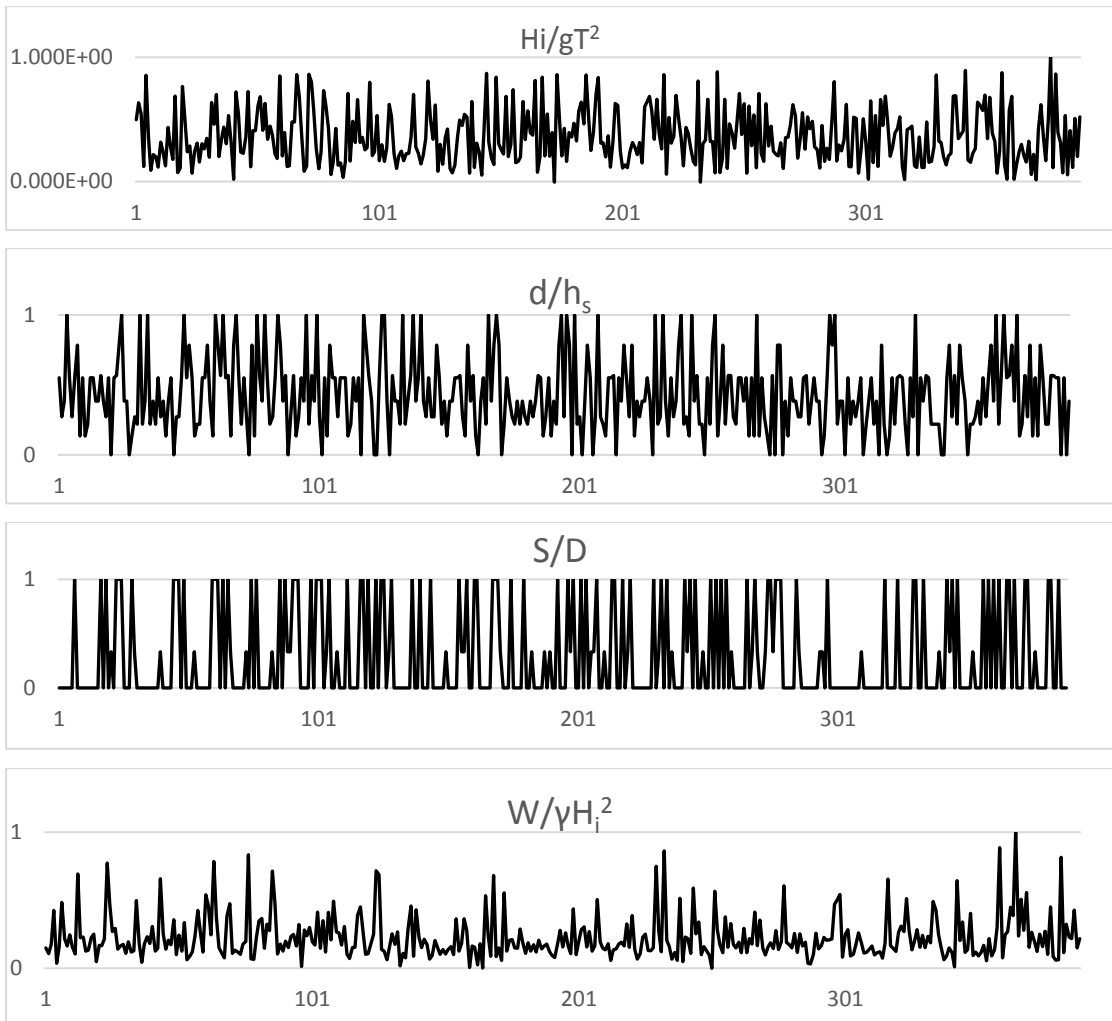


**Fig. 3.4 Data consistency of input parameters  $H_i/gT^2$ ,  $d/h_s$ ,  $S/D$ ,  $W/gH_i^2$ , in the case of stability parameter prediction**

### 3.2 METHODOLOGY FLOWCHART

The flowchart presented in Fig. 3.5 is adopted in order to achieve the objectives set in the research work.

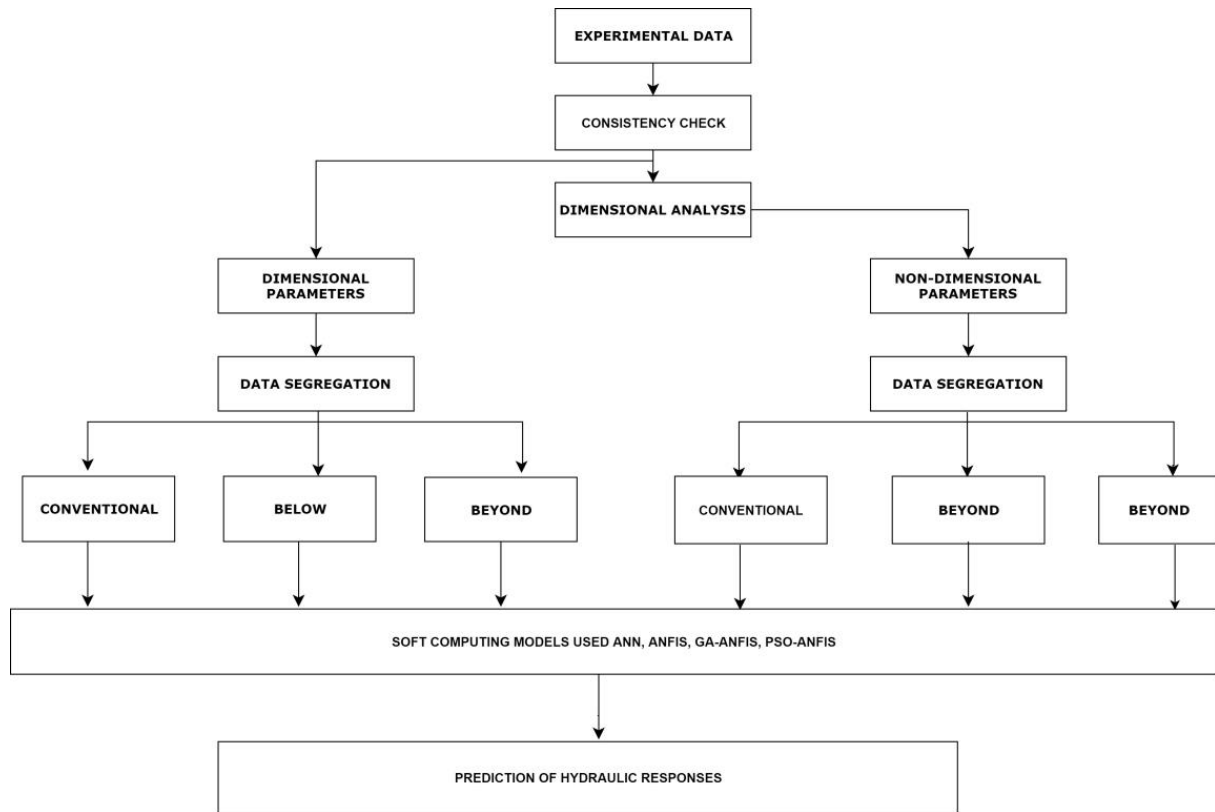


**Fig. 3.5 Flowchart of Methodology**

### 3.3 PHYSICAL EXPLANATION OF PREDICTION VARIABLES OF SEMICIRCULAR BREAKWATERS UNDER STUDY

#### 3.3.1 Reflection coefficient

When a vertical barrier such as a sea wall can reflect wave back into the ocean with little loss of energy, this process is called wave reflection. Reflected waves can make disturbances and intensify sediment scour, which can lead to dramatic loss in beach material and structure destabilization. The reflection coefficient provides an index for designing a slope of seaward face and an installed position of the structure. For an emerged non overtopping structure incident wave hits the surface with a wave height ( $H_i$ ) and some amount of energy is reflected back. Reflection of a wave from a barrier occurs at an angle

equal to the angle of approach to the barrier. Reflection coefficient ( $K_r$ ) depends upon incident wave condition, still water level and structural parameters like roughness, porosity, slope, etc.

Reflection coefficient ( $K_r$ ) increases with increase in wave steepness because in short period waves, the quantum of energy dissipated is less and hence reflection will be more. Also it is found that as depth parameter increases the value of reflection coefficient found to be decreased. This is because for smaller water depths, waves encounter more plane (relatively vertical) surface and as water depth increases the effect of curvature is more pronounced causing more energy dissipation hence less reflection. The increase in percentage of perforations creates more turbulence inside the chamber and dissipates more energy, hence the reflection coefficient decreases.

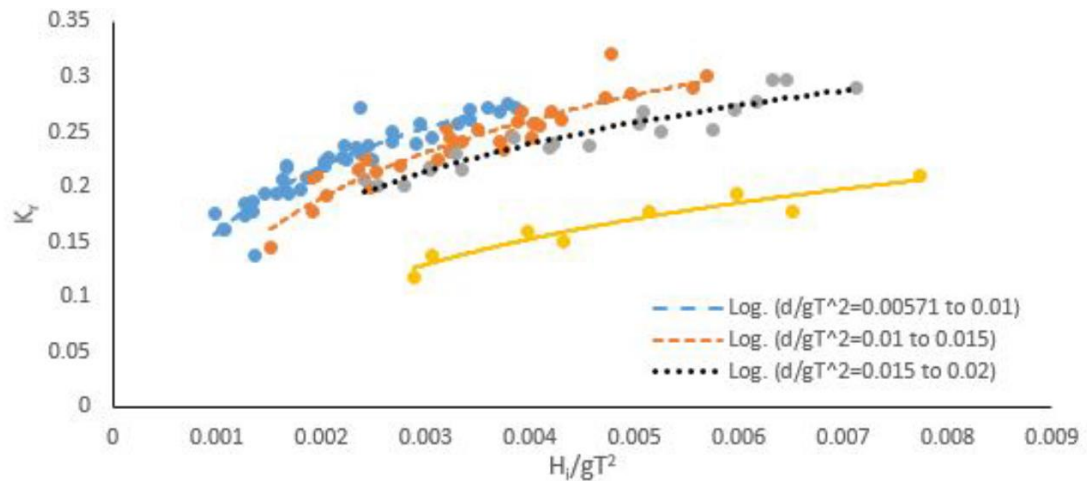


**Fig. 3.6 Variation of reflection coefficient with incident wave steepness and depth parameter for a constant  $R/h_t$  of 0.92 for a perforated SBW model with  $S/D$  ratio of 4**

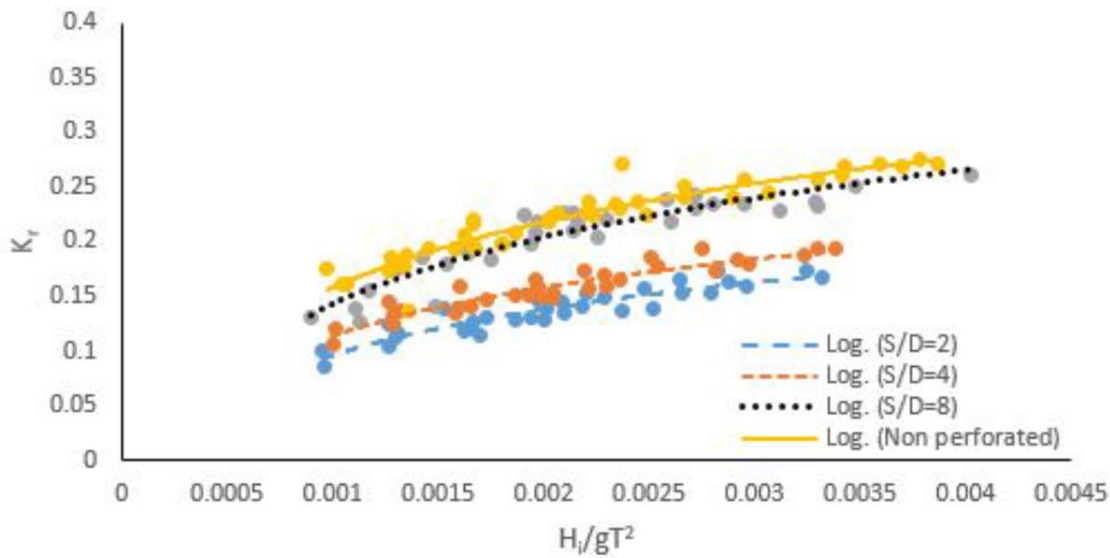


**Fig. 3.7 Influence of perforations on reflection coefficient for depth parameter of 0.01 to 0.015 and a constant  $R/h_t$  of 0.92.**

### 3.3.2 Relative runup parameter

As the wave steepness increases there is an increase in the relative runup ( $R_u/H_i$ ). This is obvious that as wave height increases, the runup also increases. It is observed that for larger wave periods the runup is more. Runup is also one of the ways of dissipation of energy. As the wave height increases there is an increase in wave energy, therefore the runup is more. The relative wave runup ( $R_u/H_i$ ) decreases with the increase in depth parameter ( $d/gT^2$ ) due to the effect of curvature. This is because as  $d/gT^2$  increases, the effect of curvature is more pronounced and hence more dissipation of energy takes place, resulting in less runup. It must also be noted that for short period waves, lesser runup happens resulting in less energy loss and higher reflection.

Since for smaller depths the radius of curvature is large, the surface almost vertical and hence there is an increase in water level at the model and if the percentage of perforations encountered is also less, then more runup. As the depth increases the radius of curvature is small thus the contact surface is more resulting in greater percolation, and if the percentage of perforations encountered is more than the there is decrease in wave runup.

Also as the S/D ratio decreases and percentage of perforation increases, there is a decrease in relative wave runup. It is obvious that as the percentage of perforation increases there is a large amount of energy loss, resulting in decrease in wave runup. Wave run-up is found to be decreasing with increase in the percentage of perforations. The increase in percentage

of perforations creates more turbulence inside the chamber and dissipates more energy, hence the run-up decreases.

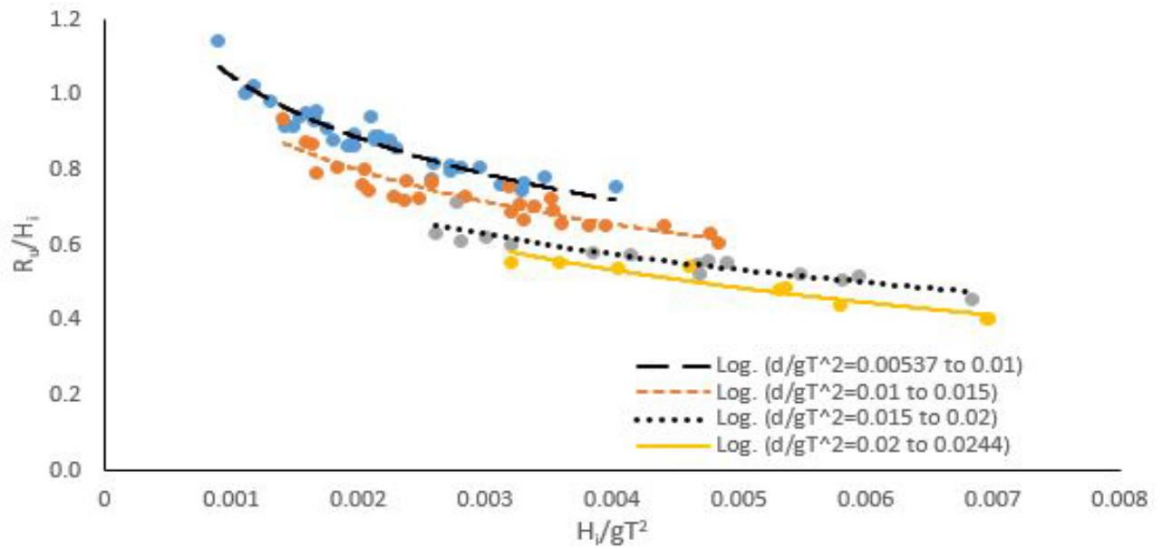


**Fig. 3.8** Variation of relative runup parameter with incident wave steepness and depth parameter for a constant  $R/h_t$  of 0.92 for a perforated SBW model with  $S/D$  ratio of 8

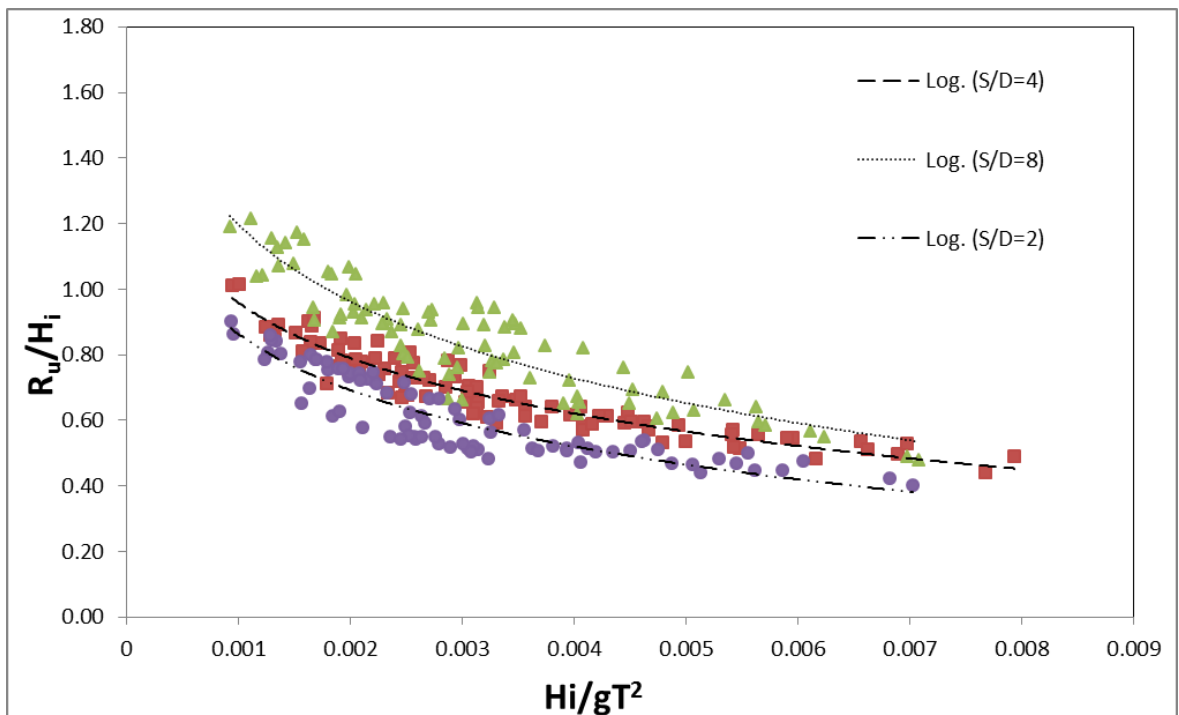


**Fig. 3.9** Influence of perforations on relative runup for depth parameter of 0.00572 to and a constant  $R/h_t$  of 0.92



### 3.3.3 Stability parameter

The stability parameter ( $W/\gamma H_i^2$ ) decreases as the incident wave steepness increases. This is because long period waves exert more force on the caisson while the short period waves will transfer less force. The sliding disturbance caused by the increased force is stabilized by increasing normal force i.e., by increasing the weight of the breakwater. It is also found that as the depth parameter  $d/gT^2$  increases, the  $W/\gamma H_i^2$  also increases. This is because higher the water depth, the greater the area of the SBW model exposed to wave action hence the increase in  $d/gT^2$  imparts more force, hence  $W/\gamma H_i^2$  increases.

The  $W/\gamma H_i^2$  decreases with the increase in percentage of perforations, due to the fact that the increase in percentage of perforations on the seaside of the SBW model generates more turbulence inside the chamber which produces more energy dissipation. Increase in percentage of perforation generates less force of impact on the SBW caisson hence the critical weight required to resist sliding found to be reduced.

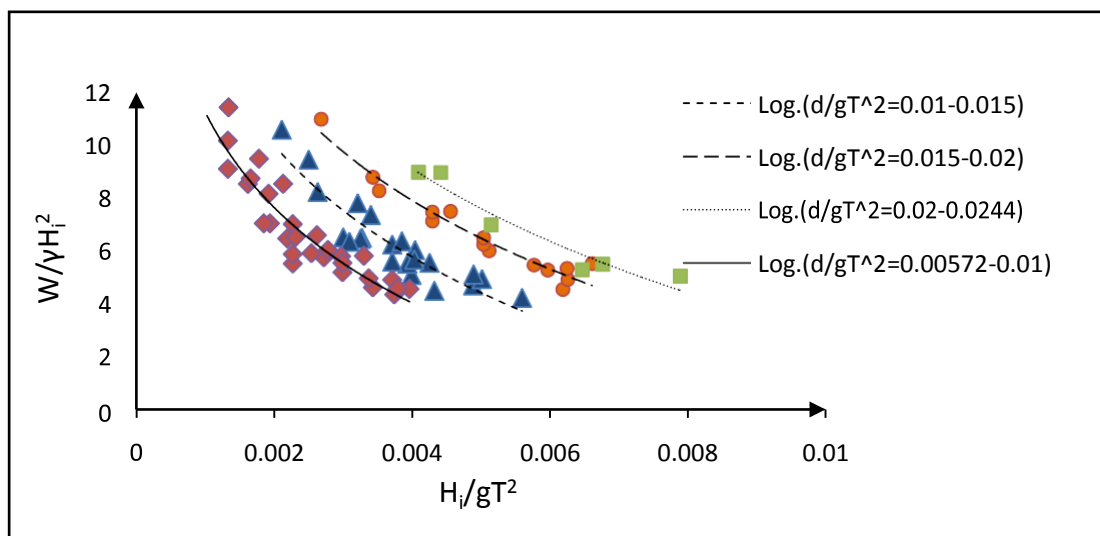


**Fig. 3.10** Variation of stability parameter with incident wave steepness and depth parameter for a constant  $R/h_t$  of 0.92 for a perforated SBW model with  $S/D$  ratio of 8

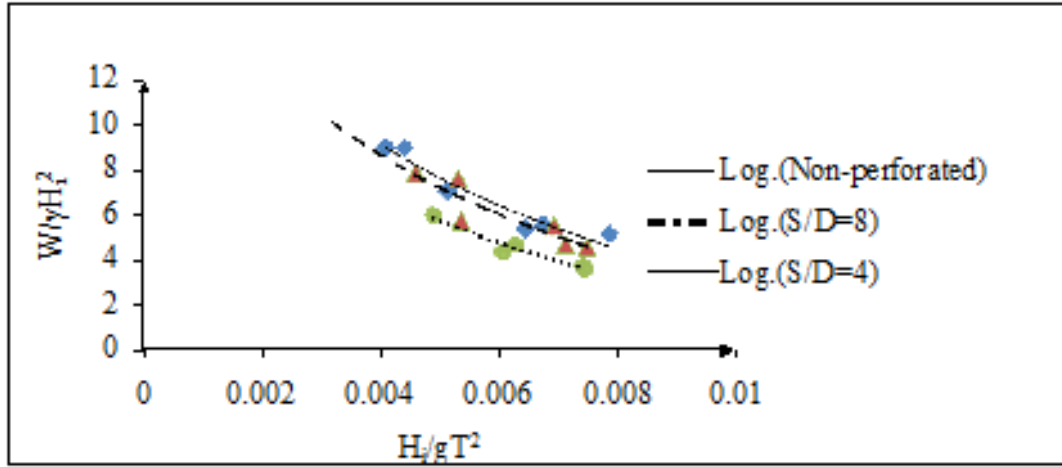


**Fig. 3.11 Influence of perforations on stability parameter with incident wave steepness**

### 3.4 DEVELOPMENT OF ANN MODEL

The basic structure of ANN has an input, a hidden and an output layer. ANN learns from the training of the input-output pairs and regulates the connection weight values in the hidden layer and bias (Azamathulla et al. 2011). A Feed Forward Back Propagation Neural Network (FFBPNN) as seen in Fig. 3.6 is used for training the input-output data sets using a Levenberg-Marquardt algorithm with transfer functions like 'tansig' (hidden layer) and 'purelin' (output layer). In a Feed Forward Back Propagation Neural Network, the error is propagated back in a direction opposite to the way activities propagate in a network.

The FFBPNN is mathematically expressed as,

$$Z_k(x) = \sum_{j=1}^m W_{kj} \times T_r(y) + b_{ko} \quad (3.2)$$

$$y_j = \sum_{i=1}^n W_{ji} \times x_i + b_{ji} \quad (3.3)$$

Wherein,  $x$  is input values from 1 to  $n$ , hidden layer neurons are  $y_j$ .  $W_{ji}$  and  $W_{kj}$  are the weights between input and hidden layer and weights between hidden and output layer

respectively. Also,  $b_{ji}$  and  $b_{ko}$  are biased at the hidden and output layer respectively. Number of hidden layer nodes are  $m$  and  $T_r(y)$  is the transfer function. A non-linear conversion of summed inputs is possible with this transfer function  $T_r(y)$ . This is done by tansig when employed between the input and hidden nodes and is expressed as,

$$T_r(y) = \left[ \frac{2}{1 + \exp(-2 \times y)} - 1 \right] \quad (3.4)$$

y- summation of input values with weights and biases

The transfer function increases the generalization capability of the network and expedites the learning process convergence. In every iteration, the bias adjustments for both hidden and output layer happens. The updated Levenberg-Marquardt algorithm calculates the weights between the hidden and output layer. Purelin a linear transfer function employed between hidden and output layer and is expressed as,

$$\text{Purelin}(n) = n \quad (3.5)$$

The objective of the algorithm is to reduce the global error,  $E$  is defined as,

$$E = \frac{1}{P} \sum_{p=1}^P \left[ \sum_{k=1}^K (d_{kp} - o_{kp})^2 \right] \quad (3.6)$$

Wherein, a total number of training patterns is  $p$ , the desired value of the  $k^{\text{th}}$  output and the  $p^{\text{th}}$  pattern is  $d_{kp}$  and  $o_{kp}$  the actual value of the  $k^{\text{th}}$  output and  $p^{\text{th}}$  pattern.

Literature supports the fact that a single hidden layer is sufficient to solve most of the nonlinear problems and the number of neurons in each layer is determined by trial and error method (Erdik et al. 2009; Karsoliya 2012; Panchal and Panchal 2014). In the current study, several ANNs were trained altering the number of neurons in the hidden layer. The network with the highest correlation coefficient with the experimental data and the least error is chosen. The Artificial Neural Networks predict well if properly trained with the datasets, however, over-training of the network should be avoided.

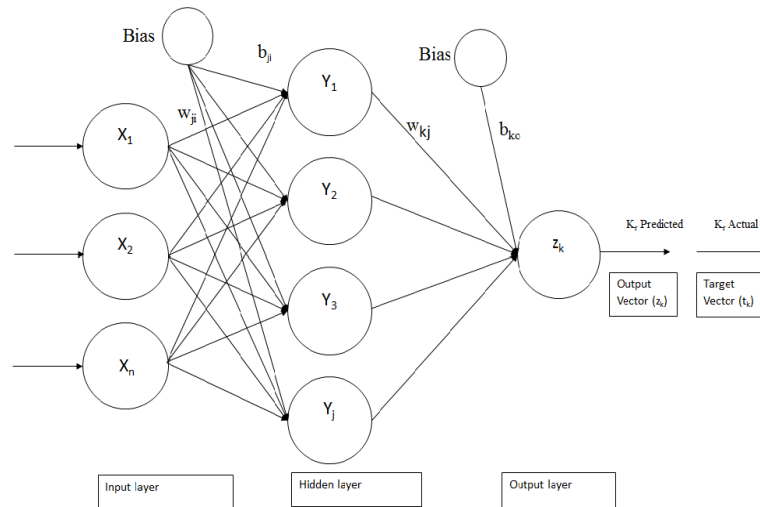


**Fig. 3.12 ANN structure of feedforward backpropagation network**

### 3.5 DEVELOPMENT OF ADAPTIVE NEURO-FUZZY INFERENCE SYSTEMS (ANFIS) MODEL

Jang (1993) originally presented the Adaptive Neuro-Fuzzy Inference Systems technique. ANFIS constructs fuzzy if-then rules with the required membership functions to generate a functional mapping of input-output pairs (Al-hmouz et al. 2012). ANFIS is a hybrid method combining the neural network learning to tune the parameters of a Fuzzy Inference System. In ANFIS, the inputs are first converted into fuzzy membership functions and then rule-based learning happens to obtain the output membership functions, by defuzzification, we get the required output (Azmathulla et al. 2011). There are a couple of methods to develop the initial fuzzy membership functions in the literature, here in the present study subtractive clustering method and Fuzzy c-means clustering has been employed.

#### 3.5.1 Subtractive clustering

The subtractive clustering algorithm is used to automatically generate Gaussian membership functions. A set of fuzzy if-then rules are generated by the algorithm which is equal to the number of cluster centers, each representing the characteristic of the cluster. The algorithm is explained in this section (Chiu 1994). C

$$\rho_i = \sum_{j=1}^n \exp \left( - \frac{\|x_i - x_j\|^2}{\left( \frac{r_a}{2} \right)^2} \right) \quad (3.7)$$

Wherein  $x_i, x_j$  are the data points with a radius of influence  $r_a$  and  $x_{c1}$  is the first cluster center with the highest density. A data point with the highest density value is chosen as the first cluster center  $x_{c1}$ . A point with the highest density occurs when there lie a large number of data points in its vicinity (Mohan Rao et al. 2015). Further, the next iteration density measure of each data point  $x_i$  is obtained from Equation 3.8 below,

$$\rho_i = \rho_i - \rho_{ci} \sum_{j=1}^n \exp \left( - \frac{\|x_i - x_j\|^2}{\left( \frac{r_a}{2} \right)^2} \right) \quad (3.8)$$

The process of changing the density of data point and finding the new cluster center is continued until all of the data points are within the range of cluster radius. Thus the FIS model is obtained and the obtained FIS is based on the first order Sugeno model which is used to initialize the ANFIS model. To map the inputs to the outputs, most commonly adopted FIS is Mamdani inference system and Sugeno inference system, it is found that the Sugeno model is more efficient and compatible (Tiwari et al. 2018).

### 3.5.2 Fuzzy C-Means Clustering

Fuzzy C-means (FCM) clustering is one of the most used clustering method developed by Bezdek (1981). Fuzzy C-Means Clustering algorithm (FCM) is usually employed in pattern recognition problems (Azamathulla et al. 2011; Alata et al. 2013; Zhou and Yang 2016). FCM limitation is that the cluster number need to be defined prior, however, it gives good modeling results (Castillo et al. 2012; Arumugadevi and Seenivasagam

2015). Clustering the data well into natural groups is performed by FCM. FCM allows each dataset to belong to multiple clusters. The entire dataset is grouped into ‘n’ clusters with every data point belonging to every cluster to a certain degree of membership. Hence FCM assigns every single data point a membership grade for each cluster. Cluster center and degree of membership for every data point is iteratively updated and pushes the cluster center to the right location in a dataset.

The two important factors influencing the performance of the fuzzy c-means algorithm is the parameter ‘m’ the weight exponent and the number of clusters ‘n’. The parameter m the weight exponent in the fuzzy membership is normally  $m = 2$  but does not work fine for all datasets. The algorithm was run for different exponent value of m from 1.1 to 2.2 and the validation is done based on RMSE, as the past researches claim that there exists no universal fuzzy clustering validity for diversified datasets in real-world formula (Ren et al. 2016). The number of clusters for each case was decided depending upon the different wave heights and the corresponding values in the datasets. Also, a cross-check was done by varying the number of clusters (Ren et al. 2016) and found that better results were obtained when the number of clusters was set to 9 for the entire dataset, based on wave heights. The minimum improvement factor was set as  $1e^{-5}$  in the objective function in between the two consecutive iterations and the maximum iterations count was set to 100.

In the FCM algorithm, the objective function as in Equation 3.9 is the generalization of the least squares method and is minimized in every iteration.

$$J_m = \sum_{i=1}^D \sum_{j=1}^N \mu_{ij}^m \left\| x_i - C_j \right\|^2 \quad (3.9)$$

Where,

D - total dataset

N – total cluster number

m - is the fuzzy partition matrix exponent which has to be greater than 1

$x_i$  - is the  $i^{\text{th}}$  data point in the dataset.

$c_j$  - is the  $j^{\text{th}}$  cluster center.

$\mu_{ij}$  - membership grade of  $x_i$  in the  $j^{\text{th}}$  cluster.

Steps involved in the fuzzy clustering are

1. Random initialization of the cluster membership values is done  $\mu_{ij}$ .
2. Cluster centers are calculated by Equation 3.10

$$c_j = \frac{\sum_{i=1}^D \mu_{ij}^m x_i}{\sum_{i=1}^D \mu_{ij}^m} \quad (3.10)$$

3. Update  $\mu_{ij}$  by Equation 3.11

$$\mu_{ij} = \frac{1}{\sum_{k=1}^N \left( \frac{\|x_i - c_j\|}{\|x_i - c_k\|} \right)^{\frac{2}{m-1}}} \quad (3.11)$$

4. Objective function  $J_m$  is calculated from Equation 3.9

5. Repeat the steps 2-4 until the set termination condition is met. Either  $J_m$  does not improve beyond the set threshold or maximum iterations is reached (Zhou and Yang 2016).

### 3.5.3 ANFIS model (Adaptive neuro-fuzzy inference systems)

ANFIS, the method is the integration of ANN and fuzzy logic models which integrates the learning ability and human knowledge to overcome the shortcomings in ANN (Jang 1993). It finds out the position and shapes for membership functions in FIS (Mohammady 2016). The membership functions of a Sugeno-type Fuzzy Inference System are tuned using the input-output datasets. It consists of five layers as seen in Figure 5 and the role of each layer is briefed here. In the first layer, a membership function is assigned to each input. The membership functions are further multiplied in the second layer and hence the output of every node in the second layer is the product of all the incoming signals. In the third layer, each of these firing strengths of the rule

is compared with the sum of all the firing strengths or say the firing strengths are averaged here. This average is the weighing factor. The Layer 4 implements the Sugeno-type inference system i.e., a linear combination of the input variables of an ANFIS plus a constant from the output of each if-then rules. In layer 5 the summation of its inputs, i.e. the defuzzification process of the fuzzy system was done using a weighted average method (Patil et al. 2011).

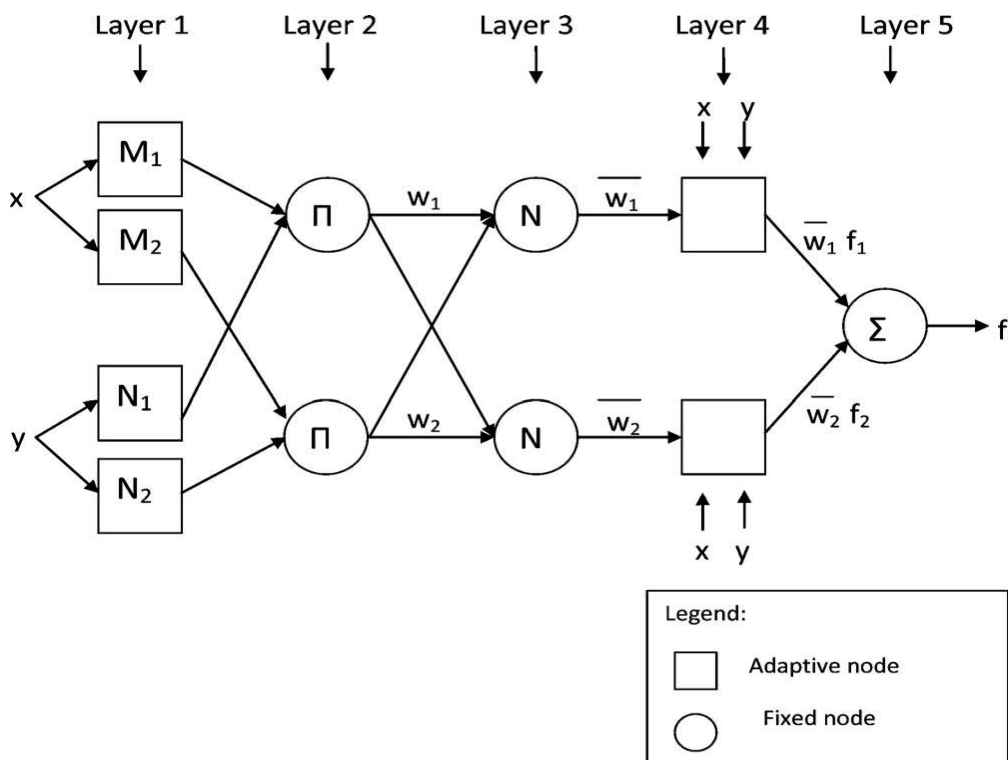


**Fig. 3.13 Basic ANFIS structure** (Azamathulla et al. 2011)

In a first-order Takegi Sugeno Kang model, if a model has only two inputs the X1 and X2 and one output Y and the rule base has only two fuzzy if-then rules then the rules can be represented as,

Rule 1: If X1 is A1 and X2 is B1 then  $F1=P1X1+Q1X2+R1$

Rule 2: If X1 is A2 and X2 is B2 then  $F2=P2X1+Q2X2+R2$  (3.12)

Where, P1, P2, Q1, Q2 and R1, R2 are the linear parameters in the consequent part of the Sugeno fuzzy inference system.

The architecture of ANFIS has five layers and each layer has several nodes defined by functions.

Layer 1 This layer is a fuzzification layer with each node representing the



membership grades of inputs ( $X_1, X_2$ ) and each nodes output denoted as  $O_i^j$  i. e., the output of  $i^{\text{th}}$  node in  $j^{\text{th}}$  layer.

$$\begin{aligned} O_i^1 &= \mu_{A_i}(X_1) & i = 1, 2 \\ O_i^1 &= \mu_{B_{i:2}}(X_2) & i = 3, 4 \end{aligned} \quad (3.13)$$

$A_i$  and  $B_i$  are the linguistic labels (like small, medium...) for particular node characterized by membership functions  $\mu(X_1)$  and  $\mu(X_2)$  respectively.  $O_i^1$  is the membership grade of the fuzzy set. The Gaussian membership function is given by,

$$\begin{aligned} \mu_{A_i}(X_1) &= e^{-\left(\frac{(x_1-b_i)^2}{2a_i^2}\right)} \\ \mu_{A_i}(X_2) &= e^{-\left(\frac{(x_2-b_i)^2}{2a_i^2}\right)} \end{aligned} \quad (3.14)$$

Where  $a_i$  and  $b_i$  is the premise parameters of the membership function in the premise part of fuzzy if-then rules that modify the shapes of membership functions.

Layer 2 is the rule layer where each node calculates the rule weight i.e., the firing strength of the associated rule as in Equation 3.15.

$$O_i^2 = w_i = \mu_{A_i}(X_1)\mu_{B_i}(X_2) \quad (3.15)$$

Layer 3 being the normalization layer represents the ratio of  $i$ th rules firing weight to the summation of all rules' firing weight as in Equation 3.16.

$$O_i^3 = \bar{w}_i = \frac{w_i}{w_1 + w_2} \quad (3.16)$$

Layer 4 being the defuzzification layer, equation 13 shows the contribution of the  $i$ th rule to the total output, where  $\bar{w}_i$  is the Layer 3 output and  $f_i$  shows the fuzzy if-then rule of the Takagi sugeno type as in Equation 3.17

$$O_i^4 = \bar{w}_i f_i = \bar{w}_i (P_i X_i + Q_i X_i + R_i) \quad (3.1)$$

Layer 5 Total output layer as in Equation 3.18 here the single node computes output ( $O_i^5$  - single output) by summation of all the rules from the previous layer.

$$O_i^5 = \sum_i \bar{w}_i f_i = \frac{\sum_i w_i f_i}{\sum_i w_i} \quad (3.18)$$

Basically, the ANFIS fine-tunes the model parameters with gradient descent backpropagation and mean least squares optimization algorithms, which is a hybrid of two techniques. This hybrid technique has a forward pass and a backward pass. The mean least square algorithm identifies the consequent parameters in the forward pass (in Layer 4). In every epoch, the sum of the squared difference error (SSE) is propagated backward to update the premise parameters by gradient descent. Once the optimal premise parameters are learned for the generated model the overall output is a linear combination of consequent parameters (Tiwari et al. 2018, Zhou et al. 2016).

### **3.6 PARTICLE SWARM OPTIMIZATION (PSO)**

Particle swarm optimization a metaheuristic method simple but powerful. PSO is good for optimization problems to find the best solution, however, the disadvantage of getting stuck in the local minima is overcome by improving different variants of PSO (Imran et al. 2013). The variants of PSO are the initialization of inertia weight and acceleration coefficients. The PSO searches for the global minimum. In PSO a level of intelligence is reached by the teamwork of entire colony of birds/fish. PSO is a swarm intelligence method it uses unintelligent particles to reach the upper level of intelligence. The population of candidate solutions is called a swarm of particles. Every particle (bird/fish) has a position in the search space of the optimization problem. Search space is a set of all probable solutions to the optimization problem and the best solution in this search space is found.

Initially, a random set of particles is chosen and the velocity vector for each particle in the swarm is calculated. In each PSO iteration, every particles new position is updated, with respect to the previous position and the updated velocity vector. The velocity vector is updated relative to global best and personal best positions for each solution particle. The velocity vector as in Equation 3.19 is a combination of Inertia component, cognitive component and social component to form a new velocity vector as shown in Fig. 3.5. The new velocity vector translates the particle position to a new position in the search space according to this model. The process of updating is repeated until the convergence is met. And hence the best new location is found. (Kennedy and Eberhart 1995; Venter and Sobieszczanski-Sobieski 2002; Ejraei et al. 2016; Bergh and

Engelbrecht 2006). A detailed review concentrating on the advances, limitations, and architecture of the PSO algorithm has been done by Bonyadi and Michalewicz (2017).

The position,  $x_i$ , of the  $i^{\text{th}}$  particle, is adjusted by a stochastic velocity  $v_i$  which depends on the distance that the particle is from its own best solution and that of its neighborhood. If  $v_{ij}$  is velocity and  $x_{ij}$  is position at the current iteration of the  $i^{\text{th}}$  particle at time  $t$  for the  $j^{\text{th}}$  component update then (Bergh and Engelbrecht 2006).

$$v_{ij}(t+1) = wv_{ij}(t) + c_1r_1(p_{ij}(t) - x_{ij}(t)) + c_2r_2(g_{ij}(t) - x_{ij}(t)) \quad (3.19)$$

$$x_{ij}(t+1) = x_{ij}(t) + v_{ij}(t) \quad (3.20)$$

Where,

$p_{ij}$  – personal best ( $P_{\text{best}}$ )

$g_{ij}$  - global best ( $G_{\text{best}}$ )

$w$  - inertia coefficient

$c_1, c_2$  – coefficients of acceleration

$r_1, r_2$  – uniformly distributed numbers between (0,1)

$t+1$  – is the time step

### 3.6.1 ANFIS training improved with PSO

For any database, the ANFIS model accuracy depends on the respective rules', premises and consequent parameters. Arriving at the optimal values of these parameters is a great challenge. In the current study, ANFIS performance is enhanced with PSO, as shown in the flow diagram of Fig. 3.6. The PSO parameters and the initial population is chosen. The fuzzy membership functions and rules of FIS are designed and the input/output variables are tuned according to PSO. The new best value is updated based on the RMSE of the individual particle solution. The PSO is used to reduce the RMSE of the prediction. The optimal parameters are thus obtained to create a fuzzy model, thus improving model prediction (Zahmatkesh et al. 2017).

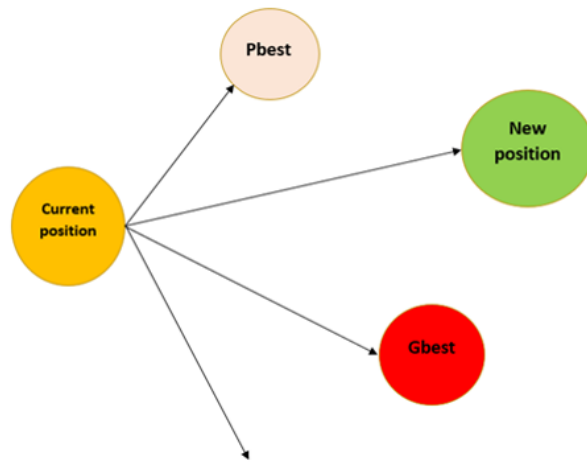


**Fig. 3.14 PSO-ANFIS simplified**

### **3.6.2 Literature on PSO application**

Particle swarm optimization is an evolutionary heuristic search model inspired by the swarming or collaborative behavior of biological population like birds flock flying together in multidimensional space searching optimum place adjusting their flight movement and distances for better search. The PSO algorithm was first introduced by Kennedy and Eberhart (1995). Since then there have been several applications of PSO. An efficient model based on Adaptive Network-based Fuzzy Interference Systems (ANFIS) optimized by using particle swarm optimization (PSO) was developed to predict the molecular diffusion of CO<sub>2</sub> in reservoir oil at elevated temperature and pressures (Ejraei et al. 2016). Benzene density can be predicted from the ambient air pollution data using ANFIS and PSO. Here, the ANFIS accuracy was increased by optimizing the multiobjective fitness cost function (Singh et al. 2017). The PSO-ANFIS and PSO-ANN was used to enhance the estimation of DSI log parameters like compressional, shear and stoneley wave velocities. The optimization technique of PSO algorithm was applied to increase the accuracy and reliability of DSI log parameters prediction in the field through using inexpensive conventional logs (Zahmatkesh et al. 2017). The short term wind power prediction in Portugal with historical wind power data as the main training input has been successful using a hybrid approach of PSO-

ANFIS (Pousinho et al. 2011). A hybrid PSO-ANFIS approach in the prediction of the optimum parameters of a protective spur dike to control the scour around the series of spur dikes has been found efficient (Basser et al. 2015).

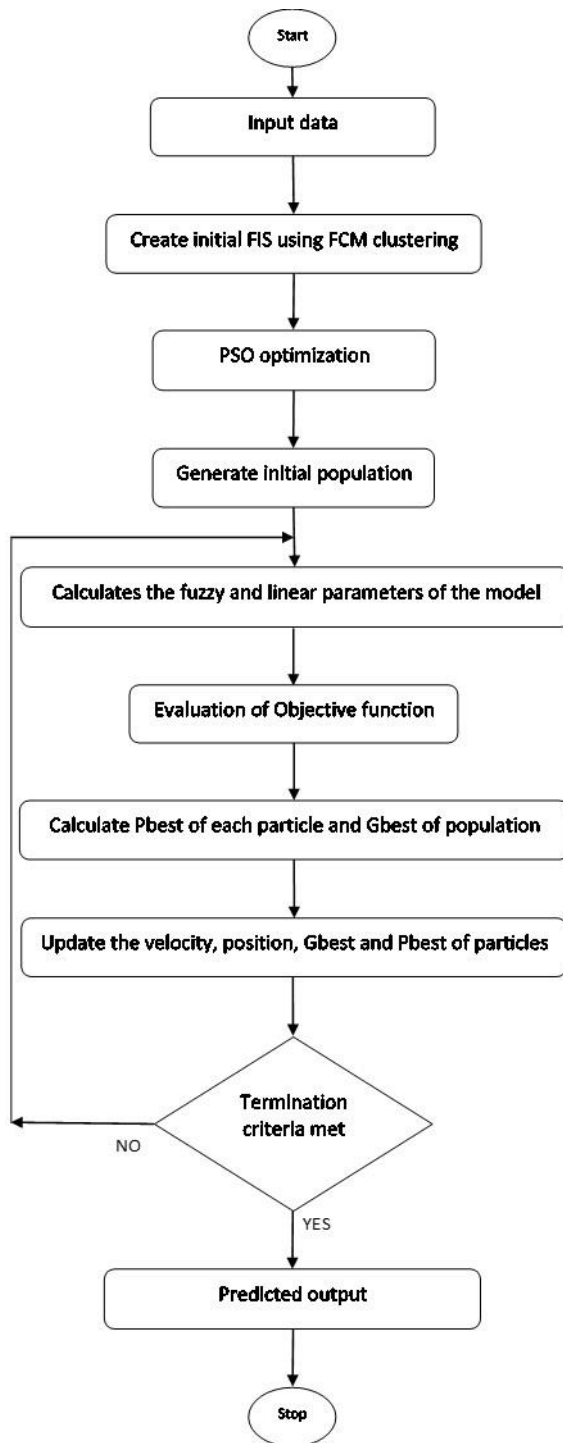


**Fig. 3.15 PSO-ANFIS flowchart**

### **3.7 GENETIC ALGORITHM**

Genetic algorithm (GA) is heuristic inspired by, Charles Darwin's theory of natural evolution. In GA, by the natural selection, the fittest individuals are selected from a population for reproduction in order to produce the offspring of the next generation. So fittest parents produce better offspring and hence the chances of surviving are better.

Three main phases involved in the genetic algorithm are:

#### **Selection:**

Initially, a set of individuals which is called a population (data variables) is chosen from the entire dataset. Each individual is a solution to the problem to be solved. A fitness function determines how to fit an individual is and gives a fitness score to each individual. Selection of a pair of the individual (chromosomes) with the highest fitness scores is done to pass on their genes to the next generation. Among the several existing operators, to choose the best individuals for the next generation the roulette wheel selection method has been employed in the current study. Followed by the most significant phase, is the crossover in genetic algorithm.

#### **Crossover:**

Crossover in genetic algorithm combines the genes of two parents to form new offspring for the next generation. This could be done by single point crossover, two-point crossover or k point crossover method. Here a single point crossover is employed in which a point is randomly picked on both parents' chromosomes and designated as a 'crossover point'. The bits to the right of the crossover point are swapped between the two parent chromosomes resulting in two offspring. Each carries some genetic information from parents and is further added to the new population.

#### **Mutation:**

In some of these new offspring formed, their genes can be subjected to a mutation with a low random probability. In order to prevent premature convergence and to maintain diversity within the population, the mutation will occur. If the population has converged then, the algorithm terminates wherein, any further produced offspring is not

significantly different from the previous generation. Thus the GA provides a set of solutions to the given problem.

### 3.7.1 Hybrid GA-ANFIS model

The fuzzy c-means clustering parameters explained in Section 3.5.2 on which the fuzzy rules of ANFIS depends are determined by trial and error. To arrive at the optimal values is attempted by employing a genetic algorithm (GA). In GA-ANFIS model the clustering parameters are optimized using GA and ANFIS is called within the GA for the fitness value evaluation of every possible candidate solution generated by GA. The objective function of the genetic algorithm as in Equation 3.21, is to reduce the RMSE of the ANFIS model prediction of resulting final FIS whose rules are controlled by FCM. Here the parameters of a FIS designed for mapping input values to targets are optimized by GA-ANFIS model thus reducing training prediction error. Stopping criteria being either the set maximum number of iterations reached or minimum improvement between two consecutive iterations not exceeding 0.01. Further, with the optimized trained model, the testing is done. The methodology of GA-ANFIS is shown in Fig. 3.7 (Habibi et al. 2018).

$$MinRMSE_{train} = \sqrt{\frac{1}{N} \sum_{i=1}^N (O_i - P_i)^2} \quad (3.21)$$

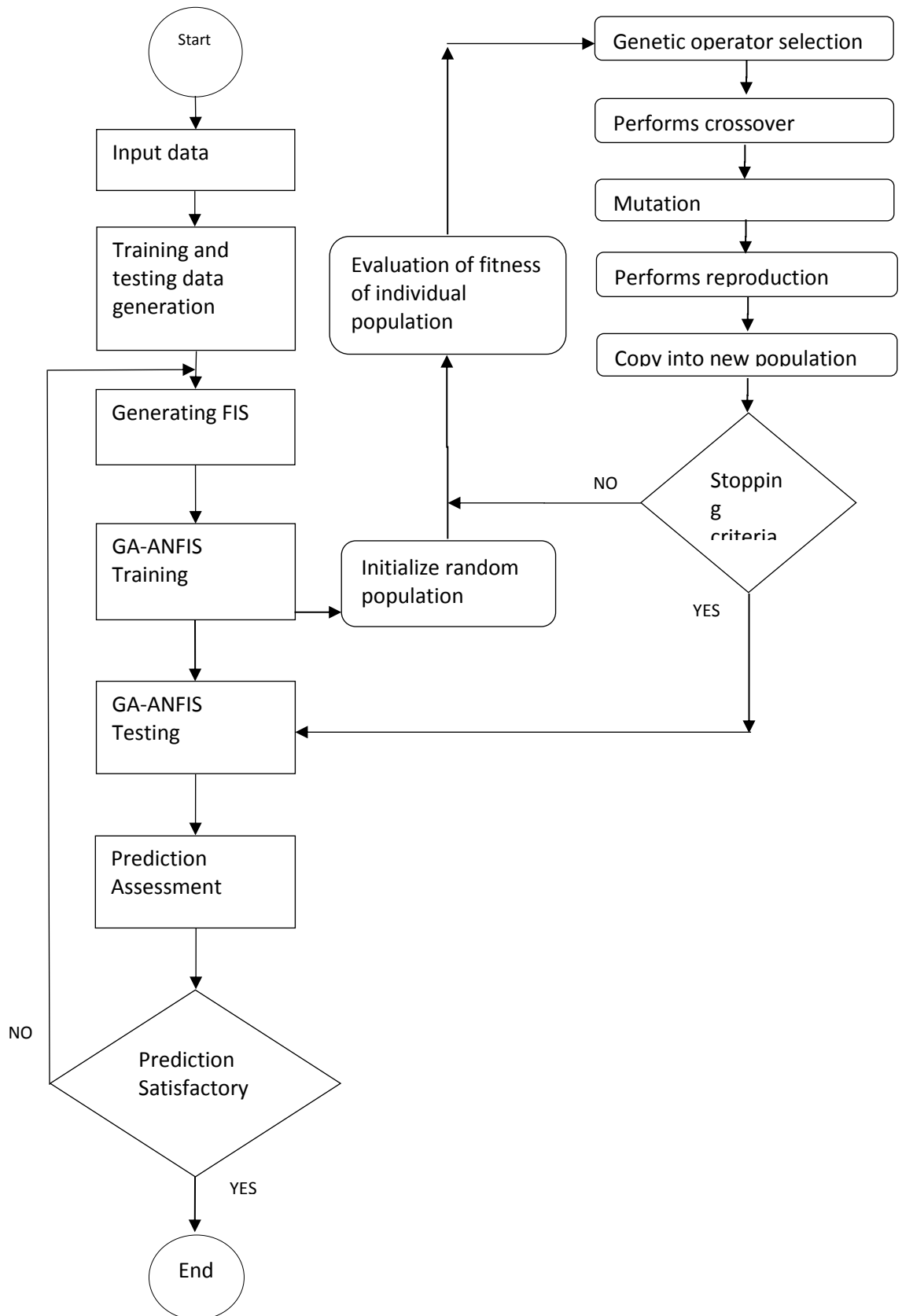


**Fig. 3.16 GA-ANFIS model (Azimi et al., 2017)**



### 3.8 STATISTICAL PARAMETERS TO VALIDATE THE MODEL PERFORMANCE

The model performance is assessed by following five statistical measures:

The Nash Sutcliffe Efficiency (NSE) can range from  $-\infty$  to 1.0, optimal being one.

$$NSE = 1 - \left[ \frac{\sum_{i=1}^N (P_i - O_i)^2}{\sum_{i=1}^N (O_i - O_{mean})^2} \right] \quad (3.22)$$

The square of the correlation coefficient is the coefficient of determination ( $R^2$ ) and is described by a linear fit. It shows the amount of variance between the model prediction and actual value. Whereas, the correlation coefficient ( $R$ ) is a measure showing a linear relationship between two variables.

$$R = \frac{N(\sum O_i P_i) - (\sum O_i)(\sum P_i)}{\sqrt{[N\sum O_i^2 - (\sum O_i)^2]} \sqrt{[N\sum P_i^2 - (\sum P_i)^2]}} \quad (3.23)$$

The Bias in the models could be positive or negative. The mean positive error indicates average overestimation and mean negative error indicates an average underestimation of the wave reflection coefficient,

$$BIAS = \frac{1}{N} \sum_{i=1}^N (P_i - O_i) \quad (3.24)$$

The scatter index (SI) is the percentage of expected error for the parameter,

$$SI = \left( \frac{RMSE}{Actual_{average}} \right) 100 \quad (3.25)$$

The Root Mean Square Error (RMSE) has the same units as the actual and predicted data. Error between measured and predicted values should always below,

$$RMSE = \sqrt{\frac{1}{N} \sum_{i=1}^N (O_i - P_i)^2} \quad (3.26)$$

In Equation 3.22 to 3.26,

$P_i$  - the model predicted the value of the output variable

$O_i$  - actual value of the output variable

$O_{mean}$  - mean of actual values of the output variable

N – Total data points



## CHAPTER 4

### PREDICTION OF REFLECTION COEFFICIENT

The reflection coefficient ( $K_r$ ) of emerged seaside perforated semicircular breakwaters has not been much explored, and there is a research gap, particularly in the application of soft computing techniques to predict  $K_r$ . The present chapter includes the data segregation, prediction of  $K_r$  using different soft computing models as well as the assessment of the models.

#### 4.1 REFLECTION COEFFICIENT

The wave reflection coefficient ( $K_r$ ) is defined as the ratio of reflected wave height ( $H_r$ ) to incident wave height ( $H_i$ ) for regular waves as in Equation 4.1

$$K_r = \frac{H_r}{H_i} \quad (4.1)$$

In the current study, the prediction of the reflection coefficient of emerged seaside perforated semicircular breakwaters is proposed. The study involves the application of soft computing models to the data obtained from the experimental study involving emerged seaside perforated semicircular breakwaters of different radii under varying wave conditions using the Issacson three probe method. The experimental parameters used can be found in Table 3.1.

The prediction of the reflection coefficient is studied separately for two sets of input variables i.e., the dimensional and dimensionless form.

- Dimensional ( $H_i$ ,  $T$ ,  $S$ ,  $D$ ,  $R$ ,  $d$ ,  $h_s$ )
- Non-dimensional ( $H_i / gT^2$ ,  $d/gT^2$ ,  $S/D$ ,  $h_s/d$ ,  $R/H_i$ ) with  $\pi$ -terms obtained from dimensional analysis using Buckingham's  $\pi$ -theorem.

#### 4.1.1 Data segregation for prediction of $K_r$

Data segregation for prediction of  $K_r$  for dimensional and non-dimensional input parameters are done as follows for the case of wave heights:

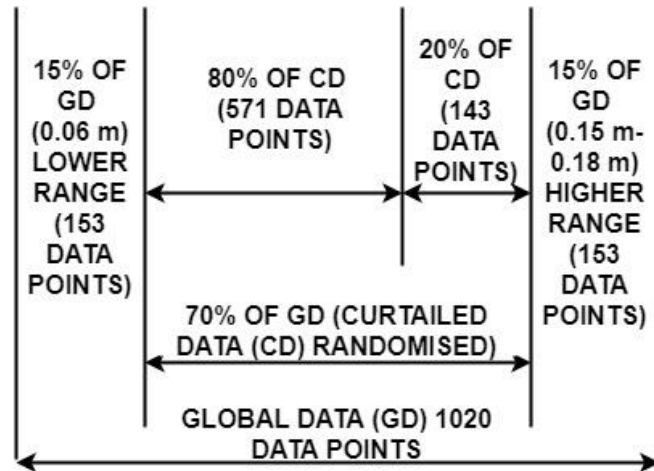


**Fig. 4.1 Typical data segregation for  $K_r$  prediction of SBW**

The data segregation procedure for the typical case of wave height

1. The entire dataset (consisting of 1020 input-output data points) is called global data (GD) and is sorted in the increasing order of wave heights ( $H_i$ ). The line diagram in Fig. 4.1 shows the data segregation.
2. The lower ranges of wave height (15%, 0.06 m, 153 data points) and higher ranges of wave height (15%, above 0.15 m - 0.18 m, 153 data points) i.e., a total of 30% is segregated.
3. The remaining 70% of the data (consisting 714 data points) is randomized and is called curtailed data (CD), of which 80% (571 data points) is used for training and the remaining 20% (143 data points) is used for testing as in the case of conventional prediction.
4. Then this 20% test data, is replaced by the available 15% lower range of data and it is named as 'below the range'. The network trained with 80% curtailed data, is used to predict the reflection coefficient for those ranges not involved in the training.

5. Similarly, a prediction for purely higher ranges of wave height (15%, above 0.15 m) not involved in the training of the network has been carried out and it is named as ‘beyond the range’ predictions.
6. A ‘conventional below’ case of prediction is done for a data division of 80:20. In which 80% of curtailed data and below the range data values 15% are grouped together and randomized and then used for prediction.
7. A ‘conventional beyond’ case of prediction is done for a data division of 80:20. In which 80% of curtailed data and beyond the range data values 15% are grouped together and randomized and then used for prediction.
8. In addition, a conventional data segregation prediction is done with a data division of 75:25 for a dataset of 1274 randomized data points.

#### **4.2 RESULTS AND DISCUSSION OF $K_r$ PREDICTION OF SEMICIRCULAR BREAKWATER USING DIFFERENT SOFT COMPUTING MODELS FOR DIMENSIONAL INPUT PARAMETERS**

The proposed approach of predicting  $K_r$  below and beyond the data ranges of available experimental data is tested with ANN and ANFIS models. The results obtained for dimensional input parameters are shown in Table (4.2 - 4.5). Further, the comparison of this prediction is done using conventional data set whose data segregation is as explained in Section 4.1.1. Among the two methods employed in ANFIS i.e., subtractive clustering (SC) and Fuzzy c-means clustering (FCM); three out of four cases the FCM outperformed in the case of dimensional input parameters. Hence for remaining cases, FCM-ANFIS is adopted. The most influencing parameter in subtractive clustering is the cluster radius of influence which is varied from 0.1 to 1.0 and the optimal FIS is chosen based on the least error, best R-value, best NSE, and SI. The most influencing parameter in FCM is the cluster number and the partition matrix. The cluster number is chosen based on the data clusters found by the subtractive clustering method. The partition matrix is varied from 1.1 to 2.0 and the optimal FIS is chosen based on the least error, best R-value, best NSE, and SI. Further, in the chapter, each proposed case the model, its optimal parameters and the assessment of results are presented.

#### **4.2.1 Reflection coefficient prediction performance of different soft computing models for the case of below the data range for dimensional input parameters**

The training and testing of ANN Model for prediction below the data range is carried out. The best ANN architecture for the available data sets is determined using a trial and error basis with respect to the error metrics. The network is fed with 7 inputs and the prediction of 1 output is done by varying the number of neurons in the only set hidden layer. Among the different model architectures tested, the model with one hidden layer consisting of 12 neurons predicted the wave reflection coefficient ( $K_r$ ) with the least error. The values of the measure of error is presented in Table 4.2. The correlation coefficient for training  $R=0.9899$  and for testing  $R=0.9875$  is found. Fig. 4.2 shows the scatter plot of model prediction and actual values of the reflection coefficient for below the data range testing using ANN.

ANFIS model with subtracting clustering was employed where the training data loaded to generate input membership function consisted of 7 inputs and 1 output data. In this case, the “genfis2” is used for training the data with a step size of 0.1 and a number of epochs 20. The radius of influence is varied from 0 to 1 and found that the RMSE to be least when the radius is 0.3 for all 7 inputs, and the genfis2, makes Gaussian membership functions for each input. Training and testing performance of the ANFIS model for below the data range is validated by error measure as shown in Table 4.2 and the scatter plot of prediction and actual values of ANFIS is as in Fig 4.2. The ANFIS model gave slightly better results with higher  $R=0.9887$  compared to ANN whose R-value for testing is 0.9875, as seen in Table 4.2.

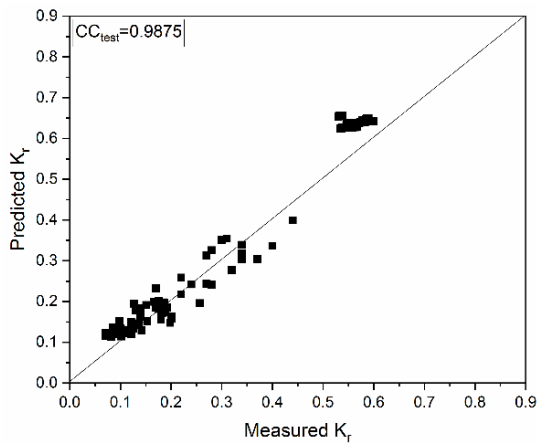
The ANFIS model with fuzzy C-means clustering is adopted with the input membership function for each input variable is ‘gaussmf’ and the output membership function type is ‘linear’ for Sugeno systems. Here the number of clusters is set as 9 as the entire dataset has 9 distinct wave heights. The exponent of partition matrix component  $m=1.2$  is set, as it gave better R-value and relatively lowest error. The minimum improvement factor was set as 0.001 in the objective function in between the two consecutive iterations and the maximum iterations count was set to 25. Training and testing performance of the

ANFIS model for below the data range is validated by error measure as shown in Table 4.2 and the scatter plot of prediction and actual values of ANFIS is as in Fig 4.2. In this case of the dimensional dataset, the input variables are 7 and the response variable is 1. Fuzzy C-means clustering constructs a fuzzy inference system (FIS) with inputs and output. The prediction of  $K_r$  for dimensional input parameters had a better correlation coefficient, lower SI, better NSE, lower positive bias and lower RMSE in the case of FCM-ANFIS model compared to the results of SC-ANFIS model. Among the three models adopted FCM-ANFIS gave relatively better results. The Fig.4.3 shows the comparison of predicted  $K_r$  by ANN, FCM-ANFIS, SC-ANFIS models with observed  $K_r$  values.

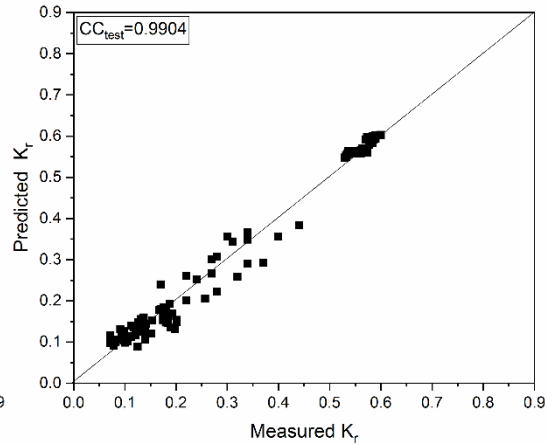
**Table 4.1 Error metrics for different soft computing models for dimensional input parameters in the case of below the data range for predicting reflection coefficient parameter**

Case	Error metrics	Soft computing models					
		ANN		ANFIS (FUZZY C-MEANS CLUSTERING)		ANFIS (SUBTRACTIVE CLUSTERING)	
		Train	Test	Train	Test	Train	Test
Below	R	0.9899	0.9875	0.9914	0.9904	0.9924	0.9887
	RMSE	0.0273	0.0517	0.0241	0.0274	0.0228	0.0303
	NSE	0.9781	0.9288	0.9829	0.9801	0.9847	0.9956
	SI	9.55	16.74	8.42	8.84	7.96	9.81
	BIAS	-0.0005	0.0311	2.821E-08	0.0009	-5.610E-09	0.0084

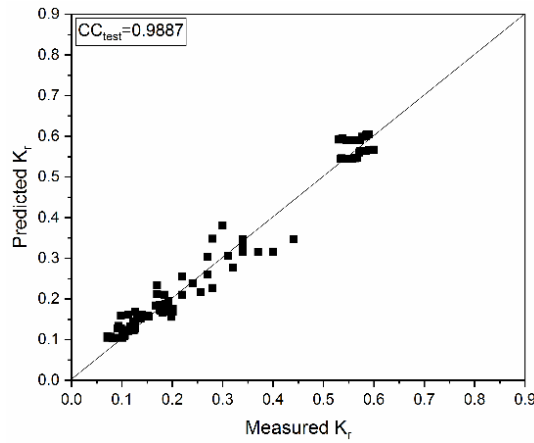




(a) ANN model



(b) FCM-ANFIS model



(c) SC-ANFIS model

**Fig. 4.2 Scatter plot of predicted versus actual values of  $K_r$  for different models for the case of below the range with dimensional input parameters**

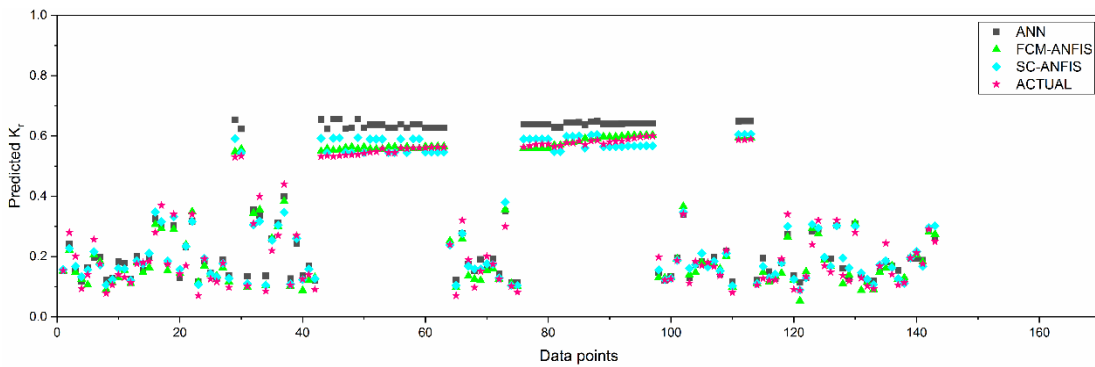


**Fig. 4.3 Comparison of predicted  $K_r$  by ANN, ANFIS, GA-ANFIS, PSO-ANFIS models for the case of below the range with dimensional input parameters with observed  $K_r$  values**

#### **4.2.2 Reflection coefficient prediction performance of different soft computing models for the case of conventional below the data range for dimensional input parameters**

The curtailed data including below the data range values are randomized and divided into two sets (80% for training and 20% for testing). This follows the typical conventional method of data segregation and prediction. As mentioned in section 4.1.1, 7 inputs are fed into the model and with the expected output being reflection coefficient ( $K_r$ ). For this case, the best ANN architecture is found to be 7-12-1, where 12 neurons are set in the hidden layer. Table 4.3 shows the error measure for training and testing by the conventional method of prediction. The  $R=0.9903$  in the case of testing is found which is closer to 1, indicating a better fit of the model compared to ANN testing of below the data range. ANN model comparison of testing RMSE of the conventional method of data segregation to the testing of below the data range shows error reduction in the conventional method of data segregation. Fig.4.4 shows the scatter plot of model prediction and actual values of the reflection coefficient for testing by the conventional below the data range method of data segregation using ANN.

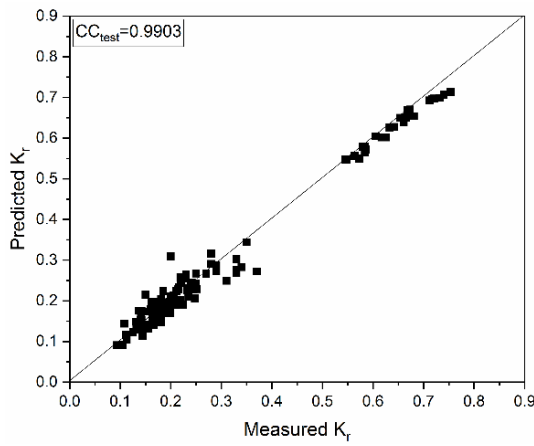
Further on the application of ANFIS subtractive clustering to training data with 7 inputs and 1 output is loaded to generate input membership function. In the study, genfis2 is used for training the data with a step size of 0.1 and a number of epochs 20 least RMSE=0.0233 is obtained when the radius is set to 0.9. Training and testing performance of ANFIS model for the conventional below method of prediction is validated by error measure as shown in Table 4.3 and found that the predictions made by ANFIS are reasonably good, slightly improved over the ANN result in terms of correlation coefficient  $R=0.9922$ . The RMSE values are found to be slightly lower in this particular case of ANFIS model testing compared to that of ANN testing errors indicating the reduction of errors in the conventional below method of prediction using SC-ANFIS. The scatter plot of  $K_r$  actual and the ANFIS model prediction is plotted in Fig.4.4.

Also, the application of FCM-ANFIS to training data with 7 inputs and 1 output is

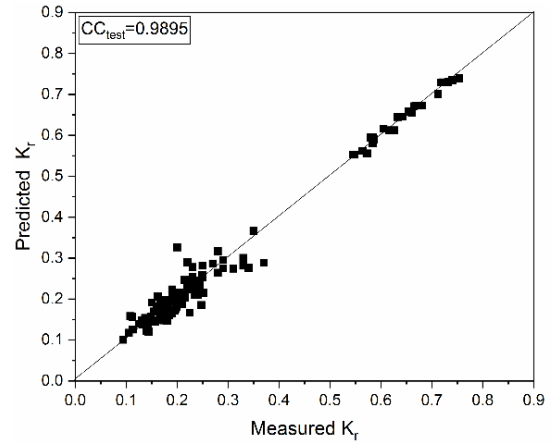
adopted with the input membership function for each input variable is ‘gaussmf’ and the output membership function type is 'linear' for sugeno systems. Here the number of clusters is set as 9 as the entire dataset has 9 distinct wave heights. The exponent of partition matrix component  $m=1.2$  is found to be the best with a lower error. The minimum improvement factor was set as 0.001 in the objective function in between the two consecutive iterations and the maximum iterations count was set to 25. Training and testing performance of the ANFIS model for below the data range is validated by error measure as shown in Table 4.3 and the scatter plot of predicted  $K_r$  value by ANFIS and actual values are as in Fig.4.4. FCM constructs a FIS with inputs and output. The prediction of  $K_r$  for dimensional input parameters by FCM had lower correlation coefficient, higher SI, lower NSE, higher negative bias and slightly higher RMSE in the case of FCM-ANFIS model compared to the results of ANFIS model with subtractive clustering. Among the three methods, SC-ANFIS gave relatively better results. The Fig.4.5 shows the comparison of predicted  $K_r$  by ANN, FCM-ANFIS, SC-ANFIS models with observed  $K_r$  values.

**Table 4.2 Error metrics for different soft computing models for dimensional input parameters in the case of conventional below the data range for predicting reflection coefficient parameter**

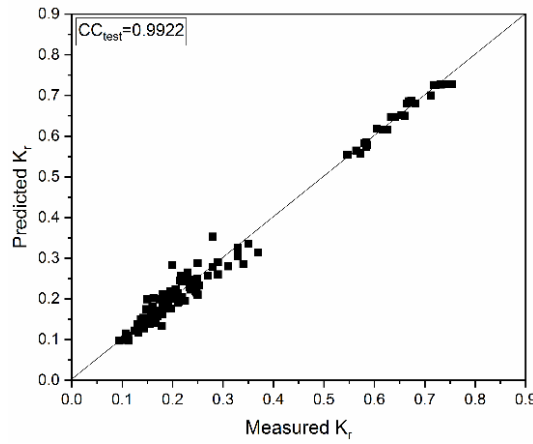
Case	Error metrics	Soft computing models					
		ANN		ANFIS (FUZZY C-MEANS CLUSTERING)		ANFIS (SUBTRACTIVE CLUSTERING)	
		Train	Test	Train	Test	Train	Test
Conventional Below	R	0.9912	0.9903	0.9908	0.9895	0.9934	0.9922
	RMSE	0.0252	0.0265	0.0251	0.0271	0.0213	0.0233
	NSE	0.9813	0.9797	0.9816	0.9788	0.9843	0.9867
	SI	8.83	8.85	8.76	9.05	7.45	7.78
	BIAS	-0.0045	0.0045	1.034E-08	-0.0010	-0.0001	-0.0001



(a) ANN model



(b) FCM-ANFIS model



(c) SC-ANFIS model

**Fig. 4.4** Scatter plot of predicted versus actual values of  $K_r$  for different models for the case of conventional below the range with dimensional input parameters

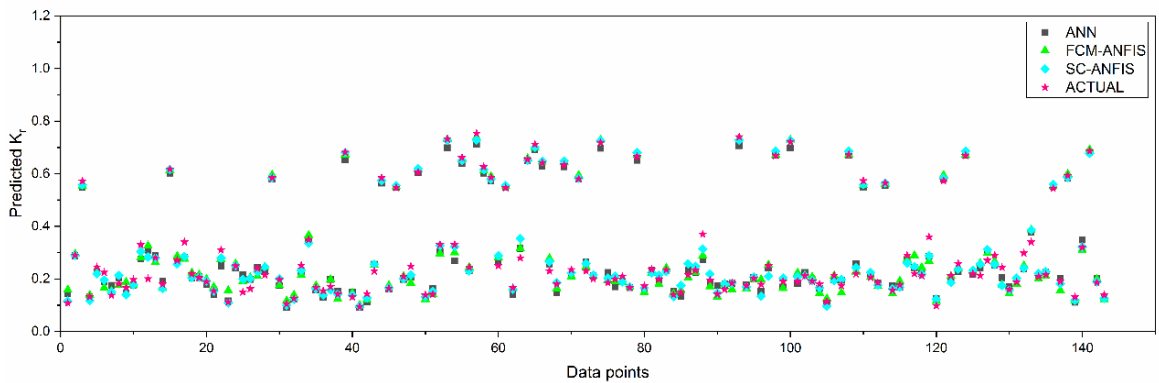


**Fig. 4.5** Comparison of predicted  $K_r$  by ANN, ANFIS, GA-ANFIS, PSO-ANFIS models for the case of conventional below the range with dimensional input parameters with observed  $K_r$  values

### **4.2.3 Reflection coefficient prediction performance of different soft computing models for the case of beyond the data range for dimensional input parameters**

The training and testing of ANN Model for prediction beyond the data range are carried out. The best ANN architecture obtained by trial and error basis is 7-12-1 with the least RMSE=0.0526 for epoch 4. The network is fed with 7 inputs and the prediction of 1 output is done by varying the number of neurons in the only set hidden layer. The values of the measure of error are presented in Table 4.4. The correlation coefficient for training  $R=0.9899$  and for testing  $R=0.9879$  was found. Fig.4.6 shows the scatter plot of model prediction and actual values of the reflection coefficient for beyond the data range testing using ANN.

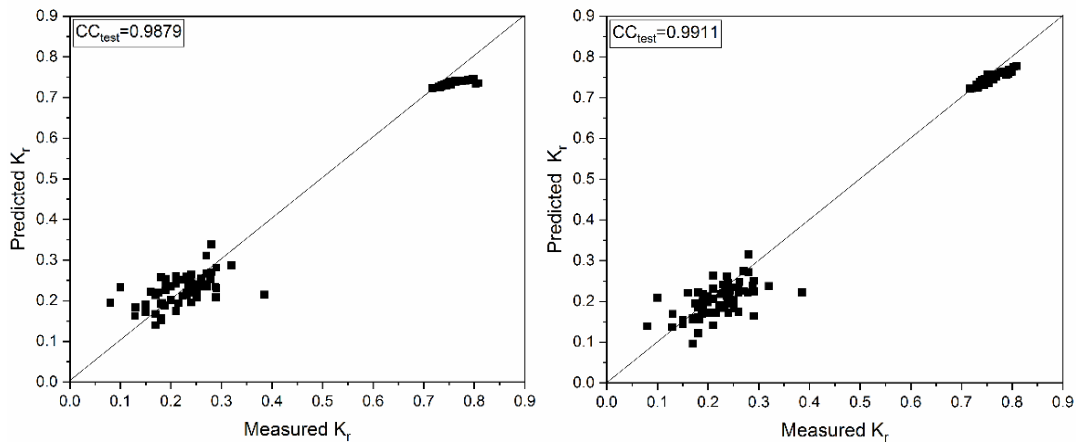
ANFIS model with subtractive clustering is employed where the training data loaded to generate input membership function consisted of 7 inputs and 1 output data. In this case, the “genfis2” is used for training the data with a step size of 0.1 and a number of epochs 20. The radius of influence was varied from 0 to 1 and found that the RMSE to be least when radius was 0.3 for all 7 inputs, and the genfis2, makes Gaussian membership functions for each input. Training and testing performance of the ANFIS model for below the data range is validated by error measure as shown in Table 4.4 and the scatter plot of prediction and actual values of SC-ANFIS is as in Fig 4.6. The SC-ANFIS model gave slightly better results with higher  $R=0.9906$  compared to ANN whose R-value for testing is 0.9879, as seen in Table 4.4.

The ANFIS model with fuzzy C-means clustering is adopted with the input membership function for each input variable is ‘gaussmf’ and the output membership function type is 'linear' for Sugeno systems. Here the number of clusters is set as 9 as the entire dataset has 9 distinct wave heights. The exponent of partition matrix component  $m=1.2$  is set as for this value, the error is minimum. The minimum improvement factor is set as 0.001 in the objective function in between the two consecutive iterations and the maximum iterations count is set to 25. Training and testing performance of FCM-ANFIS model for beyond the data range is validated by error measure as shown in Table

4.4 and the scatter plot of prediction and actual values of FCM-ANFIS is as in Fig.4.6. In this case of the dimensional dataset, the input variables are 7 and the response variable is 1. Fuzzy C-means clustering constructs a fuzzy inference system (FIS) with inputs and output. The prediction of  $K_r$  for dimensional input parameters had better correlation coefficient, lower SI, better NSE of 98%, negative bias and lower RMSE in the case of FCM-ANFIS model compared to the results of SC-ANFIS and ANN model. The Fig.4.7 shows the comparison of predicted  $K_r$  by ANN, FCM-ANFIS, SC-ANFIS models with observed  $K_r$  values.

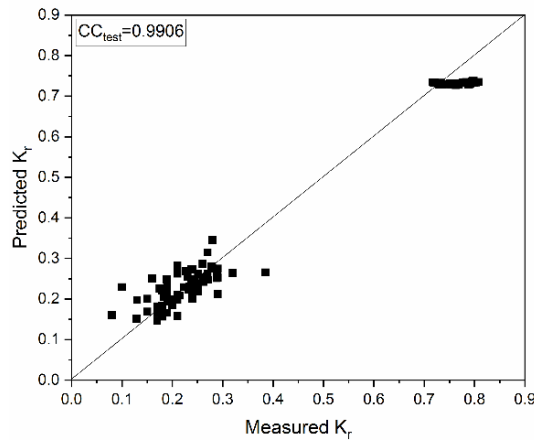
**Table 4.3 Error metrics for different soft computing models for dimensional input parameters in the case of beyond the data range for predicting reflection coefficient parameter**

Case	Error metrics	Soft computing models					
		ANN		ANFIS (FUZZY C-MEANS CLUSTERING)		ANFIS (SUBTRACTIVE CLUSTERING)	
		Train	Test	Train	Test	Train	Test
Beyond	<b>R</b>	0.9899	0.9879	0.9916	0.9911	0.9916	0.9906
	<b>RMSE</b>	0.0275	0.0526	0.0241	0.0428	0.0241	0.0497
	<b>NSE</b>	0.9778	0.9730	0.9829	0.9821	0.9829	0.9684
	<b>SI</b>	9.60	11.31	8.42	9.20	8.42	10.68
	<b>BIAS</b>	0.0081	-0.0180	0.0001	-0.0210	0.0001	-0.0186



(a) ANN model

(b) FCM-ANFIS model



(c) SC-ANFIS model

**Fig. 4.6 Scatter plot of predicted versus actual values of  $K_r$  for different models for the case of beyond the range with dimensional input parameters**

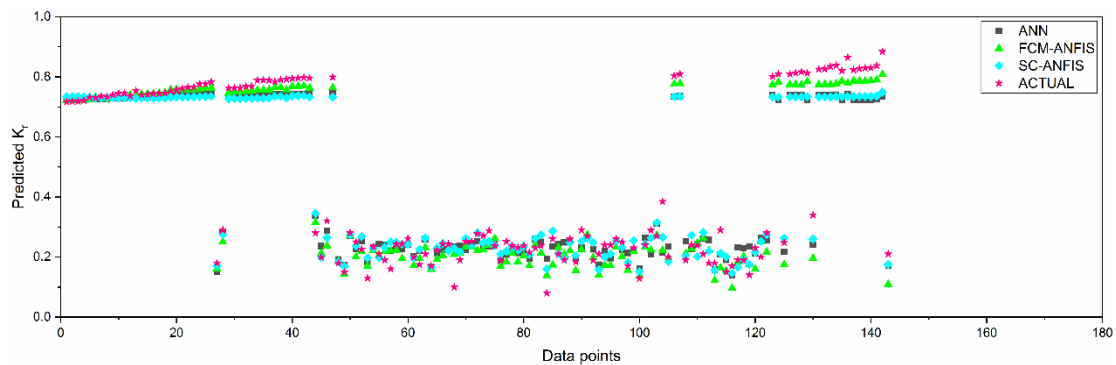


**Fig. 4.7 Comparison of predicted  $K_r$  by ANN, ANFIS, GA-ANFIS, PSO-ANFIS models for the case of beyond the range with dimensional input parameters with observed  $K_r$  values**

#### **4.2.4 Reflection coefficient prediction performance of different soft computing models for the case of conventional beyond the data range for dimensional input parameters**

The curtailed data including beyond the data range values are randomized and divided into two sets (80% for training and 20% for testing). This follows the typical conventional method of data segregation and prediction. As mentioned earlier, 7 inputs are fed into the model and with the output being reflection coefficient ( $K_r$ ). For this case, the best ANN architecture was found to be 7-12-1 at epoch 4, where 12 neurons are set in the hidden layer. Table 4.5 shows the error measure for training and testing by the conventional beyond the data range method of prediction. The R-value for training and testing is found to be 0.9895 and 0.9859 respectively. Fig. 4.8 shows the scatter plot of model prediction and actual values of the reflection coefficient for testing by the conventional beyond the data range method of data segregation using ANN.

Further on the application of ANFIS subtractive clustering (SC) to training data with 7 inputs and 1 output is loaded to generate input membership function. In the study, genfis2 is used for training the data with a step size of 0.1 and the number of epochs 20, least RMSE=0.0394 was obtained when the radius was set to 0.5. Training and testing performance of SC-ANFIS model is validated by error measure as shown in Table 4.5 and found that the prediction made by SC-ANFIS is good, however, did not improve over the ANN result in terms of correlation coefficient  $R=0.9812$ . The scatter plot of  $K_r$  actual and the SC-ANFIS model prediction is plotted in Fig. 4.8.

Also, the application of FCM-ANFIS to training data with 7 inputs and 1 output is adopted with the input membership function for each input variable is 'gaussmf' and the output membership function type is 'linear' for Sugeno systems. Here the number of clusters is set as 13 as the entire dataset has 13 distinct wave heights. The exponent of partition matrix component  $m=1.2$  IS found to have the least error with better prediction. The minimum improvement factor is set as 0.001 in the objective function in between the two consecutive iterations and the maximum iterations count was set to 50 as it gave best results. Training and testing performance of FCM-ANFIS model for

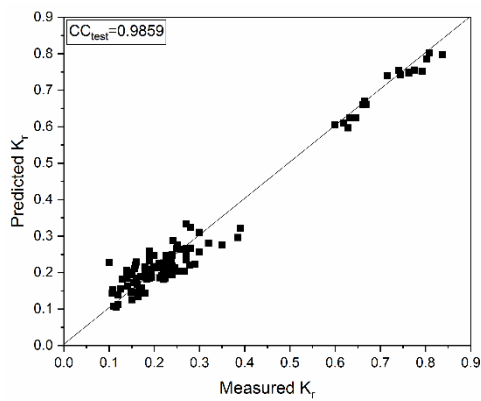


conventional beyond the data range is validated by error measure as shown in Table 4.5 and the scatter plot of prediction and actual values of FCM-ANFIS is as in Fig 4.8. FCM constructs a FIS with inputs and output. The prediction of  $K_r$  for dimensional input parameters by FCM had higher correlation coefficient, lower SI, higher NSE, lower negative bias and least RMSE in the case of FCM-ANFIS model compared to the results of ANFIS model with subtracting clustering and ANN prediction.

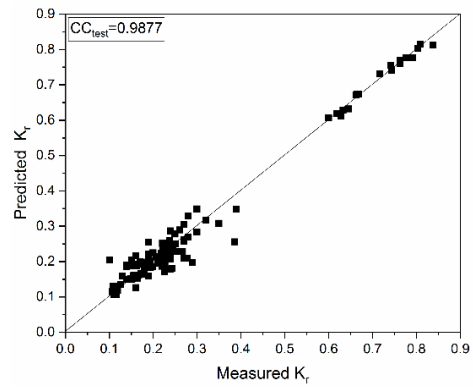
In all the above four cases presented  $K_r$  prediction is reasonably good with a test value of  $R \sim 0.99$  for FCM-ANFIS which is good and acceptable; hence no further application of any hybrid model has been attempted. The Fig.4.9 shows the comparison of predicted  $K_r$  by ANN, FCM-ANFIS, SC-ANFIS models.

**Table 4.4 Error metrics for different soft computing models for dimensional input parameters in the case of conventional beyond the data range for predicting reflection coefficient parameter**

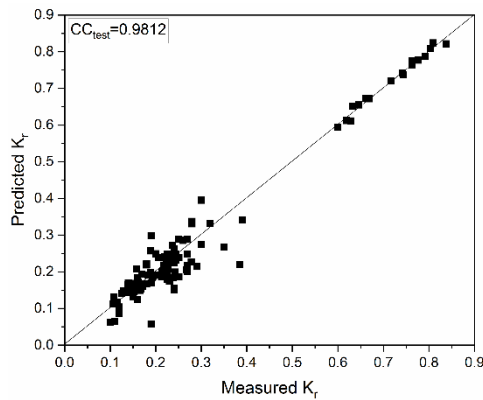
Case	Error metrics	Soft computing models					
		ANN		ANFIS (FUZZY C-MEANS CLUSTERING)		ANFIS (SUBTRACTIVE CLUSTERING)	
		Train	Test	Train	Test	Train	Test
Conventional Beyond	<b>R</b>	0.9895	0.9859	0.9931	0.9877	0.9968	0.9812
	<b>RMSE</b>	0.0308	0.0526	0.0244	0.0312	0.0167	0.0394
	<b>NSE</b>	0.9782	0.9730	0.9864	0.9755	0.9936	0.9610
	<b>SI</b>	10.09	11.31	7.9918	10.69	5.45	13.49
	<b>BIAS</b>	-0.0009	-0.0180	0	-0.0002	0	-0.0044



(a) ANN model



(b) FCM-ANFIS model



(c) SC-ANFIS model

**Fig. 4.8** Scatter plot of predicted versus actual values of  $K_r$  for different models for the case of conventional beyond the range with dimensional input parameters

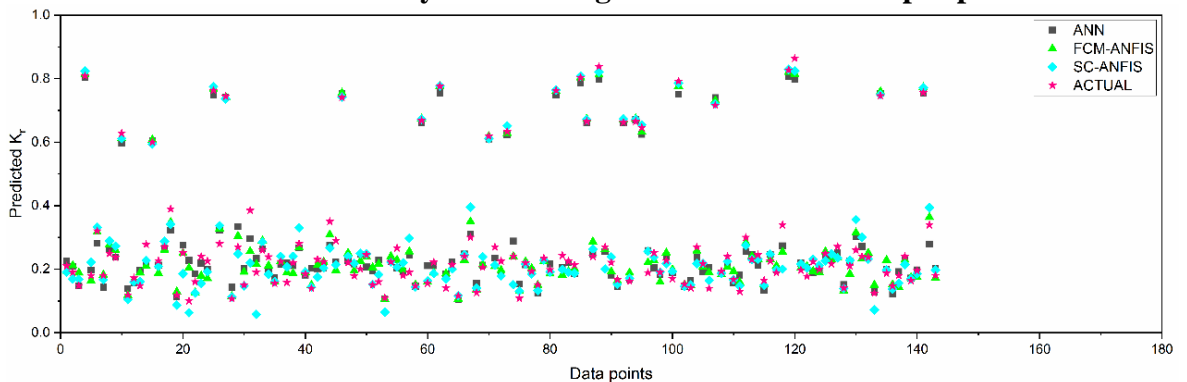


**Fig. 4.9** Comparison of predicted  $K_r$  by ANN, ANFIS, GA-ANFIS, PSO-ANFIS models for the case of conventional beyond the range with dimensional input parameters with observed  $K_r$  values

### **4.3 RESULTS AND DISCUSSION OF $K_r$ PREDICTION OF SEMICIRCULAR BREAKWATER USING DIFFERENT SOFT COMPUTING MODELS FOR NON-DIMENSIONAL INPUT PARAMETERS**

In all the four cases considered for dimensional input parameters three out of four cases the FCM-ANFIS gave better results compared to SC-ANFIS hence FCM-ANFIS alone is considered for prediction in the case of non-dimensional input parameters and not SC-ANFIS. In this case, the results obtained by ANN and ANFIS method had still scope for improvement hence further optimization of ANFIS is attempted using the genetic algorithm and particle swarm optimisation with an objective function set to reduce RMSE of best obtained FCM-ANFIS model prediction. In some cases either optimisation of GA was better than PSO or vice-versa. Non-dimensional input parameters  $H_i/gT^2$ ,  $d/gT^2$ ,  $S/D$ ,  $h_s/d$  and  $R/H_i$  obtained from dimensional analysis using Buckingham's  $\pi$ -theorem is used here to predict the reflection coefficient. The data segregation, in this case, is similar to that explained in section 4.1.1. The assessment of each model is presented in Tables (4.6-4.9), it is found that GA-ANFIS outperformed all the other models in three out of the four cases considered.

#### **4.3.1 Reflection coefficient prediction performance of different soft computing models for the case of below the data range for non-dimensional input parameters**

The training and testing of ANN Model for prediction below the data range are carried out. The best ANN architecture obtained by trial and error basis is 5-5-1 with the least testing RMSE=0.1485 for epoch 20. The network is fed with 5 inputs and the prediction of one output was done by varying the number of neurons in the only set hidden layer. The values of the measure of error are presented in Table 4.6. The correlation coefficient for training  $R=0.8764$  and for testing  $R=0.8586$  was found. Fig. 4.10 shows the scatter plot of model prediction and actual values of the reflection coefficient for below the data range testing using ANN.

The ANFIS model with fuzzy C-means clustering is adopted with the input membership function for each input variable is 'gaussmf' and the output membership function type is 'linear' for Sugeno systems. Here the number of clusters is set as 9 as the entire dataset has 9 distinct wave heights. The exponent of the partition matrix component  $m=1.4$

gave the best R-value when compared to other 'm' values. The minimum improvement factor is set as of  $1e-5$  in the objective function in between the two consecutive iterations and the maximum iterations count was set to 50. Training and testing performance of FCM-ANFIS model for below the data range is validated by error measure as shown in Table 4.6 and the scatter plot of actual and predicted values and of  $K_r$  by FCM-ANFIS is as in Fig 4.10. In this case of the non-dimensional dataset, the input variables are 5 and the response variable is 1. FCM constructs a fuzzy inference system (FIS) with inputs and output. The prediction of  $K_r$  for non-dimensional input parameters by FCM-ANFIS did not improve the correlation coefficient hence had slightly higher SI, lower NSE, higher negative bias and with higher RMSE=0.1504, compared to the results of ANN model.

To improve the ANFIS training GA-ANFIS model has been employed whose objective function is to reduce the RMSE of the prediction of  $K_r$  of the semicircular breakwater. In the FCM the number of clusters is set as 9 and with  $m=1.4$  the prediction was optimal with least RMSE, for a maximum FCM iteration of 50 and minimum improvement of  $1e-5$ . GA is sensitive to its parameters i.e., population size and the maximum number of iterations. By changing these two parameters of the GA, the training of the ANFIS model with the parameters as mentioned above is done. The GA-ANFIS model was run for various population size 10, 15, 20, 25, 30, 35, 40, 50, 100, and finally set for a population size of 60. The maximum number of iterations was set to 1000, the mutation rate is set to 0.15, the crossover percentage is set to 0.4, mutation percentage is set to 0.7, and the selection pressure is set to 8. Table 4.6 shows the comparison of GA-ANFIS and ANFIS model results in case of non-dimensional input parameters and the scatter plot of prediction and actual values of GA-ANFIS is as seen in Fig 4.10. The GA-ANFIS model prediction is better than FCM-ANFIS model. The Nash Sutcliffe efficiency of the GA-ANFIS model improved to 81% compared to 72% of testing of ANFIS model and accordingly the error reduced to least of all four cases to RMSE=0.1237, hence the scatter index is least. Though negatively biased the bias value improved over ANFIS.

Further to check if PSO is better than GA in improving the ANFIS training PSO-ANFIS model has been employed whose objective function is to reduce the RMSE of the

prediction of wave reflection ( $K_r$ ) of the semicircular breakwater. In the employment of PSO-ANFIS model, an initial FIS for the dataset of non-dimensional input parameters is generated using FCM and the PSO is applied to fine-tune the ANFIS training. The antecedent and consequent parameters of ANFIS are tuned by PSO. In the FCM the number of clusters is set as 9, as the data involved nine different wave heights. The other important parameter 'm' the exponent of the partition matrix is varied from 1.1 to 2.2 and found  $m=1.4$  is optimal with least RMSE, for a maximum FCM iteration of 100 and minimum improvement of  $1e-5$ . PSO is sensitive to its parameters i.e., the inertia weight and acceleration coefficients and the obtained heuristic ensure convergent trajectories (Bergh and Engelbrecht 2006). Further, the parameters of PSO algorithm are adjusted such as to reduce the prediction error. The cognitive coefficient and social coefficients are usually set equal to 2 (Zahmatkesh et al. 2017), in the study  $c_1=c_2=2$  predicted the  $K_r$  well. The model is run for different values of  $c_1$  and  $c_2$  but the least RMSE is attained only when the acceleration coefficient  $c_1=c_2=2$ . In PSO, the choice of size of the population is critical and it significantly affects the performance of population-based search techniques (Chen et al. 2015). The model was run for various population size 10, 15, 20, 25, 30, 35, 40, 50, 100, and finally set for a population size of 40 and 5000 iterations which gave the best prediction with least RMSE. With a lower number of iterations, the error was higher. The inertia weight of  $w=0.4$  is set for achieving a better convergence as the rate of convergence is less for any other inertia coefficients set between 1.4 to 0.4 (Eberhart and Shi 2001). Table 4.6 shows the comparison of PSO-ANFIS and ANFIS model results in case of non-dimensional input parameters.

The PSO-ANFIS model prediction is better than ANFIS-FCM model. The prediction of the reflection coefficient by PSO-ANFIS model is found to be positively biased with a bias value of 0.0034, shows slight overestimation, however, lower than the bias of ANFIS model i.e., -0.0139 which is also negatively biased. For PSO-ANFIS model, root mean square error is found to be less with Nash Sutcliffe Efficiency being higher and a lower scatter index compared to that of ANFIS model prediction statistics as, seen in Table 4.6. Also, a scatter plot of predict  $K_r$  and actual values of PSO-ANFIS is as

seen in Fig. 4.10. The Fig. 4.11 shows the comparison of predicted  $K_r$  by ANN, ANFIS, GA-ANFIS and PSO-ANFIS models with observed  $K_r$  values. Among the four models employed GA-ANFIS gave a better prediction of  $K_r$  in this case.

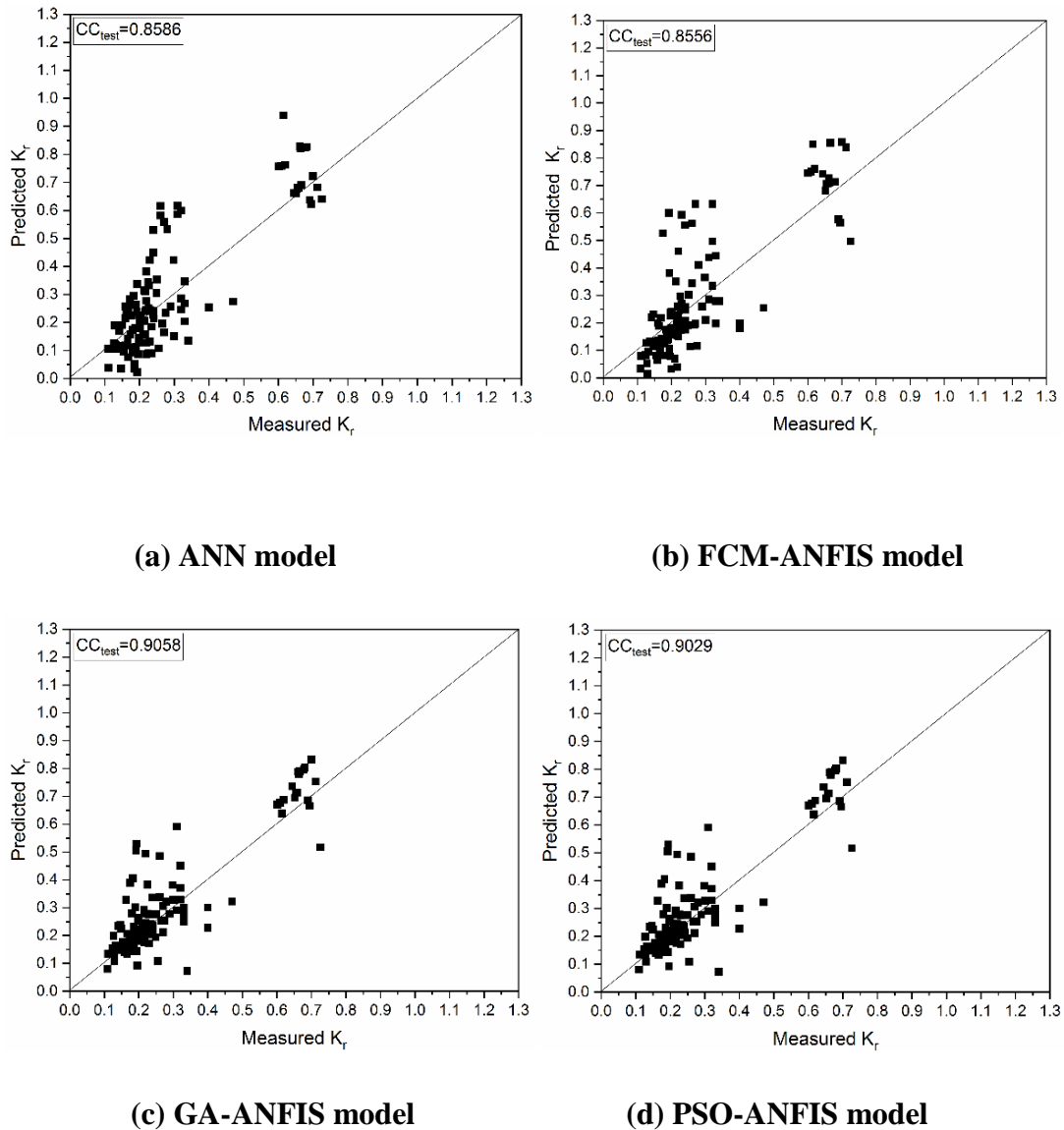


**Fig. 4.10** Scatter plot of predicted versus actual values of  $K_r$  for different models for the case of below the range with non-dimensional input parameters

**Table 4.5 Error metrics for different soft computing models for non-dimensional input parameters in the case of below the data range for predicting reflection coefficient parameter**

Case	Error metrics	Soft computing models							
		ANN		ANFIS		GA-ANFIS		PSO-ANFIS	
		Train	Test	Train	Test	Train	Test	Train	Test
Below	R	0.8764	0.8586	0.8907	0.8556	0.9088	0.9058	0.9078	0.9029
	RMSE	0.1211	0.1485	0.1142	0.1504	0.1049	0.1237	0.1064	0.1286
	NSE	0.7678	0.7362	0.7934	0.7296	0.8258	0.8171	0.8206	0.8021
	SI	45.33	44.63	42.76	45.17	39.27	37.16	39.84	38.65
	BIAS	0.004	-0.0089	2.93E-08	-0.0139	-0.0017	-0.0114	0.0043	0.003

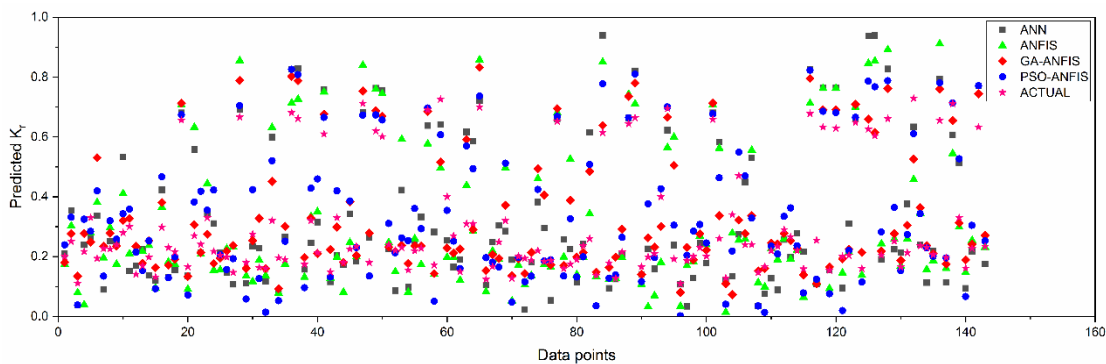


**Fig. 4.11 Comparison of predicted  $K_r$  by ANN, ANFIS, GA-ANFIS, PSO-ANFIS models for the case of below the range with non-dimensional input parameters with observed  $K_r$  values**

### **4.3.2 Reflection coefficient prediction performance of different soft computing models for the case of conventional below data range for non-dimensional input parameters**

The training and testing of ANN Model for prediction of conventional below the data range are carried out. The best ANN architecture obtained by trial and error basis is 5-6-1 with the least testing RMSE=0.1437 for epoch 22. The network is fed with 5 inputs and the prediction of single output is done by varying the number of neurons in the only set hidden layer. The values of the measure of error are presented in Table 4.7. The correlation coefficient for training  $R=0.8764$  and for testing  $R=0.8586$  was found. Fig. 4.12 shows the scatter plot of model prediction and actual values of the reflection coefficient for conventional below the data range testing using ANN.

The ANFIS model with fuzzy C-means clustering is adopted with the input membership function for each input variable is 'gaussmf' and the output membership function type is 'linear' for Sugeno systems. Here the number of clusters is set as 9 as the entire dataset has 9 distinct wave heights. The exponent of partition matrix component  $m=1.8$  is found to give better R-value with least RMSE among different trials of being' value set. The minimum improvement factor is set as of  $1e-5$  in the objective function in between the two consecutive iterations and the maximum iterations count is set to 25. Training and testing performance of the ANFIS model for conventional below the data range is validated by error measure as shown in Table 4.7 and the scatter plot of prediction and actual values of ANFIS is as in Fig. 4.12. Here FCM constructs a fuzzy inference system (FIS) with five inputs and one output. The prediction of  $K_r$  for non-dimensional input parameters by ANFIS slightly improved the correlation coefficient of training to 0.9077 and testing to 0.8655 however, relatively no significant change is observed with respect to ANN prediction.

To improve the ANFIS training GA-ANFIS model has been employed whose objective function is to reduce the RMSE of the prediction of  $K_r$  of the semicircular breakwater. In the FCM the number of clusters was set as 9, with  $m=1.8$  is found optimal with least RMSE, for a maximum FCM iteration of 25 and minimum improvement of  $1e-5$ . GA



being sensitive to its parameters population size and the maximum number of iterations. By changing these two parameters of the GA the training of ANFIS model with optimal FCM parameters as mentioned above prediction is done. The GA-ANFIS model is run for various population size 10, 15, 20, 25, 30, 35, 40, 50, 100, and finally set for a population size of 90 as the model gave best R-value for this population size and for maximum iterations set to 5000. The mutation rate is set to 0.15, the crossover percentage is set to 0.4, mutation percentage is set to 0.7, and the selection pressure is set to 8. Table 4.7 shows the comparison of GA-ANFIS and ANFIS model results in case of non-dimensional input parameters and the scatter plot of predicted and actual values of  $K_r$  by GA-ANFIS is as seen in Fig.4.12. The GA-ANFIS model prediction is better than the ANFIS model. The Nash Sutcliffe efficiency of the GA-ANFIS model improved to 77% compared to 74% of testing of ANFIS model and accordingly the error reduced to a least of all four cases to  $RMSE=0.1362$  hence the scatter index is also least with a bias value of 0.0113.

Further to check if PSO is better than GA in improving the ANFIS training PSO-ANFIS model is employed with an objective function to reduce the RMSE of the prediction of wave reflection ( $K_r$ ) of the semicircular breakwater. In the employment of PSO-ANFIS model, an initial FIS for the dataset of non-dimensional input parameters is generated using FCM and the PSO approach to fine tune the ANFIS training. The antecedent and consequent parameters of ANFIS are tuned by PSO. In the FCM the number of clusters is set as 9, as the data involved nine different wave heights. The other important parameter 'm' the exponent of the partition matrix is varied from 1.1 to 2.2 and found  $m=1.8$  is optimal with least RMSE, for a maximum FCM iteration of 25 and minimum improvement of  $1e-5$ . The model is run for different values of  $c_1$  and  $c_2$  but the least RMSE was attained only when the acceleration coefficient  $c_1=2$ ,  $c_2=2$ . The model is run for various population size and finally set for a population size of 90 and 5000 iterations which gave the best prediction with least RMSE for inertia weight of  $w=0.4$ . Table 4.7 shows the comparison of PSO-ANFIS and ANFIS model results in case of non-dimensional input parameters. The PSO-ANFIS model prediction for training  $R=0.9290$  is slightly better than ANFIS model training however, did not improve on the testing  $R=0.8623$ . On further increase of iterations in PSO-ANFIS, the model results

are not good. PSO-ANFIS model root mean square error was found slightly higher with Nash Sutcliffe Efficiency being lesser by 1% and a higher scatter compared to that of ANFIS model prediction Table 4.7. Also, a scatter plot of prediction and actual values of PSO-ANFIS is as seen in Fig. 4.12. Fig. 4.13 shows the comparison of predicted  $K_r$  by ANN, ANFIS, GA-ANFIS and PSO-ANFIS models with observed  $K_r$  values. Also among the four models employed GA-ANFIS predicted the best  $K_r$  for non-dimensional input parameters in the case of conventional below the data range.

**Table 4.6 Error metrics for different soft computing models for non-dimensional input parameters in the case of conventional below the data range for predicting reflection coefficient parameter**

Case	Error metrics	Soft computing models							
		ANN		ANFIS		GA-ANFIS		PSO-ANFIS	
		Train	Test	Train	Test	Train	Test	Train	Test
<b>Conventional Below</b>	<b>R</b>	0.8712	0.8643	0.9077	0.8655	0.9664	0.8865	0.9290	0.8623
	<b>RMSE</b>	0.1247	0.1434	0.1064	0.1437	0.0658	0.1362	0.0940	0.1470
	<b>NSE</b>	0.7583	0.7465	0.8239	0.7455	0.9326	0.7712	0.8625	0.7336
	<b>SI</b>	45.81	45.87	39.10	45.96	24.18	43.58	34.55	47.03
	<b>BIAS</b>	-0.004	-0.005	-1.83E-07	-0.0001	-0.0003	0.0113	-0.002	0.008

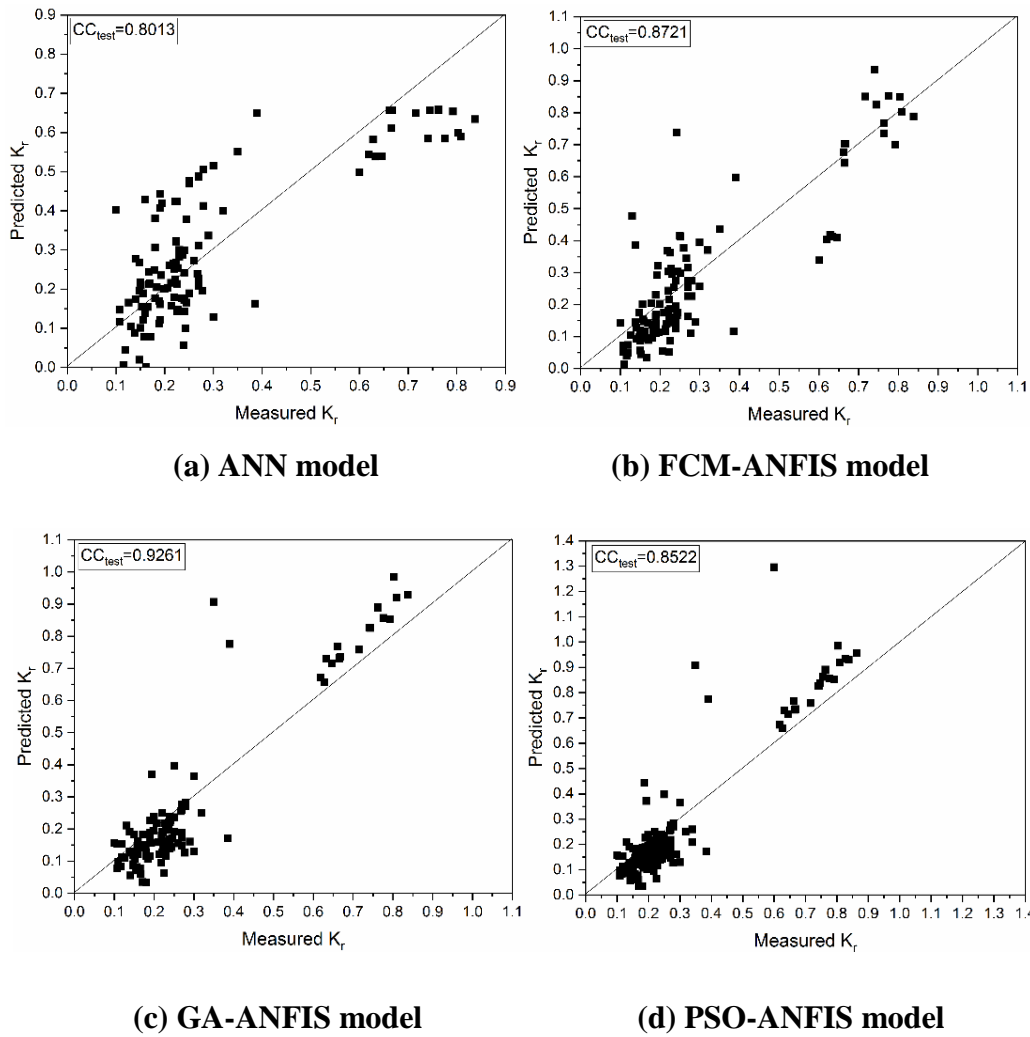


**Fig. 4.12** Scatter plot of predicted versus actual values of  $K_r$  for different models for the case of conventional below the range with non-dimensional input parameters

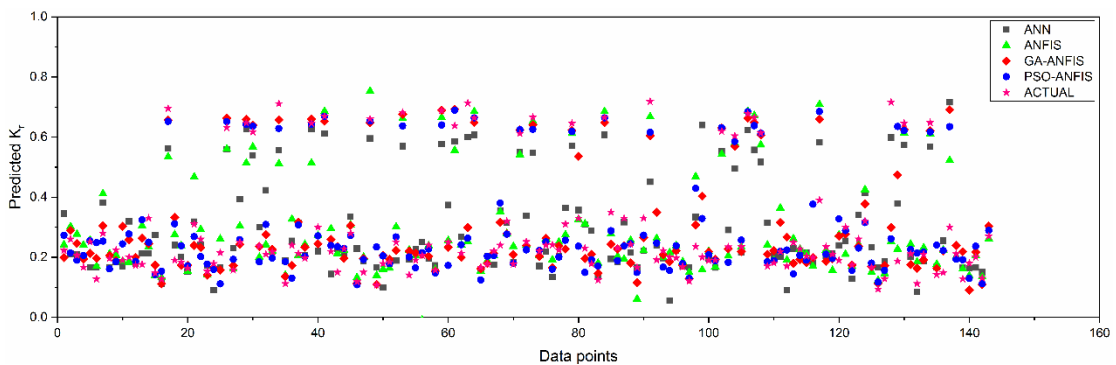


**Fig. 4.13** Comparison of  $K_r$  prediction performance of ANN, FCM-ANFIS, SC-ANFIS models in case of conventional below the range with non-dimensional input parameters

### **4.3.3 Reflection coefficient prediction performance of different soft computing models for the case of beyond data range for non-dimensional input parameters**

The training and testing of ANN Model for prediction of beyond the data range are carried out. The best ANN architecture obtained by trial and error basis is 5-11-1 with the least testing RMSE=0.3114 for epoch 26. The network is fed with 5 inputs and the prediction of single output is done by varying the number of neurons in the only set hidden layer. The values of the measure of error are presented in Table 4.8. The correlation coefficient for training  $R=0.8919$  and for testing  $R=0.7695$  is found. Fig 4.14 shows the scatter plot of model prediction and actual values of the reflection coefficient for beyond the data range testing using ANN.

The ANFIS model with fuzzy C-means clustering is adopted with the input membership function for each input variable is 'gaussmf' and the output membership function type is 'linear' for Sugeno systems. Here the number of clusters is set as 9 as the entire dataset has 9 distinct wave heights. The model prediction is best with relatively lower RMSE=0.3362 when  $m=1.2$  is set. The minimum improvement factor was set as of  $1e-5$  in the objective function in between the two consecutive iterations and the maximum iterations count was set to 50. Training and testing performance of ANFIS model for beyond the data range is validated by error measure as shown in Table 4.8 and the scatter plot of predicted  $K_r$  and actual values of ANFIS is as in Fig 4.14. Here FCM constructs a FIS with five inputs and one output. The prediction of  $K_r$  for non-dimensional input parameters by ANFIS did not improve the R-value of training and testing with respect to ANN prediction significantly.

Hence in order to improve the ANFIS training; GA-ANFIS model has been employed whose objective function is to reduce the RMSE of the prediction of  $K_r$  of the semicircular breakwater. In the FCM the number of clusters is set as 9, with  $m=1.2$  is optimal with least RMSE, for a maximum FCM iteration of 50 and minimum improvement of  $1e-5$ . GA is sensitive to its parameters i.e., population size and the maximum number of iterations. By changing these two parameters of the GA the

training of ANFIS model with the parameters as mentioned above is done. The GA-ANFIS model was run for various population size 10, 15, 20, 25, 30, 35, 40, 50, 100, and finally set for a population size of 90 and a maximum number of iterations set to 5000 as this gave better R-value. Similarly, the mutation rate is set to 0.15, the crossover percentage is set to 0.4, mutation percentage is set to 0.7, and the selection pressure is set to 8. In spite of varying the parameters to the best possible extent, the GA-ANFIS model did not improve over the ANFIS model prediction. Table 4.8 shows the comparison of GA-ANFIS and ANFIS model results in case of non-dimensional input parameters and the scatter plot of prediction and actual values of GA-ANFIS is as seen in Fig 4.14. The Nash Sutcliffe efficiency of the GA-ANFIS model of testing is very poor.

Further to check if PSO is better than GA in improving the ANFIS training PSO-ANFIS model is employed with an objective function to reduce the RMSE of the prediction of wave reflection ( $K_r$ ) of the semicircular breakwater. In the employment of PSO-ANFIS model, an initial FIS for the dataset of non-dimensional input parameters is generated using FCM and the PSO approach to fine tune the ANFIS training. The antecedent and consequent parameters of ANFIS are tuned by PSO. In the FCM the number of clusters is set as 9, as the data involved nine different wave heights. The optimal found  $m=1.8$  with least RMSE is set for a maximum FCM iteration of 25 and minimum improvement of  $1e-5$ . The model is run for different values of  $c_1$  and  $c_2$  but the least RMSE was attained only when the acceleration coefficient  $c_1=2$ ,  $c_2=2$ . The model is run for various population size and finally set for a population size of 30 and 5000 iterations which gave the best prediction with least RMSE for inertia weight of  $w=0.4$ . Table 4.8 shows the comparison of PSO-ANFIS and ANFIS model results in case of non-dimensional input parameters. The PSO-ANFIS model prediction for training  $R=0.9109$  is slightly better than ANFIS model training and for testing  $R=0.7900$ . On further increase of iterations in PSO-ANFIS, the model results are not good. Though PSO-ANFIS model root mean square error is found on the higher side, among the four models the PSO-ANFIS had lower error  $RMSE=0.1908$ . The NSE of all the models is good for training whereas for testing it was very poor. Also, a scatter plot of predicted  $K_r$  and actual

values of PSO-ANFIS is as seen in Fig 4.14. Among the four models considered PSO-ANFIS model gave better results. However, the results show that the prediction performance of different soft computing models for non-dimensional input parameters in the case of beyond the data range is not satisfactory from the statistics obtained. Fig. 4.15 shows the comparison of predicted  $K_r$  by ANN, ANFIS, GA-ANFIS and PSO-ANFIS models.

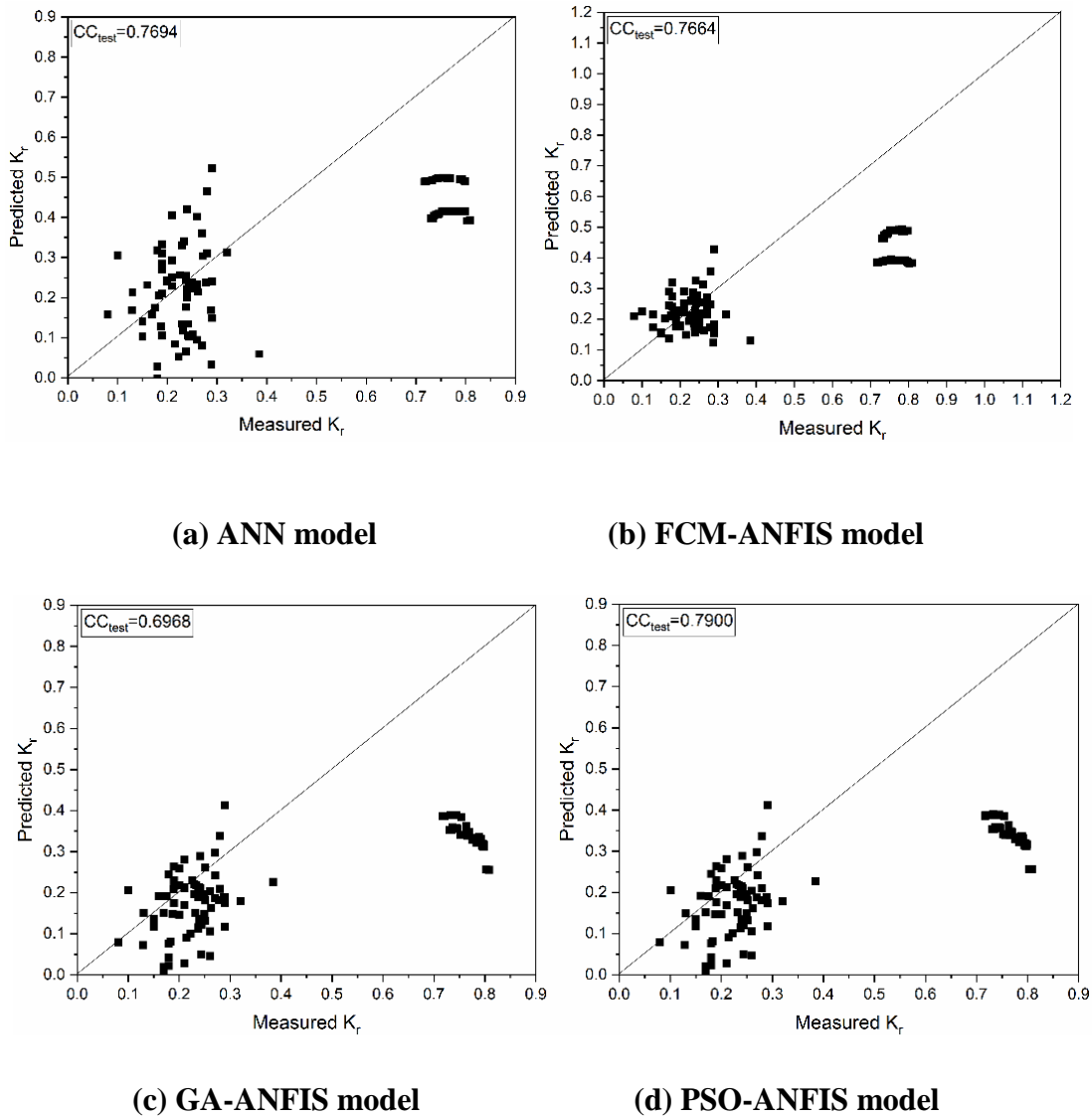


**Fig. 4.14 Scatter plot of predicted versus actual values of  $K_r$  for different models for the case of beyond the range with non-dimensional input parameters**

**Table 4.7 Error metrics for different soft computing models for non-dimensional input parameters in the case of of beyond the data range for predicting reflection coefficient**

Case	Error metrics	Soft computing models							
		ANN		ANFIS		GA-ANFIS		PSO-ANFIS	
		Train	Test	Train	Test	Train	Test	Train	Test
<b>Beyond</b>	<b>R</b>	0.8919	0.7694	0.8541	0.7664	0.9016	0.6968	0.9109	0.7900
	<b>RMSE</b>	0.0903	0.3114	0.1038	0.3362	0.0873	0.2004	0.0823	0.1908
	<b>NSE</b>	0.7949	0.2007	0.7294	0.0684	0.8081	0.1325	0.8297	0.2141
	<b>SI</b>	39.80	64.98	45.72	70.15	38.50	83.59	36.27	39.81
	<b>BIAS</b>	0.0016	-0.2039	-1.2 E -08	-0.2124	-0.0033	-0.0723	0.0004	-0.0658



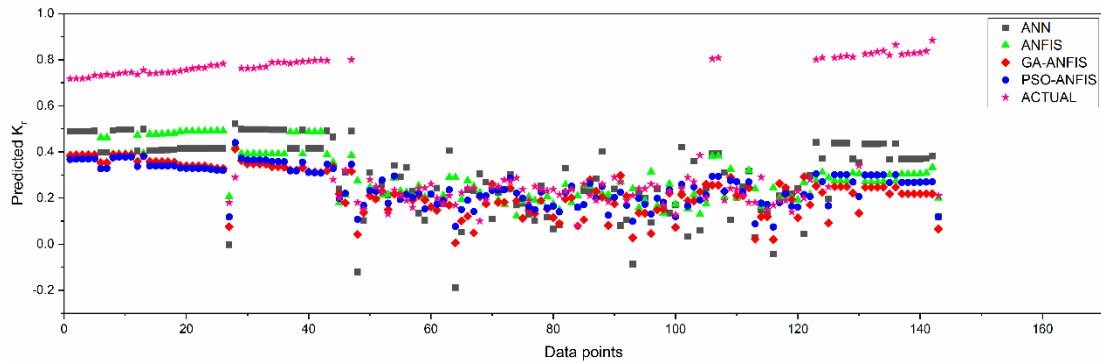


**Fig. 4.15 Comparison of predicted  $K_r$  by ANN, ANFIS, GA-ANFIS, PSO-ANFIS models for the case of beyond the range with non-dimensional input parameters with observed  $K_r$  values**

#### **4.3.4 Reflection coefficient prediction performance of different soft computing models for the case of conventional beyond data range for non-dimensional input parameters**

The training and testing of ANN Model for prediction of conventional beyond the data range are carried out. The best ANN architecture obtained by trial and error basis is 5-12-1 with the least testing RMSE=0.1524 for epoch 13. The network is fed with 5 inputs and the prediction of single output is done by varying the number of neurons in the only set hidden layer. The values of the measure of error are presented in Table 4.9. The correlation coefficient for training  $R=0.8744$  and for testing  $R=0.8013$  is found. Fig. 4.16 shows the scatter plot of model predicted  $K_r$  and actual values for conventional beyond the data range testing using ANN.

The ANFIS model with fuzzy C-means clustering is adopted with the input membership function for each input variable is 'gaussmf' and the output membership function type is 'linear' for sugeno systems. Here the number of clusters is set as 9 and the FIS is generated for five inputs and one output. The model predictions were best with relatively lower RMSE=0.1231 when the exponent of the partition matrix component was set to  $m=1.8$ . The minimum improvement factor is set as of  $1e-5$  in the objective function in between the two consecutive iterations and the maximum iterations count was set to 50. Training and testing performance of the ANFIS model for conventional beyond the data range is validated by error measure as shown in Table 4.9 and the scatter plot of prediction and actual values of ANFIS is as in Fig. 4.16. The prediction

of  $K_r$  for non-dimensional input parameters by ANFIS improved the R-value of training to 0.9015 and testing to 0.8721 with respect to ANN prediction.

An attempt to improve the ANFIS training was done by GA-ANFIS model whose objective function is to reduce the RMSE of the prediction of  $K_r$  of the semicircular breakwater. In the FCM the number of clusters was set as 9, with  $m=1.8$  was optimal with least RMSE, for a maximum FCM iteration of 50 and minimum improvement of  $1e-5$ . GA is sensitive to its parameters i.e., population size and the maximum number of iterations. The GA-ANFIS model was run for various population size 10, 15, 20, 25, 30, 35, 40, 50, 100, and finally set for a population size of 30 with maximum number of iterations set to 8000, the mutation rate was set to 0.15, the crossover percentage was set to 0.4, mutation percentage was set to 0.7, and the selection pressure was set to 8. GA-ANFIS model prediction was found to improve over the ANFIS model prediction and also was found to be the best among the four models adopted. Table 4.9 shows the comparison of GA-ANFIS and ANFIS model results in case of non-dimensional input parameters and the scatter plot of prediction and actual values of GA-ANFIS is as seen in Fig. 4.16. The Nash Sutcliffe efficiency of the GA-ANFIS model of testing is 82% best among all four models for this case of prediction. The scatter index reduced relatively with respect to the other three models shown in Table 4.9.

Further to check if PSO improves the ANFIS training, PSO-ANFIS model is employed with an objective function to reduce the RMSE of the prediction of wave reflection ( $K_r$ ) of the semicircular breakwater. In the employment of PSO-ANFIS model, an initial FIS for the dataset of non-dimensional input parameters was generated using FCM and the PSO approach to fine tune the ANFIS training. In the FCM the number of clusters was set as 9, as the data involved 9 different wave heights. The optimal found  $m=1.8$  with least RMSE was set for a maximum FCM iteration of 50 and minimum improvement of  $1e-5$ . The model was run for different values of  $c_1$  and  $c_2$  but the least RMSE was attained only when the acceleration coefficient  $c_1=2$ ,  $c_2=2$ . The model was run for various population size and finally set for a population size of 80 and 1000 iterations which gave the best prediction with least RMSE for inertia weight of  $w=0.4$ . Table 4.9 shows the comparison of PSO-ANFIS and ANFIS model results in case of non-dimensional input parameters. The PSO-ANFIS model prediction for training

$R=0.9234$  was slightly better than ANFIS model training however, did not improve on the testing  $R=0.8522$ . On further increase of iterations in PSO-ANFIS, the model results did not improve. A scatter plot of predicted  $K_r$  and actual values of PSO-ANFIS is as seen in Fig. 4.16. Among the four models considered GA-ANFIS model gave better results. However, the results show that the prediction performance of different soft computing models for non-dimensional input parameters in the case of conventional beyond the data range is satisfactory from the statistics obtained. Fig. 4.17 shows the comparison of predicted  $K_r$  by ANN, ANFIS, GA-ANFIS and PSO-ANFIS models with observed  $K_r$  values.

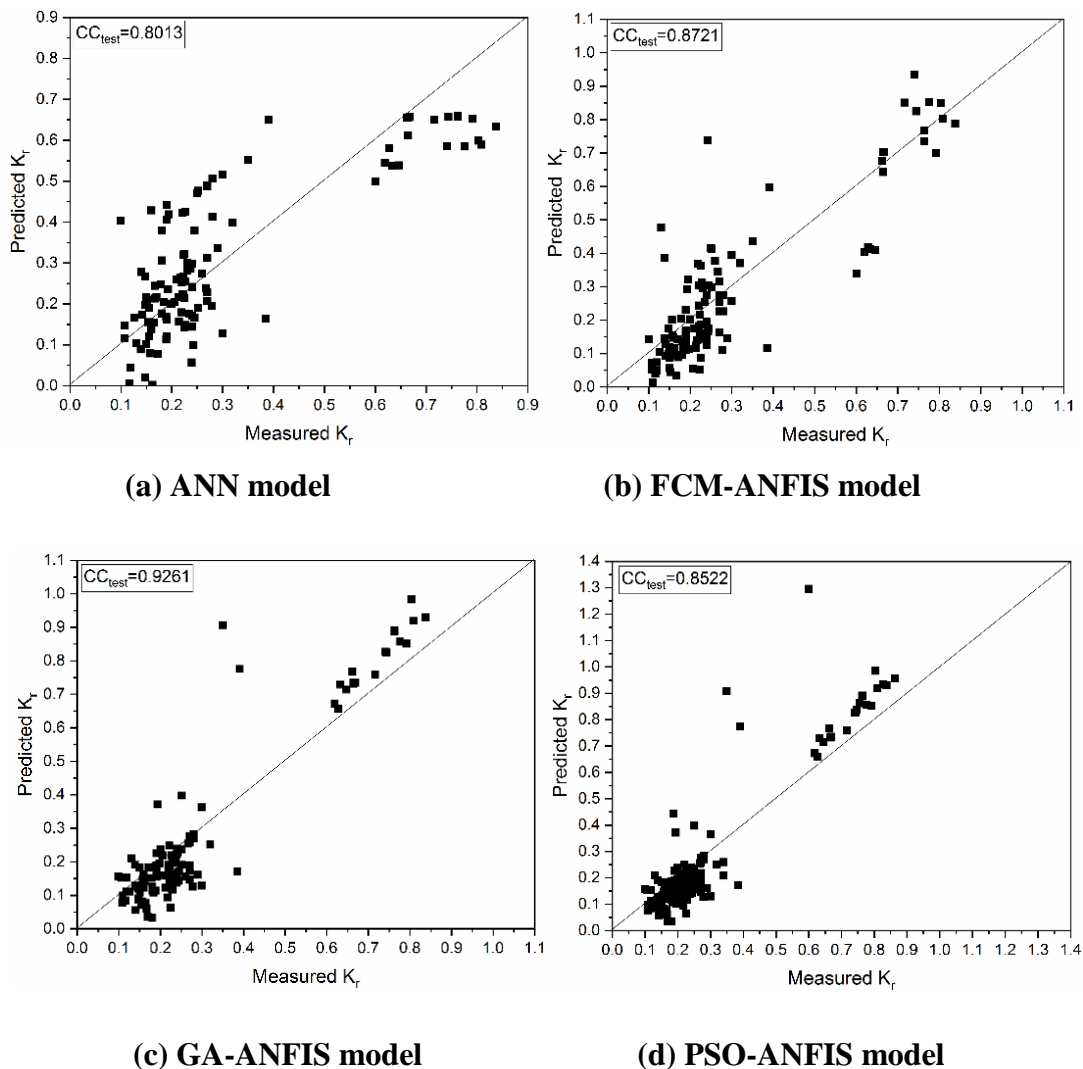


**Fig. 4.16** Scatter plot of predicted versus actual values of  $K_r$  for different models for the case of conventional beyond the range with non-dimensional input parameters

**Table 4.8 Error metrics for different soft computing models for non-dimensional input parameters in the case of conventional beyond the data range for predicting reflection coefficient**

Case	Error metrics	Soft computing models							
		ANN		ANFIS		GA-ANFIS		PSO-ANFIS	
		Train	Test	Train	Test	Train	Test	Train	Test
Conventional beyond	R	0.8744	0.8013	0.9015	0.8721	0.9755	0.9261	0.9234	0.8522
	RMSE	0.1266	0.1524	0.1124	0.1231	0.0571	0.1039	0.0999	0.1420
	NSE	0.7717	0.6240	0.7717	0.7551	0.9500	0.8252	0.8578	0.6737
	SI	45.10	57.74	45.10	46.60	20.33	39.36	35.59	53.79
	BIAS	-0.0132	-0.0006	-0.0132	0.0031	-0.0002	0.0044	-0.0030	0.0044

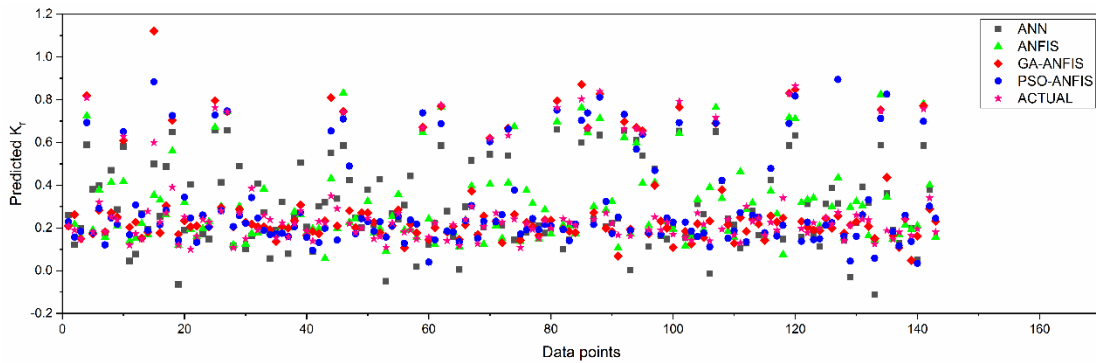


**Fig. 4.17 Comparison of predicted  $K_r$  by ANN, ANFIS, GA-ANFIS, PSO-ANFIS models for the case of conventional beyond the range with non-dimensional input parameters with observed  $K_r$  values**

#### **4.4 RESULTS AND DISCUSSION OF $K_r$ PREDICTION OF SEMICIRCULAR BREAKWATER USING DIFFERENT SOFT COMPUTING MODELS FOR 1274 GLOBAL DATA POINTS**

Apart from the previously mentioned cases, the reflection coefficient prediction performance of different soft computing models for dimensional and non-dimensional input parameters for 1274 data points is done by conventional data segregation method. This particular case was carried out when additional dataset of 250 points was available. The entire dataset was randomized, normalized and a data division of 75% for training and 25% for testing was taken up to check the prediction possibility for both dimensional and non-dimensional input parameters.

##### **4.4.1 Reflection coefficient prediction performance of different soft computing models using dimensional input parameters for global data of 1274 points**

The training and testing of ANN Model for prediction of the Reflection coefficient are carried out. The best ANN architecture obtained by trial and error basis is 5-11-1 with the least testing RMSE=0.0321 for epoch 18.

The network is fed with 7 inputs and the prediction of single output is done by varying the number of neurons in the only set hidden layer. The values of the measure of error are presented in Table 4.10. The correlation coefficient for training  $R=0.9834$  and for

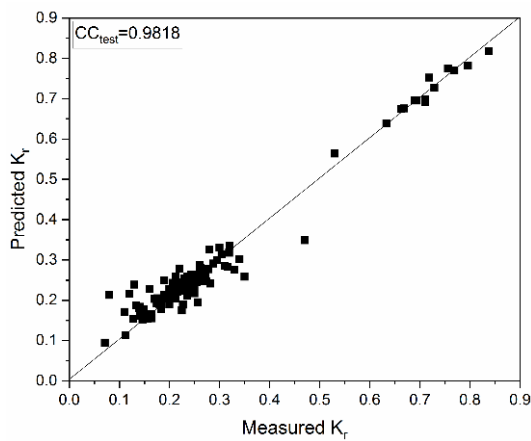
testing  $R=0.9697$  is found. Fig. 4.18 shows the scatter plot of model predicted  $K_r$  and actual values for 1274 global data points using ANN. The ANN prediction had better correlation with respect to actual values and outperformed the other three models used. The model efficiency is highest of all models i.e., 96% with relatively least RMSE having a lower scatter index and a small positive bias of 0.0043.

The ANFIS model with fuzzy C-means clustering is adopted with the input membership function for each input variable is 'gaussmf' and the output membership function type is 'linear' for sugeno systems. Here the number of clusters is set as 9. The model prediction is best with relatively lower  $RMSE=0.0499$  when the exponent of partition matrix component was set to  $m=2.0$ . The minimum improvement factor was set as of  $1e-5$  in the objective function in between the two consecutive iterations and the maximum iterations count is set to 25. Training and testing performance of the ANFIS model for conventional data segregation is validated by error measure as shown in Table 4.10 and the scatter plot of predicted  $K_r$  and actual values of ANFIS is as in Fig 4.18. Here FCM constructs a FIS with seven inputs and one output. The prediction of  $K_r$  for non-dimensional input parameters by ANFIS improved the R-value of training to 0.9875 whereas, testing reduced to 0.9589 with respect to the R-value of ANN prediction.

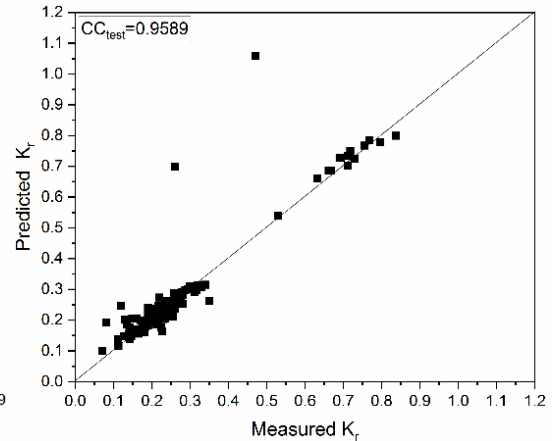
An attempt to improve the ANFIS training is done by GA-ANFIS model whose objective function is to reduce the RMSE of the prediction of  $K_r$  of the semicircular breakwater. In the FCM the number of clusters is set as 9, with  $m=2.0$  was optimal with least RMSE, for a maximum FCM iteration of 25 and minimum improvement of  $1e-5$ . GA is sensitive to its parameters i.e., population size and the maximum number of iterations. The GA-ANFIS model was run for various population size 10, 15, 20, 25, 30, 35, 40, 50, 100, and finally set for a population size of 70 with a maximum number of iterations set to 1000 which gave better R-value. The mutation rate was set to 0.15, the crossover percentage was set to 0.4, mutation percentage was set to 0.7, and the selection pressure was set to 8. GA-ANFIS model prediction is found to improve over the ANFIS model prediction with an R-value of training as 0.9819 and for testing as 0.9753 but did not improve over the ANN prediction. Accordingly the scatter index is

found lesser than that of the ANFIS model and the efficiency of the GA-ANFIS model is 95% and lower RMSE=0.0373 with lesser bias than the ANFIS model. Table 4.10 shows the comparison of GA-ANFIS and ANFIS model results in case of non-dimensional input parameters and the scatter plot of predicted  $K_r$  and actual values of GA-ANFIS is as seen in Fig 4.18. The Nash Sutcliffe efficiency of the GA-ANFIS model of testing is 82% best among all four models for this case of prediction. The scatter index reduced relatively with respect to the other three models shown in Table 4.10.

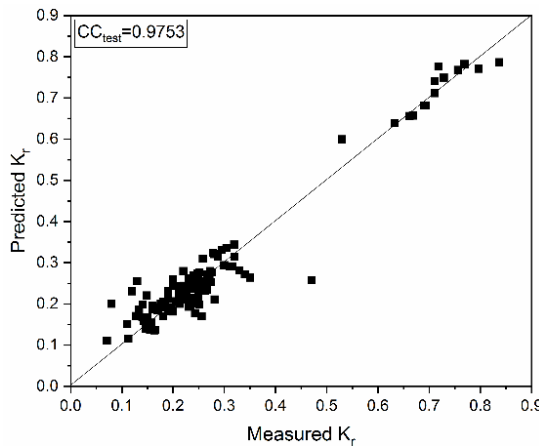
Further to check if PSO is better than GA in improving the ANFIS training PSO-ANFIS model is employed with an objective function to reduce the RMSE of the prediction of  $K_r$  of the semicircular breakwater. In the employment of PSO-ANFIS model, an initial FIS for the dataset of non-dimensional input parameters is generated using FCM and the PSO is applied to fine-tune the ANFIS training. In the FCM the number of clusters was set as 9, as the data involved 9 different wave heights. The optimal found  $m=2$  with least RMSE was set, for a maximum FCM iteration of 25 and minimum improvement of  $1e-5$ . The model is run for different values of  $c_1$  and  $c_2$  but the least RMSE is attained only when the acceleration coefficient  $c_1=2$ ,  $c_2=2$ . The model is run for various population size and finally set for a population size of 70 and 1000 iterations which gave the best prediction with least RMSE for inertia weight of  $w=0.4$ . Table 4.10 shows the comparison of PSO-ANFIS and ANFIS model results in case of non-dimensional input parameters. The PSO-ANFIS model prediction for testing  $R=0.9711$  is better than ANFIS model however, could not improve over the results of ANN model prediction. A scatter plot of predict  $K_r$  and actual values of PSO-ANFIS is as seen in Fig 4.18 and the performance is presented in Table 4.10. Among the four models considered the ANN model gave best results this shows that even individual models predict well for some datasets. Fig. 4.19 shows the comparison of predicted  $K_r$  by ANN, ANFIS, GA-ANFIS and PSO-ANFIS models with observed  $K_r$  values.



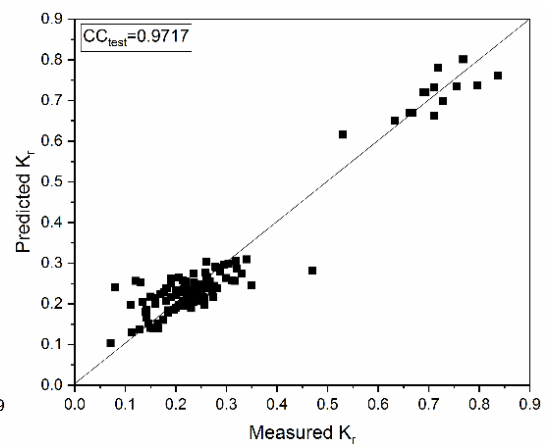
(a) ANN model



(b) FCM-ANFIS model



(c) GA-ANFIS model



(d) PSO-ANFIS model

**Fig. 4.18** Scatter plot of predicted versus actual values of  $K_r$  for different models in case of 1274 global data points with dimensional input parameters

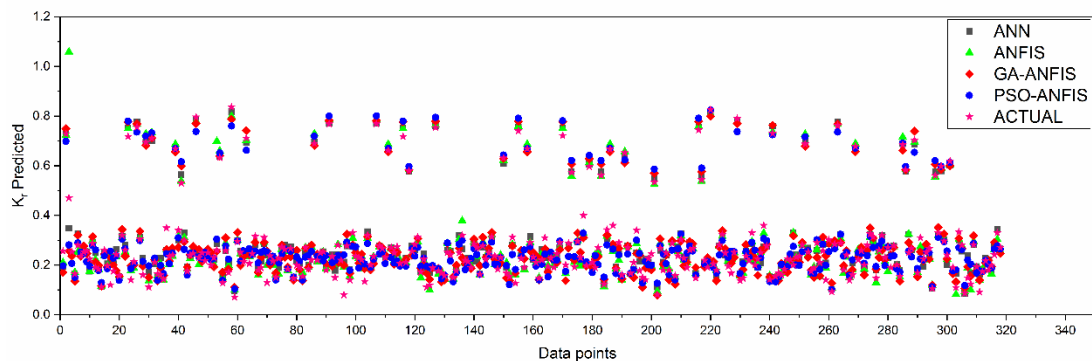


**Fig. 4.19** Comparison of predicted  $K_r$  by ANN, ANFIS, GA-ANFIS, PSO-ANFIS models for the case of dimensional input parameters with observed  $K_r$  values



**Table 4.9 Error metrics for different soft computing models for dimensional input parameters in the case of global data of 1274 points for predicting reflection coefficient**

Input form	Error metrics	Soft computing models							
		ANN		ANFIS		GA-ANFIS		PSO-ANFIS	
		Train	Test	Train	Test	Train	Test	Train	Test
<b>Dimensional</b>	<b>R</b>	0.9869	0.9818	0.9875	0.9589	0.9819	0.9753	0.9862	0.9711
	<b>RMSE</b>	0.0297	0.0321	0.0289	0.0499	0.0347	0.0373	0.0298	0.0402
	<b>NSE</b>	0.9738	0.9633	0.9750	0.9116	0.9641	0.9503	0.9735	0.9424
	<b>SI</b>	9.83	11.31	9.59	15.29	11.50	13.17	9.88	14.18
	<b>BIAS</b>	0.0018	0.0043	2.20084E-08	0.0050	-0.0001	0.0025	-0.0003	0.0021

#### **4.4.2 Reflection coefficient prediction performance of different soft computing models using non-dimensional input parameters for global data of 1274 points**

The training and testing of ANN Model for prediction of  $K_r$  for 1274 global data points are carried out. The best ANN architecture obtained by trial and error basis is 5-11-1 with the least testing RMSE=0.1703 for epoch 133. The network is fed with 5 inputs and the prediction of single output is done by varying the number of neurons in the only set hidden layer. The values of the measure of error are presented in Table 4.11. The correlation coefficient for training  $R=0.6803$  and for testing  $R=0.6003$  is found. Fig. 4.20 shows the scatter plot of model predicted  $K_r$  and actual values for the case of 1274 global data points testing using ANN.

The ANFIS model with fuzzy C-means clustering is adopted with the input membership function for each input variable is 'gaussmf' and the output membership function type is 'linear' for sugeno systems. Here the number of clusters is set as 9 as the entire dataset has 9 distinct wave heights. The model prediction for  $m=2$  with the minimum improvement factor set as of 0.001 in the objective function in between the two consecutive iterations and the maximum iterations count is set to 25 for which RMSE=0.1282 is obtained. Training and testing performance of ANFIS model for the case of 1274 global data points is validated by error measure as shown in Table 4.11 and the scatter plot of predict  $K_r$  and actual values of ANFIS is as in Fig. 4.20. Here FCM constructs a FIS with five inputs and one output. ANFIS predicted the  $K_r$  value for non-dimensional input parameters with an improvement in the R-value of training and testing with respect to ANN prediction as seen in Table 4.11.

An attempt to further improve the ANFIS training was done by GA-ANFIS model whose objective function is to reduce the RMSE of the prediction of  $K_r$  of the semicircular breakwater. In the FCM the number of clusters was set as 9, with  $m=1.2$  was optimal with least RMSE, for a maximum FCM iteration of 50 and minimum improvement of  $1e-5$ . GA parameters population size and the maximum number of iterations ARE varied to arrive at the best R values and lower RMSE. Finally, a

population size of 20 with a maximum number of iterations 8000 was found optimal. Also, the mutation rate is set to 0.15, the crossover percentage is set to 0.4, mutation percentage is set to 0.7, and the selection pressure is set to 8. GA-ANFIS model prediction is found to improve over the ANFIS model prediction and is found to be the best among the four models adopted. Table 4.11 shows the comparison of GA-ANFIS and ANFIS model results in case of non-dimensional input parameters and the scatter plot of prediction and actual values of GA-ANFIS is as seen in Fig. 4.20. The Nash Sutcliffe efficiency of the GA-ANFIS model of testing is 66% best among all four models for this case of prediction. The scatter index for testing reduced relatively with respect to the other three models as shown in Table 4.11.

Further to check if PSO is better than GA in improving the ANFIS training PSO-ANFIS model is employed with an objective function to reduce the RMSE of the prediction of wave reflection ( $K_r$ ) of the semicircular breakwater. In the employment of PSO-ANFIS model, an initial FIS for the dataset of non-dimensional input parameters is generated using FCM and the PSO is applied to fine-tune the ANFIS training. In the FCM the number of clusters was set as 9, as the data involved 9 different wave heights. The optimal found  $m=1.7$  with least RMSE is set for a maximum FCM iteration of 50 and minimum improvement of  $1e-5$ . The model is run for different values of  $c_1$  and  $c_2$  but the least RMSE was attained only when the acceleration coefficient  $c_1=2$ ,  $c_2=2$ . The model is run for various population size and finally set for a population size of 50 and 1000 iterations which gave the best prediction with least RMSE for inertia weight of  $w=0.7$ . Table 4.11 shows the comparison of PSO-ANFIS and ANFIS model results in case of non-dimensional input parameters. The PSO-ANFIS model prediction for training  $R=0.8886$  is better than ANFIS model training and for the testing  $R=0.7569$ . On further increase of iterations in PSO-ANFIS, the model results did not improve. A scatter plot of prediction and actual values of PSO-ANFIS is as seen in Fig. 4.20. Among the four models considered GA-ANFIS model gave better results. Fig. 4.21 shows the comparison of predicted  $K_r$  by ANN, ANFIS, GA-ANFIS and PSO-ANFIS models with observed  $K_r$  values.

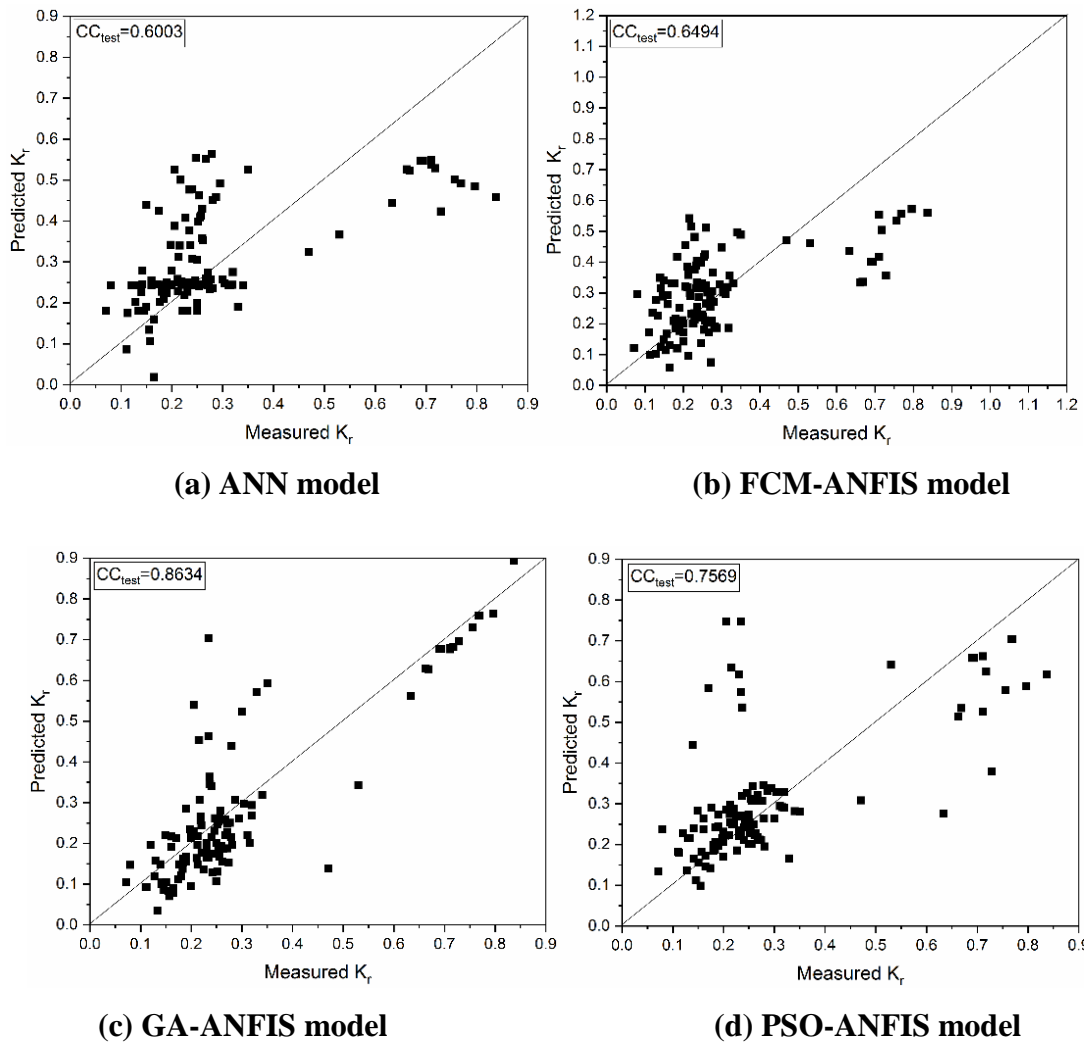


**Fig. 4.20** Scatter plot of predicted versus actual values of  $K_r$  for different models in case of 1274 global data points with non-dimensional input parameters

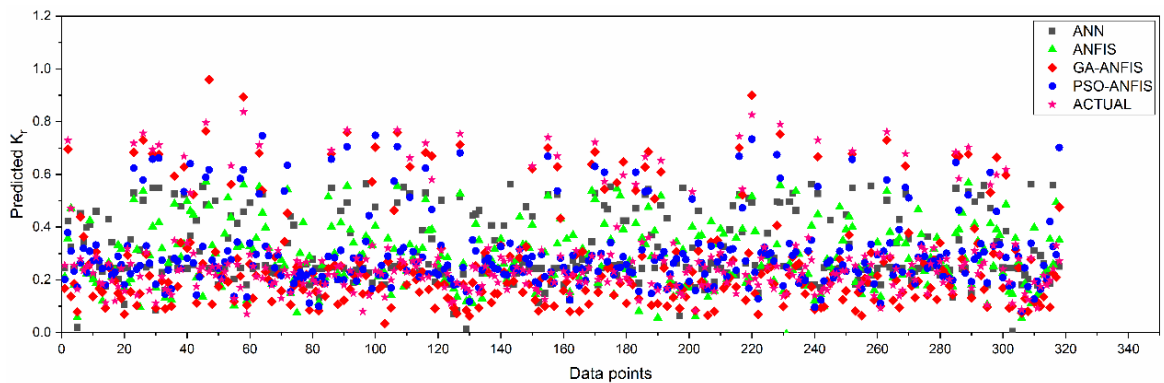


**Fig. 4.21** Comparison of predicted  $K_r$  by ANN, ANFIS, GA-ANFIS, PSO-ANFIS models for the case of non-dimensional input parameters with observed  $K_r$  values

**Table 4.10 Error metrics for different soft computing models for non-dimensional input parameters in the case of global data of 1274 points for predicting reflection coefficient**

Input form	Error metrics	Soft computing models							
		ANN		ANFIS		GA-ANFIS		PSO-ANFIS	
		Train	Test	Train	Test	Train	Test	Train	Test
Non-dimensional	R	0.6803	0.6003	0.6991	0.6494	0.9096	0.8634	0.8886	0.7569
	RMSE	0.1656	0.1703	0.1312	0.1282	0.0869	0.0974	0.0785	0.1116
	NSE	0.4621	0.3190	0.4886	0.4158	0.7757	0.6626	0.8209	0.5580
	SI	58.26	65.07	43.45	45.20	28.78	34.34	25.97	39.32
	BIAS	-0.0060	0.0258	3.129E-05	0.0074	-0.0184	-0.0151	-0.0097	0.0160

#### **4.5 CLOSURE**

The proposed approach of predicting  $K_r$  in below, conventional below, beyond, and conventional beyond the data ranges of available experimental data is carried out successfully and presented. Prediction is reasonably good for all the cases except in the case of beyond the range data particularly when the input data was non-dimensional form. With dimensional as well as non-dimensional input parameters though the improvement of ANFIS prediction statistics after optimization by GA, PSO is not significant, any improvement in the prediction of the reflection coefficient is considered good. The maximum  $K_r$  value obtained from experimental data is 0.884 and from prediction, the value is 1.05. As the values are corresponding to the scale down model of the actual sea conditions even a small improvement in the prediction value of output ( $K_r$ ) is good.



5.1 PREDICTION OF RELATIVE WAVE RUN-UP ( $R_u/H_i$ )

Wave run-up ( $R_u$ ) is defined as the height of rising of the incident waves on the face of the breakwaters above the still water level. Wave run-up is a process influenced by various wave characteristics, structural parameters, and local effects. In the study, the wave run-up ( $R_u$ ) has been expressed as a non-dimensional parameter ( $R_u/H_i$ ). The relative wave run-up parameter ( $R_u/H_i$ ) of the emerged seaside perforated semicircular breakwater has not been much explored, and there is a research gap, particularly in the application of soft computing techniques to predict  $R_u/H_i$ . All of the possible available literature regarding  $R_u/H_i$  has been discussed in chapter 2. The present chapter includes the data segregation, prediction of  $R_u/H_i$  using different soft computing models as well as the assessment of the models.

5.1.1 Data segregation for prediction of relative wave run-up ( $R_u/H_i$ )

The experimental input parameters for the set of data obtained from Marine structure Laboratory, NITK, Surathkal, India, is given in the Table 3.3 Data segregation for prediction of relative wave run-up parameter ( $R_u/H_i$ ) for dimensional and non-dimensional input parameters is done as follows:

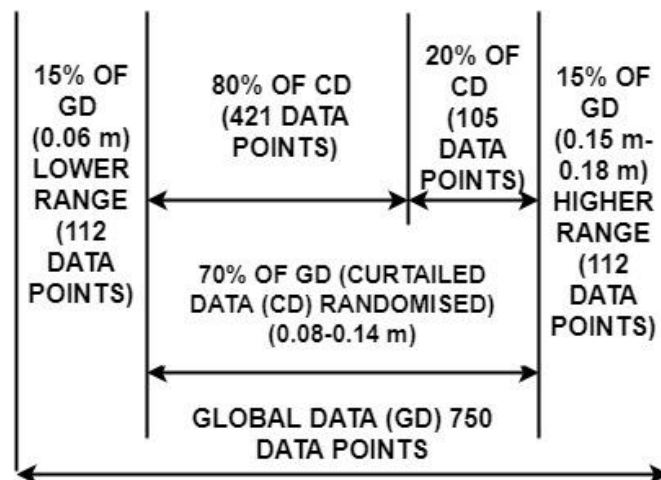


Fig. 5.1 Typical data segregation for  $R_u/H_i$  prediction of SBW



The data segregation procedure for the typical case of wave height ( $H_i$ ) for Run-up is,

- 1) The entire ensemble, called here as Global data (GD) is sorted in the increasing order of wave heights ( $H_i$ )
- 2) Now, the lowest 15% of the Global data and the highest 15% of the Global data is carved out.
- 3) The remaining 70% of Global data, which is called as curtailed data is randomized for application of soft computing techniques.
- 4) The curtailed data is again divided into two parts 80% and 20% for training and testing respectively.
- 5) The case I: Below the range, data is introduced in the testing data for prediction of the performance of emerged perforated SBW.
- 6) Case II: Beyond the range, data is introduced in the testing data for prediction of the performance of emerged perforated SBW.
- 7) Also the conventional data segregation of 70:30 and corresponding prediction is undertaken for the randomized Global data (GD)

## **5.2 RESULTS AND DISCUSSION OF $R_u/H_i$ PREDICTION OF SEMICIRCULAR BREAKWATER USING DIFFERENT SOFT COMPUTING MODELS FOR DIMENSIONAL INPUT PARAMETERS**

In the current study the prediction of relative wave run-up parameter is done for dimensional input parameters i.e.,  $H_i$ ,  $T$ ,  $S$ ,  $D$ ,  $R$ ,  $d$  and  $h_s$ . The conventional data segregation was done as 70% for training and 30% for testing and the corresponding prediction is undertaken. The prediction of the relative wave run-up parameter by using ANN, ANFIS, GA-ANFIS, and PSO-ANFIS was carried out successfully.

The training and testing of ANN model for prediction of relative wave run-up parameter are carried out. The best ANN architecture for the available data sets is determined on a trial and error basis with respect to the error metrics. The ANN network was designed for 7 inputs and single output the relative wave run-up parameter. The ANN with a single hidden layer consisting of 11 neurons in it predicted the  $R_u/H_i$  very well with R-

value 0.9810 and 0.8095 for training and testing respectively. Table 5.2 represents the optimal parameters for the ANN model arrived in the study.

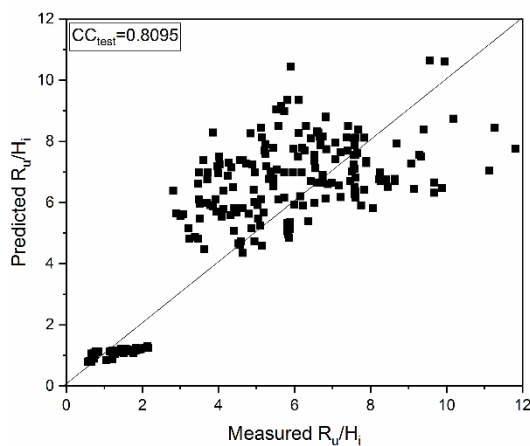
In order to improve this result, ANFIS was employed. The ANFIS model with fuzzy C-means clustering is adopted with the input membership function for each input variable is 'gaussmf' and the output membership function type is 'linear' for sugeno systems. Fuzzy C-means clustering constructs a fuzzy inference system (FIS) with 7 inputs and single output the relative wave run-up parameter. Although several combinations of the models were tried altering the exponent of partition matrix' the ANFIS model training and testing did not improve in the case of dimensional parameters. Table 5.2 represents the optimal parameters arrived in the study for the ANFIS model. ANFIS predicted the  $R_u/H_i$  parameter for dimensional input parameters with an improvement in the R-value of training but, for testing, it is similar to ANN prediction as seen in Table 5.3.

Further, the ANFIS was optimized with GA and PSO techniques individually. The model parameters set were crossover rate as 0.7, mutation rate as 0.4 and selection pressure as 8. In the case of GA-ANFIS model the prediction of  $R_u/H_i$  did not improve the correlation coefficient value of ANFIS, it is found to be 0.9822 for training and 0.8075 for testing. The population size was varied from 10 to 100, and the number of iterations was also altered and among the different combinations tried better results were obtained when the population size is set to 90 and iterations is set to 7000. Table 5.2 represents the optimal parameters arrived in the study for GA-ANFIS model.

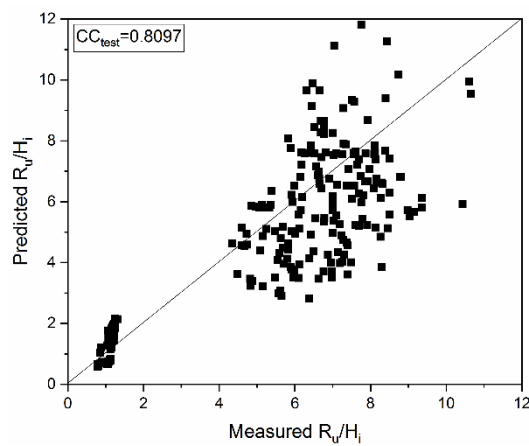
Whereas, in the case of PSO-ANFIS model the prediction of  $R_u/H_i$  improved with R-value of 0.9836 and 0.8149 for training and testing respectively. Here the population size is varied from 10 to 100, and the number of iterations is also varied, and best results were obtained when the population size is set to 100 and iterations is set to 1000. The other model parameters set were inertia weight 0.4 cognitive acceleration ( $c_1$ )=2, social acceleration ( $c_2$ )=2. Among the four models employed the PSO-ANFIS model well predicted the  $R_u/H_i$  parameter with the highest R-value and least error RMSE= 0.1497.

If we look into the Nash Sutcliffe efficiency of PSO-ANFIS model it is found to be the highest among all the four models i.e., 0.5870. However, the model efficiency of 58% is not highly appreciable in the prediction of ( $R_u/H_i$ ). Table 5.2 represents the optimal parameters arrived in the study for PSO-ANFIS model.

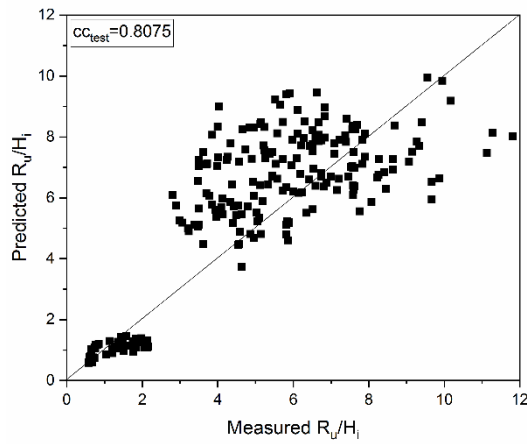
The scatter plot for the individual model is as seen in Fig 5.1 and among the scatter index of all the four models it is best for the PSO-ANFIS. The performance of each model is presented in Table 5.3, and it is found that PSO improved the ANFIS result whereas GA did not. However, the hybrid methods consumed time when the population size and number of iterations were increased. The PSO-ANFIS model has a slight overestimation of values being positively biased. Also, the  $R=0.8149$  of PSO-ANFIS is better than the ANFIS and GA-ANFIS models. The scatter index of PSO-ANFIS being 37.30 is better than 38.06 (ANFIS) and 38.25 (GA-ANFIS). Hence the application of PSO to ANFIS improved the training of the ANFIS model and finally a better prediction is possible reducing the root mean square error compared to the other three models considered. The Fig.5.3 shows the comparison of predicted  $R_u/H_i$  by ANN, ANFIS, GA-ANFIS, PSO-ANFIS models for the case of dimensional input parameters with observed values.



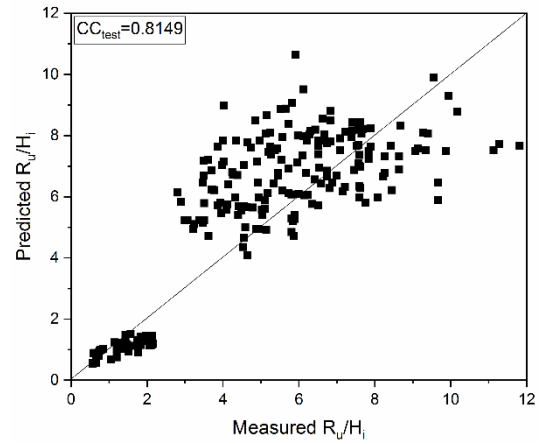
**(a) ANN model**



**(b) ANFIS model**



(c) GA-ANFIS model



(d) PSO-ANFIS model

**Fig. 5.2** Scatter plot of predicted versus actual values of  $R_u/H_i$  for different models with dimensional input parameters

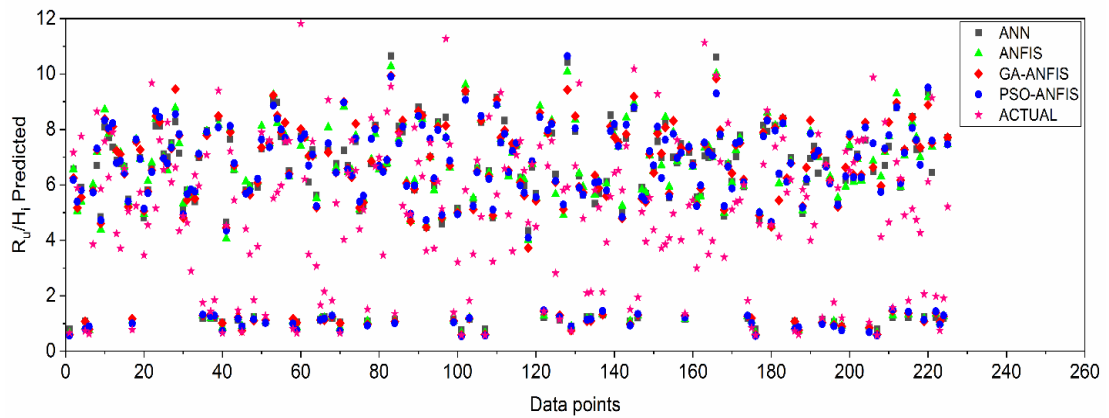


**Fig. 5.3** Comparison of predicted  $R_u/H_i$  by ANN, ANFIS, GA-ANFIS, PSO-ANFIS models for the case of dimensional input parameters with observed values

**Table 5.1 Optimal parameters of different models for dimensional input parameters**

<b>Model</b>	<b>Parameters</b>	<b>Values</b>
ANN	Number of neurons	11
	Epochs	8
ANFIS	Partition matrix	1.8
	Minimum improvement factor	0.001
	Number of clusters	9
GA-ANFIS	Population size	90
	Number of generations	7000
PSO-ANFIS	Number of iterations	1000
	Number of Particles	100

**Table 5.2 Error metrics for different soft computing models for dimensional input parameters in the case of 750 data points for predicting relative wave run-up parameter**

Input form	Error Metrics	Soft computing models							
		ANN		ANFIS (FCM)		GA-ANFIS		PSO-ANFIS	
		Train	Test	Train	Test	Train	Test	Train	Test
Dimensional	R	0.9810	0.8095	0.9838	0.8097	0.9822	0.8075	0.9836	0.8149
	RMSE	0.0488	0.1502	0.0449	0.1527	0.0469	0.1535	0.0450	0.1497
	NSE	0.9618	0.5620	0.9677	0.5470	0.9647	0.5425	0.9675	0.5648
	SI	10.75	37.42	9.88	38.06	10.33	38.25	9.92	37.30
	BIAS	-0.0044	0.0499	8.19185E-09	0.0542	-2.328E-05	0.5425	-0.0009	0.0517

### 5.3 RESULTS AND DISCUSSION OF $R_u/H_i$ PARAMETER PREDICTION OF SEMICIRCULAR BREAKWATER USING DIFFERENT SOFT COMPUTING MODELS FOR NON-DIMENSIONAL INPUT PARAMETERS

In the present study the prediction of relative wave run-up parameter ( $R_u/H_i$ ) is done for non-dimensional input parameters i.e.,  $H_i/gT^2$ ,  $d/gT^2$ ,  $S/D$ ,  $h_s/d$  and  $R/H_i$  obtained from dimensional analysis using Buckingham's  $\pi$ -theorem. The conventional data segregation is done as 70% for training and 30% for testing and the corresponding prediction is undertaken. The prediction of  $R_u/H_i$  by ANN, ANFIS, GA-ANFIS and PSO-ANFIS models is carried out successfully and compared as in Fig 5.5.

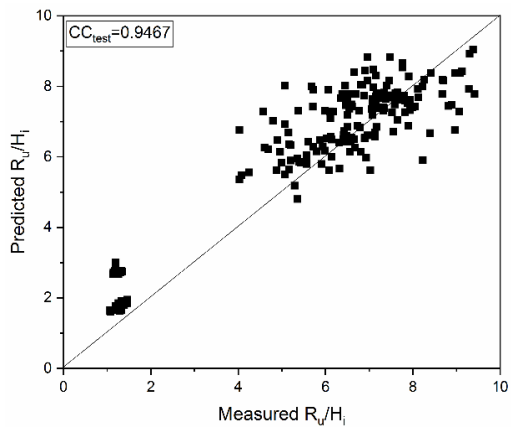
The ANN model is trained with 5 inputs and one output relative wave run-up parameter and tested to predict the relative wave run-up parameter. The best ANN architecture for the available data sets is arrived on a trial and error basis based on the error metrics. Table 5.4 represents the optimal parameters arrived in the study for the ANN model. The ANN with a single hidden layer consisting of 7 neurons in it predicted the  $R_u/H_i$  very well with higher  $R=0.9467$ , with least  $RMSE=0.0874$ , higher  $NSE=0.8694$ ,  $SI=20.41$  whereas, there is a positive bias of 0.0343. Among the four models employed the ANN prediction is found best, as seen in the error metrics of Table 5.5.

The ANFIS model predicted  $R_u/H_i$  parameter did not improve the ANN model results hence, needed further improvement. In order to improve the ANN model result, ANFIS was employed. The FCM-ANFIS model with the input membership function for each input variable is 'gaussmf' and the output membership function type is 'linear' for sugeno systems. Altering the exponent of the partition matrix 'm' from 1.1 to 2.2 the ANFIS model training and testing did not improve in this case. Fuzzy C-means clustering constructs a FIS with 5 inputs and single output the relative wave run-up parameter. Table 5.4 represents the optimal parameters arrived in the study for the ANFIS model.

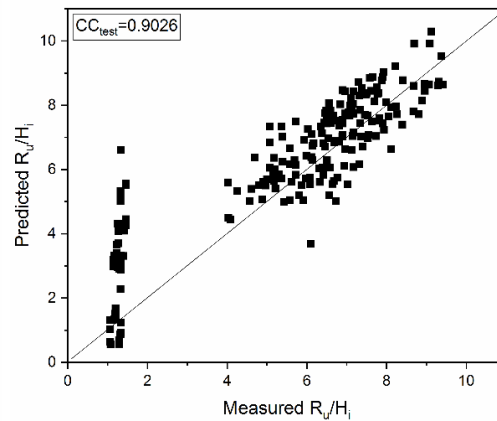
Two hybrid models are developed i.e GA-ANFIS and PSO-ANFIS. The optimization techniques GA and PSO are individually clubbed to ANFIS and prediction are compared. The optimal parameters for each algorithm used in the study are tabulated in Table 5.4. The model parameters set in GA were crossover rate as 0.7, mutation rate

as 0.4 and selection pressure as 8. The other model parameters set in PSO were inertia weight 0.4 cognitive acceleration ( $c_1$ )=2, social acceleration ( $c_2$ )=2. The performance of each model is presented in Table 5.5, and it is found that GA and PSO improved the ANFIS model result.

However, the hybrid methods consumed time when the population size and number of iteration is increased. From Table 5.5 as seen the NSE of GA-ANFIS model being 81% is higher compared to ANFIS and PSO-ANFIS models with a very small underestimation of values happened being negatively biased. Also, the testing  $R=0.9149$  of GA-ANFIS is better than the ANFIS and PSO-ANFIS models. The scatter index of GA-ANFIS being 24.12 is better than 27.15 (ANFIS) and 31.20 (PSO-ANFIS). Hence the application of GA to ANFIS improved the training of the ANFIS model and a better prediction is possible reducing the root mean square error. However, among the four models employed the ANN model best predicted the  $R_u/H_i$  parameter.

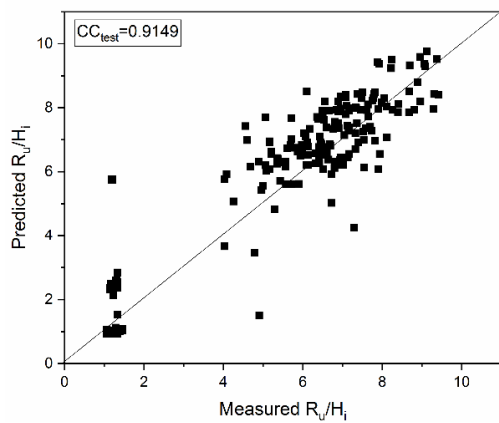


**(a) ANN model**

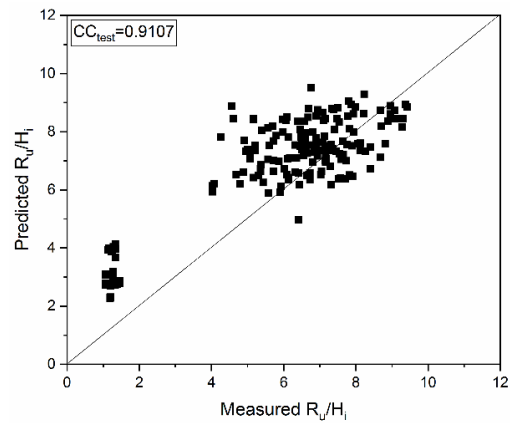


**(b) ANFIS model**





(c) GA-ANFIS model



(d) PSO-ANFIS model

**Fig. 5.4** Scatter plot of predicted versus actual values of  $R_u/H_i$  for different models with non-dimensional input parameters

**Table 5.3** Optimal parameters of different models for non-dimensional input parameters

Model	Parameters	Values
ANN	Number of neurons	7
	Epochs	50
ANFIS	Partition matrix	2
	Minimum improvement factor	0.001
	Maximum iterations	25
GA-ANFIS	Number of clusters	9
	Population size	30
PSO-ANFIS	Number of generations	7000
	Number of iterations	1000
	Number of Particles	80

**Table 5.4 Error metrics for different soft computing models for non-dimensional input parameters in the case of 750 data points for predicting relative wave run-up parameter**

Input form	Error Metrics	Soft computing models							
		ANN		ANFIS (FCM)		GA-ANFIS		PSO-ANFIS	
		Train	Test	Train	Test	Train	Test	Train	Test
Non-dimensional	<b>R</b>	0.9662	0.9467	0.9227	0.9026	0.9718	0.9149	0.9249	0.9107
	<b>RMSE</b>	0.0652	0.0874	0.0975	0.1162	0.0595	0.1032	0.0961	0.1336
	<b>NSE</b>	0.9334	0.8694	0.8513	0.7690	0.9444	0.8178	0.8555	0.6950
	<b>SI</b>	12.94	20.41	19.34	27.15	11.82	24.12	19.07	31.20
	<b>BIAS</b>	0.0013	0.0343	-2.167E-09	0.0495	0.0293	-0.0002	0.0002	0.0827

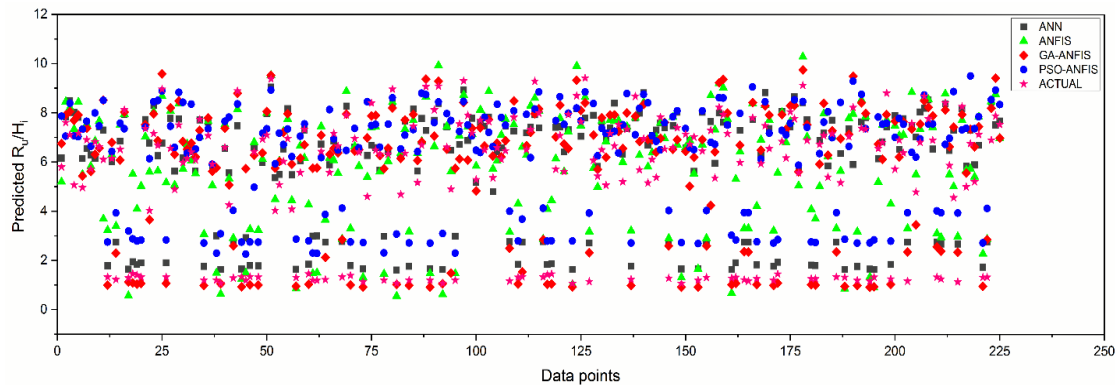


**Fig. 5.5 Comparison of predicted  $R_u/H_i$  by ANN, ANFIS, GA-ANFIS, PSO-ANFIS models for the case of non-dimensional input parameters with observed values**

#### **5.4 RESULTS AND DISCUSSION OF $R_u/H_i$ PREDICTION OF SEMICIRCULAR BREAKWATER USING DIFFERENT SOFT COMPUTING MODELS FOR DIMENSIONAL AND NON-DIMENSIONAL INPUT PARAMETERS FOR BELOW THE DATA RANGE PREDICTION**

As proposed in the present study an attempt to estimate relative wave run-up parameter ( $R_u/H_i$ ) using dimensional input parameters for below the data ranges of training data is carried out. The data division can be found in Section 5.1.1 and four soft computing models i.e., ANN, ANFIS, GA-ANFIS, PSO-ANFIS are employed. The ANN model predicted the  $R_u/H_i$  parameter with an R-value of 0.9720 and 0.9713 for training and testing respectively for 12 neurons set in a hidden layer at epoch 3. And ANFIS model predicted the  $R_u/H_i$  parameter with an R-value of 0.9715 and 0.9634 for training and testing respectively a partition matrix  $m=1.4$  and the number of clusters in the available data was 6. The application of GA to ANFIS did not improve the results of ANFIS as the R-value of 0.9671 and 0.5249 for training and testing respectively were found. This is a poor prediction. There was no improvement in the results in spite of varying the population size and increasing the iterations. An attempt was also done to change the crossover percentage and mutation rate however, the results of GA-ANFIS did not improve on prediction say poor generalization. Further, the application of PSO-ANFIS failed to predict the  $R_u/H_i$  parameter.

Also, an attempt to estimate relative wave run-up parameter ( $R_u/H_i$ ) using non-dimensional input parameters for below the data ranges of training data is carried out in the study. The data division can be found in Section 5.1.1 and four soft computing models i.e., ANN, ANFIS, GA-ANFIS, PSO-ANFIS are employed. The ANN model predicted the  $R_u/H_i$  parameter with an R-value of 0.9511 and 0.7469 for training and testing respectively for 10 neurons set in a hidden layer at epoch 18. And ANFIS model predicted the  $R_u/H_i$  parameter with an R-value of 0.7750 and 0.7116 for training and testing respectively a partition matrix  $m=1.4$  and the number of clusters in the available data was 6. The application of GA to ANFIS improved the results of ANFIS training with the R-value of 0.8967 whereas for testing it was 0.6755 thus prediction is not satisfactory. There was no improvement in the results in spite of varying the population size, increasing the iterations and mutation. Further, the application of PSO-ANFIS also did not show any improvement over the results of ANFIS with the R-value of 0.7702 and 0.6253 for training and testing respectively in the prediction of the  $R_u/H_i$  parameter.

## **5.5 RESULTS AND DISCUSSION OF $R_u/H_i$ PREDICTION OF SEMICIRCULAR BREAKWATER USING DIFFERENT SOFT COMPUTING MODELS FOR DIMENSIONAL AND NON-DIMENSIONAL INPUT PARAMETERS FOR BEYOND THE DATA RANGE PREDICTION**

As proposed in the present study an attempt to estimate relative wave run-up parameter using dimensional input parameters beyond the data ranges of training is carried out. The data division can be found in Section 5.1.1. and four soft computing models i.e., ANN, ANFIS, GA-ANFIS, PSO-ANFIS are employed. Among which the GA-ANFIS failed to predict the  $R_u/H_i$ . Whereas, the prediction of the other three models is reasonably good with the testing R-value of 0.9214, 0.9651 and 0.9515 in the case of ANN, ANFIS, PSO-ANFIS respectively with the respective training R being 0.9734, 0.9731, 0.9733. Which shows that PSO did not improve the ANFIS training result and the prediction is not satisfactory.

Similarly, the study to estimate relative wave run-up parameter using non-dimensional input parameters for beyond the data ranges of training is carried out using the same four models and data segregation may be referred to in Section 5.1.1. The ANN

predicted the  $R_u/H_i$  parameter well for training with an R-value of 0.9617 and poor for testing with  $R=0.6597$  shows purely the overfitting of the model. The ANFIS poorly predicted the  $R_u/H_i$  parameter with very low R-value positively correlated in the case of training and negatively correlated in the case of testing. Further, the application of optimization techniques GA and PSO to ANFIS improved the  $R_u/H_i$  prediction with testing R-value of 0.8550 and 0.9712 respectively which is better than ANN.

## 5.6 CLOSURE

The estimation of relative wave run-up parameter ( $R_u/H_i$ ) is vital for the design of the crest level of the breakwater. An approach to predict the relative wave run-up parameter ( $R_u/H_i$ ) on emerged semicircular breakwater for conventional data range has been carried out in the present study. The study presents four different soft computing models i.e., ANN, ANFIS, GA-ANFIS, and PSO-ANFIS for estimating the  $R_u/H_i$  parameter for dimensional and non-dimensional input parameters. In the case of dimensional input parameters,  $R_u/H_i$  predicted by PSO-ANFIS gave better results whereas, ANN prediction was better in the case of non-dimensional input parameters. However, if you compare the relative wave run-up parameter prediction made for dimensional and non-dimensional input parameters, the prediction made by the non-dimensional input parameters are better compared to the dimensional input parameters. Amongst the two cases under consideration, the ANN predictions have the least error in the prediction of  $R_u/H_i$  parameter. This shows that individual method like ANN also performs well in comparison with the hybrid models in the prediction of hydraulic response of emerged seaside perforated semicircular breakwater. Also, the prediction of  $R_u/H_i$  of the emerged semicircular breakwater for below and beyond the data range used for training has been attempted. However, this did not give satisfactory results hence details are not included in the thesis. This shows that such a prediction in the case of relative wave run-up parameter is not satisfactory for the emerged seaside perforated semicircular breakwater with the available dataset.

**GENERAL**

The stability parameter ( $W/\gamma H_i^2$ ) of emerged seaside perforated semicircular breakwaters has not been much explored, and there is a research gap, particularly in the application of soft computing techniques to predict  $W/\gamma H_i^2$ . All of the possible available literature regarding stability parameter has been discussed in chapter 2. The present chapter includes the data segregation, prediction of  $W/\gamma H_i^2$  using different soft computing models as well as the assessment of the models.

**6.1 STABILITY PARAMETER ( $W/\gamma H_i^2$ ) OF SEMICIRCULAR BREAKWATER**

The breakwaters are continuously subjected to highly vulnerable environments; to provide adequate service during their designed life and to provide safety against different modes of failure the stability analysis needs to be performed. A cost-effective structure is to be designed as the cost of the structure varies exorbitantly depending on the depth of water, wave climate, and foundation conditions. The design and the breakwater position is highly influenced by these factors. By determining the stability parameter we can arrive at the critical (minimum) weight required for safeguarding the structure stability, thus minimizing the total expenditure of the breakwater installation. The sliding stability parameter of the emerged seaside perforated semicircular breakwater is expressed as a non-dimensional parameter as,

$$\text{Stability parameter} = \frac{W}{\gamma H_i^2} \quad (6.1)$$

Where,

W- Weight added

Y- Specific weight

H<sub>i</sub>- Incident wave height

The current study focusses on predicting the stability parameter of the emerged seaside perforated semicircular breakwater using the inputs influencing the stability in two forms.

### **6.1.1 Data segregation for prediction of the Stability parameter**

For the data segregation for the typical case of wave height ( $H_i$ ) the entire ensemble, called here as Global data (GD) is sorted in the increasing order of wave height ( $H_i$ ). With the conventional procedure of data segregation 70:30 for training and testing the prediction of stability parameter is done for the entire set of data with of 389 points, the perforation diameter being constant 0.016 m. The two sets of input parameters are :

(1) Dimensional ( $H_i$ , T, S, R, d,  $h_s$ )

(2) Non-dimensional ( $H_i / gT^2$ ,  $d/h_s$ , S/D)

The dimensional parameters being wave height ( $H_i$ ), wave period (T), the spacing between the perforations (S), the radius of the semicircular caisson (R), water depth (d), structure height ( $h_s$ ). The dimensionless parameters wave steepness ( $H_i/gT^2$ ), relative depth parameter ( $d/h_s$ ), and perforation spacing to the diameter of the perforation (S/D), is used to predict the stability parameter ( $W/\gamma H_i^2$ ). The experimental parameter ranges are as in Table 3.3.

## **6.2 RESULTS AND DISCUSSION OF $W/\gamma H_i^2$ PARAMETER PREDICTION OF SEMICIRCULAR BREAKWATER USING DIFFERENT SOFT COMPUTING MODELS FOR DIMENSIONAL INPUT PARAMETERS**

The prediction of stability parameter for an emerged seaside perforated semicircular breakwater using different soft computing models ANN, ANFIS, GA-ANFIS and PSO-ANFIS for dimensional input parameters proposed has been performed here. In this case, a data length of 389 points is used and a conventional procedure of data segregation of 70% for training and 30% for testing is used in all the four models. The optimal parameters of each of the model have been presented in Table 6.2. Also, Table 6.3 presents the results using different models.

By trial and error approach, the best architecture for ANN was found to be 6-13-1 with  $R=0.9189$  for training and lower RMSE of 0.0572 and for testing  $R=0.8642$  with slightly higher RMSE of 0.0875. As seen in Table 6.3 the efficiency of training was 83% with lower scatter of prediction and efficiency of testing was 74% with higher scatter of prediction.

The application of ANFIS model with the partition matrix of 1.8, with the minimum improvement factor of 0.001, maximum iterations 25 and number of clusters set to 13 slightly improved the R-value of ANFIS prediction to 0.9215 and 0.8828 for training and testing respectively. Accordingly, the scatter index reduced, RMSE improved, scatter index improved over ANN results. Whereas, the result obtained for ANFIS is more negatively biased than ANN.

To further improve the ANFIS model results GA was applied whose objective function is to reduce the RMSE of the prediction of  $R_0/H_i$  parameter of the semicircular breakwater. In the FCM the number of clusters is set as 13 and with  $m=1.8$  the prediction was optimal with least RMSE, for a maximum FCM iteration of 25 and minimum improvement of  $1e-5$ . Population size and the maximum number of iterations, by changing these two most sensitive parameters of the GA, the training of the ANFIS model are done arriving at the optimal parameters as in Table 6.1. The model parameters set were crossover rate as 0.7, mutation rate as 0.4 and selection pressure as 8. However, among the four models, GA-ANFIS had the highest value of R being 0.9221 for training and 0.8874 for testing with the lowest RMSE 0.0572 and 0.0823 respectively. The NSE for training was 6% better than that for testing and scatter plot for GA-ANFIS was better than the other three models with the least scatter index of 34.92.

The PSO-ANFIS model was employed to check if could predict better than the GA-ANFIS model. PSO-ANFIS is run for various population size 10, 15, 20, 25, 30, 35, 40, 50, 100, and finally set for a population size of 50. The maximum number of iterations was set to 5000. The training of the ANFIS model is done arriving at the optimal parameters for PSO as in Table 6.2. The other model parameters set were inertia weight 0.4 cognitive acceleration ( $c1$ )=2, social acceleration ( $c2$ )=2. The scatter index is highest among all the four models for PSO-ANFIS testing with the value of 41.91 with slightly higher underestimated bias of -0.0190. Also, the PSO-ANFIS had a higher error with poor correlation with the measured value as seen in Table 6.3.

In the prediction of stability parameter using all the four models the best was the prediction made by GA-ANFIS. The Fig.6.1 shows the scatter plot of individual models



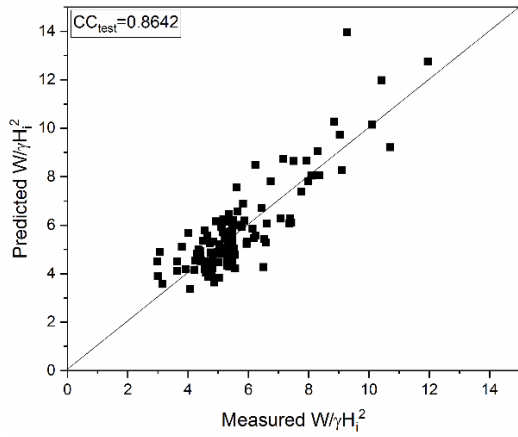
and Fig.6.2 shows the comparison of best prediction of each employed model in the prediction of stability parameter ( $W/\gamma H_i^2$ ) of the semicircular breakwater for dimensional input parameters.

**Table 6.1 Optimal parameters of different models for dimensional input parameters**

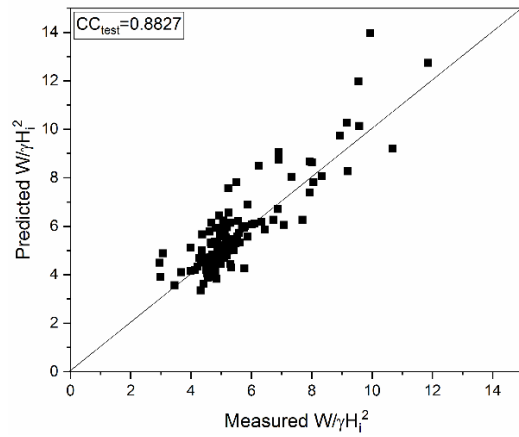
<b>Model</b>	<b>Parameters</b>	<b>Values</b>
ANN	Number of neurons	13
	Epochs	4
ANFIS	Partition matrix	1.8
	Minimum improvement factor	0.001
	Maximum iterations	25
	Number of clusters	13
GA-ANFIS	Population size	90
	Number of generations	12000
PSO-ANFIS	Number of iterations	5000
	Number of Particles	50

**Table 6.2 Error metrics for different soft computing models for dimensional input parameters in the case of 389 data points for predicting stability parameter**

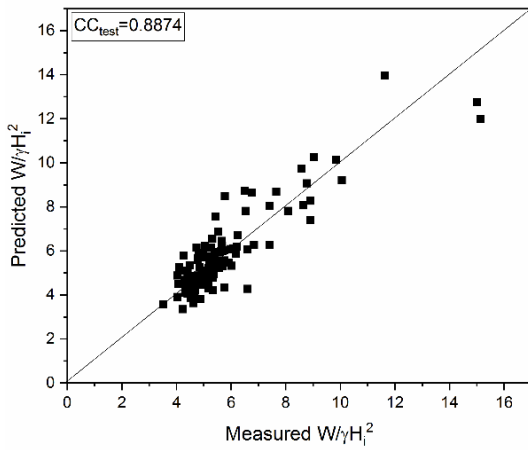
Input form	Error Metrics	Soft computing models							
		ANN		ANFIS		GA-ANFIS		PSO-ANFIS	
		Train	Test	Train	Test	Train	Test	Train	Test
Dimensional	R	0.9189	0.8642	0.9215	0.8828	0.9221	0.8874	0.9220	0.8284
	RMSE	0.0572	0.0875	0.0565	0.0845	0.0572	0.0823	0.0562	0.0987
	NSE	0.8309	0.7438	0.8350	0.7614	0.8309	0.7737	0.8363	0.6741
	SI	25.54	37.16	25.23	35.85	25.54	34.92	25.13	41.91
	BIAS	0.0043	-0.0095	-0.0019	-0.0215	0.0043	-0.0060	-0.0008	-0.0190



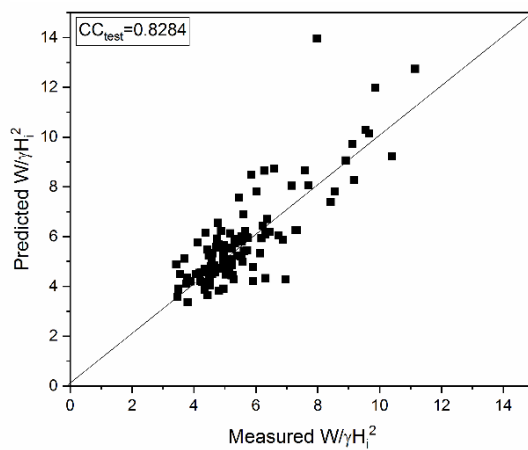
(a) ANN model



(b) ANFIS model



(c) GA-ANFIS model



(d) PSO-ANFIS model

**Fig. 6.1** Scatter plot of predicted versus actual values of  $W/\gamma H_i^2$  parameter of different models for dimensional input parameters

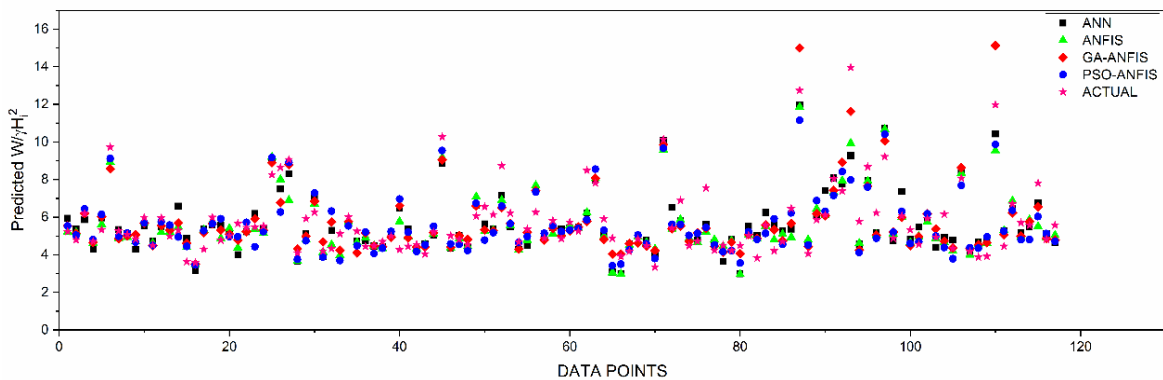


**Fig. 6.2** Comparison of predicted  $W/\gamma H_i^2$  by ANN, ANFIS, GA-ANFIS, PSO-ANFIS models for the case of dimensional input parameters with observed values

### **6.3 RESULTS AND DISCUSSION OF $W/\gamma H^2$ PARAMETER PREDICTION OF SEMICIRCULAR BREAKWATER USING DIFFERENT SOFT COMPUTING MODELS FOR NON-DIMENSIONAL INPUT PARAMETERS**

The prediction of stability parameter for an emerged seaside perforated semicircular breakwater using different soft computing models ANN, ANFIS, GA-ANFIS and PSO-ANFIS for non-dimensional input parameters proposed has been performed here. In this case, a data length of 389 points is used and a conventional procedure of data segregation of 70% for training and 30% for testing is used in all the four models. The optimal parameters of each of the model have been presented in Table 6.3. Also, Table 6.4 presents the results using different models.

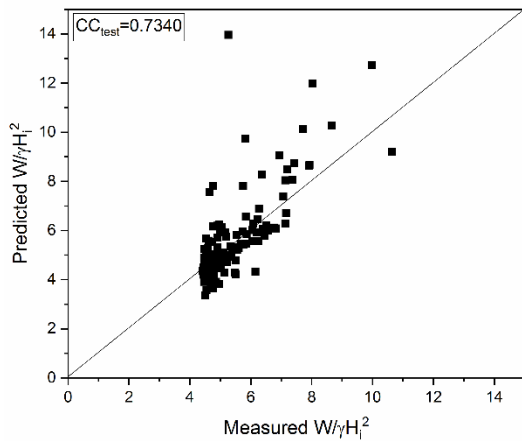
Among different trials of neurons set in the hidden layer the best architecture for ANN was found to be 6-2-1 with  $R=0.8087$  for training with lower RMSE of 0.0930 and for testing  $R=0.7340$  with slightly higher RMSE of 0.1214. It also shows that the efficiency of training was 64% with relatively lower scatter of prediction and the model efficiency of testing was 50% with higher scatter of prediction.

The application of ANFIS model with the partition matrix of 2, with the minimum improvement factor of 0.001, maximum iterations 25 and number of clusters set to 13 slightly improved the R-value of ANN prediction to 0.8406 and 0.7447 for training and testing respectively. Accordingly, the model efficiency of training improved to 70% and testing to 53% with improvement in the respective scatter index as seen in Table 6.4.

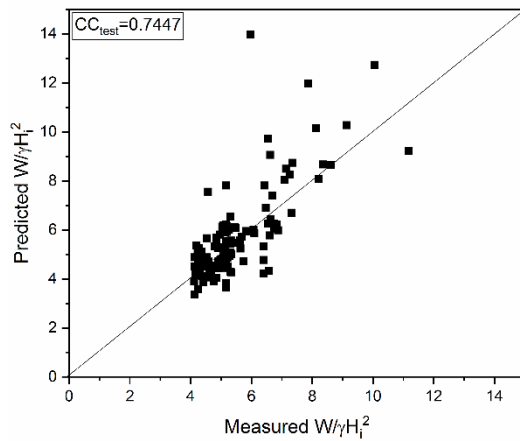
Further improvement of ANFIS prediction is expected by the application of GA and PSO. In both cases, the employment of optimization techniques did not significantly improve the prediction of the ANFIS model. In the case of GA-ANFIS model though the training-value slightly improved to 0.8488 and the testing  $R=0.7353$  did not improve in spite of several trials of varying the population size and the iteration number. The GA-ANFIS model parameters were set as crossover rate to 0.7, mutation rate as 0.4 and selection pressure as 8. Among the four models, PSO-ANFIS had the better value of R is 0.8459 for training and 0.7452 for testing. But the RMSE of 0.0838 and

0.1188 for training and testing was similar to that in the case of ANFIS, there is no significant decrease in the error. Also, the NSE for training and testing was close to that of ANFIS. The PSO-ANFIS model parameters were set with inertia weight 0.4 cognitive acceleration (c1)=2, social acceleration (c2)=2.

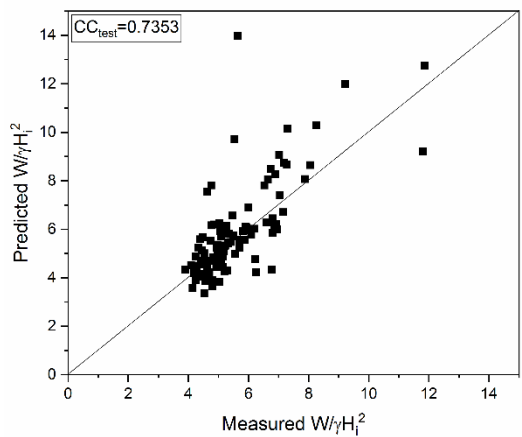
Fig.6.3 shows the scatter plot of individual models and Fig.6.4 shows the comparison of the best prediction of each employed model in the prediction of stability parameter ( $W/\gamma H_i^2$ ) of the semicircular breakwater.



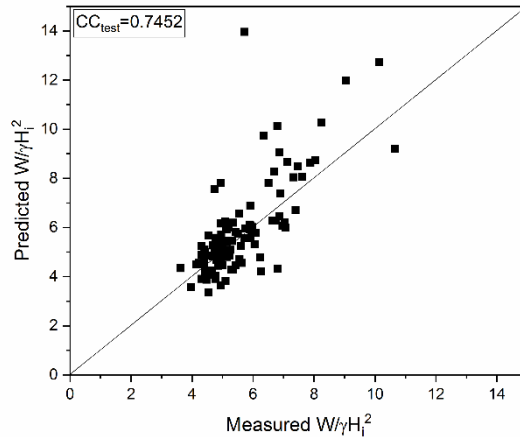
(a) ANN model



(b) ANFIS model



(c) GA-ANFIS model



(d) PSO-ANFIS model

**Fig. 6.3 Scatter plot of predicted versus actual values of  $W/\gamma H_i^2$  for different models with non-dimensional input parameters**

**Table 6.3 Optimal parameters of different models for non-dimensional input parameters**

<b>Model</b>	<b>Parameters</b>	<b>Values</b>
ANN	Number of neurons	2
	Epochs	4
ANFIS	Partition matrix	2
	Minimum improvement factor	0.001
	Maximum iterations	25
	Number of clusters	13
GA-ANFIS	Population size	20
	Number of generations	3000
PSO-ANFIS	Number of iterations	1000
	Number of Particles	30

**Table 6.4 Error metrics for different soft computing models for non-dimensional input parameters in the case of 389 data points for predicting stability parameter**

Input form	Error Metrics	Soft computing models							
		ANN		ANFIS (FUZZY C-MEANS CLUSTERING)		GA-ANFIS		PSO-ANFIS	
		Train	Test	Train	Test	Train	Test	Train	Test
Non-dimensional	<b>R</b>	0.8087	0.7340	0.8406	0.7447	0.8488	0.7353	0.8459	0.7452
	<b>RMSE</b>	0.0930	0.1214	0.0851	0.1178	0.0830	0.1197	0.0838	0.1188
	<b>NSE</b>	0.6495	0.5076	0.7066	0.5365	0.7205	0.5211	0.7155	0.5287
	<b>SI</b>	41.55	51.52	38.01	49.99	37.10	50.81	37.43	50.40
	<b>BIAS</b>	-0.0057	-0.0228	1.596E-07	-0.0205	-4.70E-05	-0.0236	0.0009	-0.0225

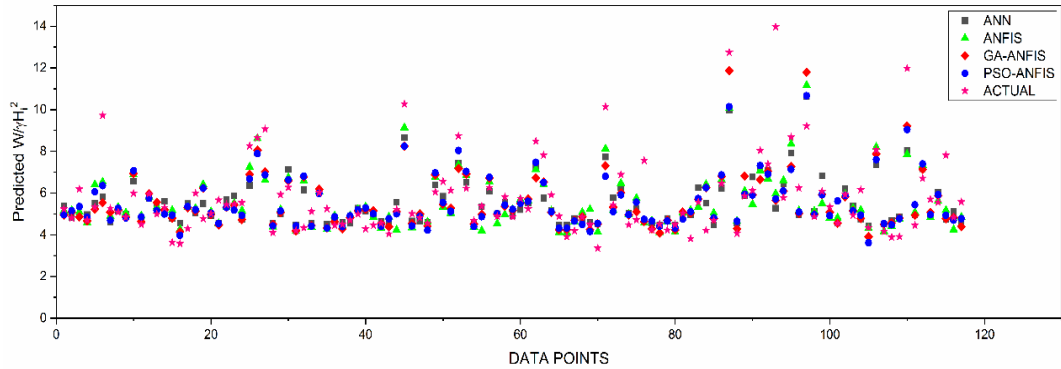


**Fig. 6.4 Comparison of predicted  $W/\gamma H_i^2$  by ANN, ANFIS, GA-ANFIS, PSO-ANFIS models for the case of non-dimensional input parameters with observed values**

#### 6.4 CLOSURE

In the case of  $W/\gamma H_i^2$  prediction performance of ANN, ANFIS, GA-ANFIS, PSO-ANFIS models for dimensional input parameters and non-dimensional input parameters did not improve significantly over the individual models. The data length being 389 could be one of the reasons for not getting accurate predictions in both cases. In the case of dimensional input parameters, the training R-value is reasonably good but testing R-value is low in case of all the four models. Whereas, in the case of non-dimensional input parameters, the training and testing R-value is found similar in the case of ANFIS, GA-ANFIS, and PSO-ANFIS. However, test R values are low in case of all the four models. The model was also run for different non-dimensional input parameters to predict the  $W/\gamma H_i^2$  but, the results are better only when the input is limited to  $H_i/gT^2$ ,  $d/h_s$ , and  $S/D$ ; these parameters being the most important parameters in estimating the stability parameter with the available data set.





## **CHAPTER 7**

### **SUMMARY AND CONCLUSIONS**

#### **7.1 SUMMARY**

The present study of developing soft computing models to predict the hydraulic responses of emerged seaside perforated semicircular breakwater by the conventional approach of data segregation has been successfully carried out. Also, it is first of its kind wherein certain ranges of data is excluded from training the models and the prediction of hydraulic responses is done and compared with the conventional approach. The possibility of such a prediction is checked for both below the range prediction as well as beyond the range prediction. Such a study is attempted to facilitate the coastal engineers in the prediction of hydraulic responses of emerged seaside perforated semicircular breakwaters to be installed in similar site conditions. Especially when physical model data is available only for certain ranges, the hydraulic responses for lower and higher wave ranges could be predicted. Several different cases considered are discussed in the previous chapters based on which it is found that GA-ANFIS gave good results in most of the cases.

#### **7.2 CONCLUSIONS**

Based on the present study the following conclusions are drawn:

- Reflection coefficient prediction performance of ANN, ANFIS, GA-ANFIS AND PSO-ANFIS models are tested for 1274 data points shows that ANN produced the best prediction in the case of dimensional parameters, however, in the case of non-dimensional input parameters GA-ANFIS outperformed the rest.
- In the study a comparison of two ANFIS methods i.e., subtractive clustering and fuzzy c-means clustering in the reflection coefficient prediction shows that fuzzy c-means clustering works better in most of the cases.

- The reflection coefficient prediction for ‘below the data range’ approach is close to the prediction by a conventional approach using ANN and ANFIS models in case of dimensional input parameters and hence such a prediction is acceptable. The study found that below the data range prediction made by the FCM-ANFIS model (0.9904) is better than the ANN model (0.9875) and SC-ANFIS model (0.9887).
- The reflection coefficient prediction made by SC-ANFIS model (0.9922) for ‘conventional below the data range’ approach in the case of dimensional input parameters is better than the ANN model (0.9903) and FCM-ANFIS model (0.9922).
- The reflection coefficient prediction for ‘beyond the data range’ approach is close to the prediction made by a conventional approach using ANN and ANFIS models in case of dimensional input parameters and hence such a prediction is acceptable. The study found that beyond the data range prediction made by the FCM-ANFIS model (0.9911) outperformed the ANN model (0.9879) and SC-ANFIS model (0.9906).
- In the case of non-dimensional input parameters, the prediction of reflection coefficient using ANN and ANFIS is found to improve with the application of hybrid methods like GA-ANFIS and PSO-ANFIS.
- The reflection coefficient prediction for ‘below the data range’ approach is close to the prediction made by a conventional approach using ANN, ANFIS, GA-ANFIS and PSO-ANFIS models in case of non-dimensional input parameters hence such a prediction is acceptable. The study found that ‘below the data range prediction’ in the case of non-dimensional input parameters made by the GA-ANFIS model (0.9058) was better than the other models.
- The reflection coefficient prediction made by GA-ANFIS model (0.8865) for ‘conventional below the data range’ approach in the case of non-dimensional input parameters was better than the other three models.
- The reflection coefficient prediction for ‘beyond the data range’ approach did not give satisfactory results compared to the prediction made by the conventional approach in the case of non-dimensional input parameters using

ANN, ANFIS, GA-ANFIS, and PSO-ANFIS models and hence such a prediction was not acceptable.

- The reflection coefficient prediction made by GA-ANFIS model (0.9261) for ‘conventional beyond the data range’ approach in the case of non-dimensional input parameters was better than the other three models.
- Relative wave runup parameter prediction done by using non-dimensional input parameters gave better results compared to the dimensional input parameters in the case of the conventional data segregation method.
- Relative wave runup parameter predicted by GA-ANFIS is found to give better  $R=0.8201$ , compared to the other three model  $R$ -values in the case of dimensional parameters.
- Relative wave runup parameter predicted by ANN is found to outperform the other three models in the case of non-dimensional input parameters shows that even individual models are capable of good prediction. However, the runup parameter prediction in the case of below and beyond the data range prediction was not found satisfactory.
- Stability parameter prediction using dimensional input parameters outperformed the prediction done using non-dimensional input parameters, using all four soft computing models.
- Stability parameter predicted by GA-ANFIS was found to be slightly higher compared to the other three models in the case of dimensional parameters.
- Stability parameter prediction by PSO-ANFIS was found to be better than the other three models in the case of non-dimensional parameters.
- Among the two optimization techniques applied to ANFIS, GA- ANFIS gave better results in most of the cases considered.

### **7.3 CONTRIBUTIONS FROM THE STUDY**

- This study verified the possibility of prediction of hydraulic responses of semicircular breakwater subjected to regular waves using four soft computing models.
- Prediction of hydraulic responses of semicircular breakwater using four soft computing models for both below and beyond the data ranges is made.

### **7.4 LIMITATIONS AND FUTURE SCOPE**

- The major limitation of the study is models are site specific and can be applied only if similar site conditions exist.
- The data segregation could be done with respect to the frequency of the data.
- There is a scope to carry out a similar study for semicircular breakwater employing other soft computing techniques like Extreme Learning Machines, Ant Colony optimization or Firefly optimization algorithm could be explored.

## REFERENCES

- Aburatani, S., Koizuka, T., Sasayama, H., Tanimoto, K. & Namerikawa, N., (1996). Field test on a semi-circular caisson breakwater. *Coastal Engineering Journal in Japan*, 39(1), 59-78.
- Alata, M., Molhim, M., Ramini, A., & Arabia, S. (2013). Using GA for Optimization of the Fuzzy C-Means Clustering Algorithm. *Research Journal of Applied Sciences, Engineering, and Technology*, 5(3), 695–701.
- Al-hmouz A., Shen J., Al-Hmouz R. & Yan J. (2012). Modeling and Simulation of an Adaptive Neuro-Fuzzy Inference System (ANFIS) for Mobile Learning. *IEEE transactions on learning technologies*, 5(3), 226-237.
- Arumugadevi, S., & Seenivasagam, V. (2015). Comparison of Clustering Methods for Segmenting Color Images. *Indian Journal of Science and Technology*, 8(7), 670–677.
- Arunjith, A., Sannasiraj, S. A., & Sundar, V. (2013). Wave Overtopping over Crown Walls and Run-up on Rubble Mound Breakwaters with Kolos Armour under Random Waves. *The International Journal of Ocean and Climate Systems*, 4(2), 125–132.
- Azamathulla, H. Md., & Ghani, A. A. (2011). ANFIS-based approach for predicting the scour depth at culvert outlets. *Journal of Pipeline Systems Engineering and Practice*, 2(1), 35–40.
- Balas, C. E., Koç, M. L., & Tür, R. (2010). Artificial neural networks based on principal component analysis, fuzzy systems and fuzzy neural networks for preliminary design of rubble mound breakwaters. *Applied Ocean Research*, 32(4), 425–433.
- Basser, H., Karami, H., Shamshirband, S., Akib, S., Amirmojahedi, M., Ahmad, R., Jahangirzadeh, A., & Javidnia, H. (2015). Hybrid ANFIS – PSO approach for predicting optimum parameters of a protective spur dike. *Applied Soft Computing Journal*, 30, 642–649.
- Bataineh, K. M., Naji M., & Saqer, M., (2011) A Comparison Study between Various Fuzzy Clustering Algorithm. *Jordan Journal of Mechanical and Industrial Engineering*, 5(4), 335–343.

- Bergh, F. Van Den, & Engelbrecht, A. P. (2006). A study of particle swarm optimization particle trajectories. *Journal Information Sciences*, 176(8), 937–971.
- Bezdek, J.C. (1981). *Pattern Recognition with Fuzzy Objective Function Algorithms*. Advanced Applications in Pattern Recognition, ISBN 0-306-40671-3.
- Bonyadi, M. R. & Michalewicz Z. (2017). Particle Swarm Optimization for Single Objective Continuous Space Problems : A Review. *Evolutionary Computation*, 25(1), 1–54.
- Bruun, P., & Günbak, A. R. (1977). New design principles for rubble mound structures. *Coastal Engineering*, 2429-2473.
- Bryant, M. A., T. Hesser, and R. E. Jensen. 2016. *Evaluation Statistics Computed for the Wave Information Studies (WIS)*. ERDC/CHL CHETN-I-91. Vicksburg, MS: U.S. Army Engineer Research and Development Center.
- Castillo, O., Rubio, E., Soria, J., & Naredo, E. (2012). Optimization of the Fuzzy C-Means Algorithm using Evolutionary Methods. *Engineering Letters*. 20.
- Castro, A., Pinto, F. T., & Iglesias, G. (2011). Artificial intelligence applied to plane wave reflection at submerged breakwaters. *Journal of Hydraulic Research*, 49 (2011), 465-472.
- Chau, K., (2006). A review on the integration of artificial intelligence into coastal modelling. *Journal of Environmental Management*, 80(1), 47-57.
- Chen, S., Montgomery, J., & Boluf'e-R'ohler, A. (2015). Measuring the curse of dimensionality and its effects on particle swarm optimization and differential evolution. *Applied Intelligence* 42(3):514–526
- Chiu, S. (1994). Fuzzy Model Identification Based on Cluster Estimation, *Journal of Intelligent & Fuzzy Systems*, 2(3), 1994.
- Deo, M. C. (2010). Artificial neural networks in coastal and ocean engineering. *Indian Journal of Geo-Marine Science*, 39, 589–596.
- Dhinakaran, G., Sundar, V., & Sundaravadivelu, R. (2002). Dynamic pressures and forces exerted on impermeable and seaside perforated semicircular breakwaters due to regular waves. *Ocean Engineering*, 29, 1981–2004.
- Dhinakaran, G., Sundar, V., Sundaravadivelu, R., & Graw, K. U. (2009). Effect of perforations and rubble mound height on wave transformation characteristics of

- surface piercing semicircular breakwaters. *Ocean Engineering*, 36(15–16), 1182–1198.
- Dhinakaran, G. (2011). Hydrodynamic Characteristics of Semi-circular Breakwaters: Review Article. *Asian Journal of Applied Sciences*, 4(1), 1–21.
- Dwarakish, G. S., & Nithyapriya, B. (2016). Application of soft computing techniques in coastal study – A review. *Journal of Ocean Engineering and Science*, 1(4), 247–255.
- Eberhart, R. C., and Shi, Y. (2001). Particle Swarm Optimization: Developments, applications and resources. *Proceedings of the IEEE Congress on Evolutionary Computation*, IEEE Press, Seoul, Korea, 81–86
- Etemad-Shahidi, A., and Bonakdar, L. (2009). Design of rubble-mound breakwaters using M5 ' machine learning method. *Applied Ocean Research*, Elsevier Ltd, 31(3), pp. 197–201.
- Ejraei, A., Sahebi, H., Ghiasi, M. M., Mirjordavi, N., Esmailzadeh, F., Lee, M., & Bahadori, A. (2016). Prediction of CO<sub>2</sub>–oil molecular diffusion using adaptive neuro-fuzzy inference system and particle swarm optimization technique. *Fuel*, 181, 178–187.
- Erdik, T., Savci, M. E., & Şen, Z. (2009). Artificial neural networks for predicting maximum wave runup on rubble mound structures. *Expert Systems with Applications*, 36(3), pp. 6403–6408.
- Erdik, T. (2009). Fuzzy logic approach to conventional rubble mound structures design. *Expert Systems with Applications*., 36(3), 4162–4170.
- Etemad-Shahidi, A., & Bonakdar, L. (2009). Design of rubble-mound breakwaters using M5' machine learning method. *Applied Ocean Research*, 31(3), 197–201.
- Gadre, M. R., Poonawala, I. Z., & Kudale, M. D. (1985). Design of reclamation bunds for Madras port. In *Proceedings of first National Conference on Dock and Harbour Engineering*, IIT Bombay, B113-B123.
- Ganesh, C. (2009). Hydrodynamic performance characteristics of semicircular breakwater. M. tech Thesis, National Institute of Technology Karnataka, Surathkal, Mangaluru, India.
- Garrido, J. M., & Medina, J. R. (2012). New neural network-derived empirical formulas



- for estimating wave reflection on Jarlan-type breakwaters. *Coastal Engineering*, 62, 9–18.
- Ghasemi, H., Kollahdoozan, M., Pena, E., Ferreras, J., & Figueroa A. (2016). A new hybrid ann model for evaluating the efficiency of  $\pi$ -type floating breakwater. *Coastal Engineering Proceedings*. (35).
- Goda, Y., & Suzuki, T., (1976). Estimation of incident and reflected waves in random wave experiments. *Proceedings of 15<sup>th</sup> Coastal Engineering, Hawaii, ASCE*, 828-845.
- Gope, V. K., Aggarwal A., & Hegde, A. V., (2016). Simulation using Computational fluid Dynamics (CFD) for Semi-Circular Breakwater during flow over it. *International Journal of Scientific and Engineering Research*. 7.
- Goyal, R., Singh, K., & Hegde, A. V. (2014). Quarter Circular Breakwater : Prediction and Artificial Neural Network. *Marine Technological Society Journal*, 48, 1–7.
- Goyal, R., Singh, K., Hegde, A. V., & Thakur, G. S. (2015). Prediction of Hydrodynamic Characteristics of Quarter Circular Breakwater Using Stepwise Regression. *International Journal of Ocean Climate Systems*, 6(1), 47–54.
- Graw, K. U., Knapp, S., Sundar, V. & Sundaravadivelu, R. (1998). Dynamic pressures exerted on semicircular breakwater, *Leipzig Annual Civil Engineering Report*, 3, 333-344.
- Harish, N., Lokesha., Mandal, S., Rao, S. & Patil, S.G. (2014). Parameter Optimization using GA in SVM to Predict Damage Level of Non-Reshaped Berm Breakwater. *International Journal of Ocean and Climate Systems*. 5, 79-88.
- Harish, N., Mandal, S., Rao, S., and Patil, S. G. (2015). Particle Swarm Optimization based support vector machine for damage level prediction of non-reshaped berm breakwater. *Applied Soft Computing*, 27, 313–321.
- Hegde, A. V., & Samaga, B. R. (1996). Study on the Effect of Core Porosity on Rubble Mound Breakwater. In *Proceedings of Tenth Congress of the Asian and Pacific Regional Division of the International Association for Hydraulic Research, IAHR*, 287.
- Hegde, A. V., Ganesh, C., & Kumar, V. (2010). Hydrodynamic performance characteristics of semicircular breakwater wave run-up and run-down. *Journal of*

- Hydraulic Engineering. 16, 99-108.
- Hegde, A. V., & Naseeb, S.M. (2014). Transmission Performance of Submerged Semicircular Breakwaters for Different Radii and Submergence Ratios. *The International Journal of Ocean and Climate Systems*. 5. 151-162. 10.1260/1759-3131.5.3.151.
- Hegde, A., Sharhabeel, P. S., & Mohan, S. (2015). Stability of a Perforated Quarter Circle Breakwater. *International Journal of Ocean Climate Systems*, 6(4), 185–194.
- Hegde, A.V., Mohan, S., Pinho, J. L. S., & Sharhabeel P. S., (2018). Physical model studies on the stability of emerged seaside perforated semicircular breakwaters, *Indian Journal of Geo-Marine Sciences*, 47(3), 681-685.
- Hodaiei, S. M. R., Chamani, M. R., Moghim, M. N., Mansoorzadeh, S., & Kabiri-Samani, A. (2016). Experimental study on reflection coefficient of curved perforated plate. *Journal of Marine Science and Applications*, 15(4), 382–387.
- Hudson, R. Y. (1959). Laboratory investigation of rubble-mound breakwaters. *Journal of the Waterways and Harbors Division*, 85 (WW3), 93-121.
- Imran, M., Hashim, R., & Khalid, N. E. A. (2013). An overview of particle swarm optimization variants. *Procedia Engineering*, 53(1), 491–496.
- Issacson M. (1991). Measurement of regular wave reflection. *Journal of Waterways, Port, Coastal and Ocean Engineering*. ASCE, 117(6), 553 –569.
- Janardhan, P., Harish, N., Rao, S., and Shirlal, K. G. (2015). Performance of Variable Selection Method for the Damage Level Prediction of Reshaped Berm Breakwater. *Aquatic Procedia*, Elsevier B.V., 4(ICWRCOE), 302–307.
- Jang, J. R. (1993). ANFIS : Adaptive-Network-Based Fuzzy Inference System. *IEEE Transactions on Systems, Man, and Cybernetics*. 23(3), 665–685.
- Jabbari, E., & Talebi, O. (2011). Using Artificial Neural Networks for estimation of scour at the head of vertical wall breakwater. *Journal of Coastal Research*, (64), 521–526.
- Jafari, E. & Etemad-Shahidi, A. (2012). Derivation of a new model for prediction of wave overtopping at rubble-mound structures. *Journal of Waterway Port Coastal and Ocean Engineering*, 138, 42-52.

- Jain, P., & Deo, M. C. (2008). Artificial Neural Networks for Coastal and Ocean studies. 12<sup>th</sup> International Association for Computer Methods and Advances in Geomechanics, 1655–1663.
- Jiang, X., Zou, Q. & Zhang, N. (2017). Wave load on submerged quarter-circular and semicircular breakwaters under irregular waves. *Coastal Engineering*, 121, 265–277.
- Karsoliya, S. (2012). Approximating Number of Hidden layer neurons in Multiple Hidden Layer BPNN Architecture. *International Journal of Engineering Trends and Technology*, 3(6), 713-717.
- Kaur, R. P., and Klair, A. S. (2012). Investigation of Grid partitioning and Subtractive Clustering based Neuro-Fuzzy Systems for Evaluation of Fault-Proneness in Open source software system. *International Conference on Computer Graphics, Simulation and Modeling. Pattaya (Thailand)*143–145.
- Kennedy, J., & Eberhart, R. (1995). Particle Swarm Optimization. *Proceedings of the IEEE International Conference on Neural Networks, (Perth Australia)*, 4, 1942-1948.
- Kingston K., & Murphy J. (1996). Thematic report: Wave runup/rundown, MAST II report.
- Kim, D. H., Kim, Y. J., & Hur, D. S. (2014). Artificial neural network based breakwater damage estimation considering tidal level variation. *Ocean Engineering*, 87, 185–190.
- Kirkgöz, M.S., & Aköz, M.S. (2005). Geometrical properties of perfect breaking waves on composite breakwaters. *Ocean Engineering*, 32, 1994–2006.
- Koç, M. L., & Balas, C. E. (2012). Genetic algorithms based on logic-driven fuzzy neural networks for stability assessment of rubble-mound breakwaters. *Applied Ocean Research*, 37, 211–219.
- Koç, M. L., Balas, C. E., & Koç, D. İ. (2016). Stability assessment of rubble-mound breakwaters using genetic programming. *Ocean Engineering*, 111, 8–12.
- Kudumula, S. R., and Mutukuru, M. R. G. (2013). Experimental Studies on Low crested Rubble Mound, Semicircular Breakwaters and Vertical wall System. *International Journal of Ocean and Climate Systems*, 4(3), 213–226.

- Kuntoji, G., Rao, M., & Rao, S., (2018). Prediction of wave transmission over the submerged reef of tandem breakwater using PSO-SVM and PSO-ANN techniques. *ISH Journal of Hydraulic Engineering*, DOI: 10.1080/09715010.2018.1482796
- Lee, A., Kim, S. E., & Suh, K.D. (2015). Estimation of Stability Number of Rock Armor Using Artificial Neural Network Combined with Principal Component Analysis. *Procedia Engineering.*, 116(1), 149–154.
- Liu, Y., & Li, Y. (2011). Wave interaction with a wave absorbing double curtain-wall breakwater. *Ocean Engineering*, 38, 1237–1245
- Mandal S., Patil S. G., & Hegde A. V. (2009). Wave transmission prediction of multilayer floating breakwater using a neural network. *International conference in Ocean Engineering*, IIT Madras, Chennai, India.
- Mandal, S., Rao, S., Harish, N., & Lokesha (2012). Damage level prediction of non-reshaped berm breakwater using ANN, SVM, and ANFIS models. *International Journal of Naval Architecture and Ocean Engineering*, 4(2), 112–122.
- Mani, J. S., & Jayakumar, S. (1995). Wave transmission by suspended pipe breakwater. *Journal of the waterway, port, coastal, and ocean engineering*, 121(6), 335-338.
- Mase, H., Sakamoto, M., & Sakai, T., (1995). Neural network for stability analysis of rubblemound breakwaters. *Journal of Waterway, Port, Coastal and Ocean Engineering* 121, 294–299.
- Mohammady, S. (2016). Optimization of adaptive neuro-fuzzy inference system based urban growth model. *City, Territory and Architecture*, 3: 10.
- Mohan Rao, U., Sood, Y. R., & Jarial, R. K. (2015). Subtractive clustering fuzzy expert system for engineering applications. *Procedia Computer Science*, 48, 77–83.
- Moriasi, D. N., Arnold, J. G., Liew, M. W. Van, Bingner, R. L., Harmel, R. D., & Veith, T. L. (2007). Model Evaluation Guidelines for Systematic Quantification of Accuracy in Watershed Simulations, *Transactions of the ASABE*, 50(3), 885-900.
- Muni-Reddy, M. G., & Neelamani, S. (2006). Wave interaction with caisson defenced by an offshore low-crested breakwater. *Journal of Coastal Research*, 1767-1770.
- Neelamani, S., Sumalatha, B. V., & Rao Narasimhan, S. (2002). Hydrodynamics of seaward defenced by a detached breakwater. In *Conference on Hydraulics, Water*

- resources, and Ocean Engineering, HYDRO. 244-249.
- Nikoo, M. R., Varjavand, I., Kerachian, R., Pirooz, M. D., & Karimi, A. (2014). Multi-objective optimum design of double-layer perforated-wall breakwaters: Application of NSGA-II and bargaining models. *Applied Ocean Research*, 47, 47–52.
- Nishanth, N. (2008). Sliding stability and hydrodynamic performance of emerged semicircular breakwater. M. Tech Thesis, National Institute of Technology Karnataka, Surathkal, Mangaluru, India.
- Panchal, F. S., & Panchal, M. (2014). Review on methods of selecting number of hidden nodes in artificial neural network. *International Journal of Computer Science and Mobile Computing*. 3(11), 455–464.
- Patil, S. G., Mandal, S., & Hegde, A. V. (2012). Genetic algorithm based support vector machine regression in predicting wave transmission of horizontally interlaced multi-layer moored floating pipe breakwater. *Advances in Engineering Software*, 45(1), 203–212.
- Patil, S. G., Mandal, S., Hegde, A. V., & Alavandar, S. (2011). Neuro-fuzzy based approach for wave transmission prediction of horizontally interlaced multilayer moored floating pipe breakwater. *Ocean Engineering*, 38(1), 186–196.
- Pousinho, H. M. I., Mendes, V. M. F., & Catalão, J. P. S. (2011). A hybrid PSO – ANFIS approach for short-term wind power prediction in Portugal. *Energy Conversion and Management*, 52(1), 397–402.
- Pourzangbar, A., Losada, M. A., Saber, A., Ahari, L. R., Larroudé, P., Vaezi, M., and Brocchini, M. (2017b). “Prediction of non-breaking wave induced scour depth at the trunk section of breakwaters using.” *Genetic Programming and Artificial Neural Networks Coastal Engineering*, Vol. 121, pp. 107–118,
- Rahmat, O. K., Hassan, A., Alauddin, M., and Ali, M. (2005). Generation of fuzzy rules with subtractive clustering. *Journal of Technology*, 43(D), 143–153.
- Rajendra, K., Balaji, R. & Mukul, P. (2017) Review of Indian research on innovative breakwaters. *India Journal of Geo-Marine Sciences*, 46, 431–453
- Raju, B., Hegde, A. V., & Chandrashekar, O. (2015). Computational Intelligence on Hydrodynamic Performance Characteristics of Emerged Perforated Quarter Circle

- Breakwater. *Procedia Engineering*, 116(1), 118–124.
- Rao, U. M., Sood, Y. R., & Jarial, R. K., (2015). Subtractive clustering fuzzy expert system for engineering applications", *Procedia Computer Science*. 48, pp. 77-83.
- Ratrout, N. T., (2011). Subtractive Clustering-Based K-means Technique for Determining Optimum Time-of-Day Breakpoints. 380–387.
- Ren, M., Liu, P., Wang, Z., & Yi, J., (2016). A Self-Adaptive Fuzzy Means Algorithm for Determining the Optimal Number of Clusters. *Comput. Intell. Neurosci.*, (2016).
- Sasajima, H., Koizuka, T., & Sasayama, H., (1994). Field demonstration test of a semicircular breakwater, *Proc., HYDROPORT' 94, PHRI, Yokosuka, Japan*, 593-610.
- Shankar, N.J. & Jayaratne, M.P.R. (2003) Wave run-up and overtopping on smooth and rough slopes of coastal structures. *Ocean Engineering*, 30(2), 221–238.
- Shi, Y. & Eberhart, R.C (1998), A modified particle swarm optimizer. *Proceedings of the IEEE International Conference on Evolutionary Computation*. Piscataway, N.J, 69-73.
- Shinsuke Aburatani, Takashi Koizuka, Hiroshi Sasayama, Katutoshi Tanimoto & Nobutaka Namerikawa (1996). Field Test on a Semi-Circular Caisson Breakwater, *Coastal Engineering in Japan*, 39:1, 59-78
- Singh, H., Dilbag, P., Avleen, S., & Malhi, K. (2017). Multi-objective particle swarm optimization-based adaptive neuro-fuzzy inference system for benzene monitoring. *Neural Computing and Applications*. <https://doi.org/10.1007/s00521-017-3181-7>
- Sooraj, M. (2015). Sliding stability and hydrodynamic performance of emerged semicircular breakwater. M.Tech. Thesis, National Institute of Technology Karnataka, Surathkal, Mangaluru, India, Appendix II.
- Sreejith, M. (2016). Sliding stability and hydrodynamic performance of emerged semicircular breakwater. M.Tech. Thesis, National Institute of Technology Karnataka, Surathkal, Mangaluru, India.
- SriKrishnapriya, M., Roopsekhar, K.A., Sundar, V., Sundaravadivelu, R., Graw, K.U., Susanne K., (2000). Hydrodynamic Pressures on Semicircular Breakwaters. In:

- CD Proceedings of Fourth International Conference on Hydroscience and Engineering, IAHR, Seoul, South Korea, 26–29.
- Sundar, V., and Ragu, V. (1998). Dynamic pressures and run-up on semicircular breakwaters due to random waves. *Ocean Engineering.*, 25(2–3), 221–241.
- Sundar, V, Sundaravadivelu R., Dhinakaran, G., Roopshekar K. A., & Graw K. U., (2001). Pressure and forces on a semicircular breakwater due to regular waves, *Oceanic Engineering. International*, 5: 73-83.
- Surakshitha, (2017). Sliding stability and hydrodynamic performance of emerged non-perforated and seaside perforated semicircular breakwaters. M. Tech Thesis, National Institute of Technology Karnataka, Surathkal, Mangaluru, India.
- Tanimoto, K. & Goda, Y. (1992). Historical development of breakwater structures in the world. *Coastal structures and breakwaters*. Institution of Civil Engineers. London, UK.
- Tanimoto, K., & Takahashi, S., (1994). Japanese experiences on composite breakwaters. *Proceedings International Workshop on Wave Barriers in Deepwater*. Port and Harbour Research Institute in Yokosuka, Japan. 1-22.
- Teh, H. M., Vengatesan, V., & Bruce, T. (2010). Hydrodynamic performance of a free surface semicircular perforated breakwater. *Coastal Engineering*, 1–13.
- Teh, H. M., & Venugopal, V. (2013). Performance evaluation of a semicircular breakwater with truncated wave screens. *Ocean Engineering*, 70, 160–176.
- Tiwari, S., Babbar, R., & Kaur, G. (2018). Performance evaluation of two ANFIS models for predicting water quality index of river satluj. *Advances in Civil Engineering*, 2018.
- US Army Corps of Engineers (2002). *Coastal engineering manual*, US army corps of engineers. Washington, DC [in 6 volumes].
- Van der Meer, J.W., 1988. *Rock slopes and gravel beaches under wave attack*. Delft Hydraulics, Communication No. 396.
- Van der Meer, Jentsje & Stam, Cor-Jan. (1992). Wave Runup on Smooth and Rock Slopes of Coastal Structures. *Journal of Waterway Port Coastal and Ocean Engineering* 118:5(534).
- Varghese, R. V., Shirlal, K.G., Hari, B., & Mohanan, S. (2016) Review of

- Developments in Estimation of Wave Reflection from Coastal Structures. IOSR Journal of Mechanical and Civil Engineering, 30-32.
- Venter, G., & Sobieszczanski-Sobieski, J. (2002). Particle swarm optimization. 43<sup>rd</sup> AIAA 2002-1235, Structures, Structural Dynamics, and Materials Conference, Denver, Colorado.
- Vishal Kumar, (2010). Hydrodynamic performance characteristics of one side and two sides perforated semicircular breakwater. M. Tech Thesis, National Institute of Technology Karnataka, Surathkal, Mangaluru, India.
- Xie, S. L. (2001). Design of semi-circular breakwaters and estuary jetties, Proceedings of XXIX IAHR Congress, Beijing, 90-95.
- Yagci, O., Mercan, D.E., Cigizoglu, H.K., & Kabdasli, M.S. (2005). Artificial intelligence methods in breakwater damage ratio estimation. Ocean Engineering, 32, 2088–2106.
- Young, D.M. & Testik, F.Y. (2011). Wave reflection by submerged vertical and semicircular breakwaters. Ocean Engineering, 38, 1269–1276.
- Yuan, D., & Tao, J. (2003). Wave forces on submerged, alternately submerged and emerged semicircular breakwaters. Coastal Engineering, 48, 75–93.
- Yu, Y.X., Zhang, N.C. & Rao, Y.H., (1999). Hydraulic experimental study on semicircular breakwaters. The Ocean Engineering, 17(4), 39-48.
- Zahmatkesh, I., Soleimani, B., Kadkhodaie, A., & Golalzadeh, A. (2017). Estimation of DSI log parameters from conventional well log data using a hybrid particle swarm optimization – adaptive neuro-fuzzy inference system. Journal of Petroleum Science and Engineering, 157, 842–859.
- Zanaganeh, M., Mousavi, S. J., Farshad, A., & Shahidi, E. (2009). A hybrid genetic algorithm – adaptive network based fuzzy inference system in prediction of wave parameters. Engineering Applications of Artificial Intelligence, 22(8), 1194–1202.
- Zanuttigh, B., & Van der Meer, J.W. (2008). Wave reflection from coastal structures in design conditions. Coastal Engineering, 55, 771–779.
- Zanuttigh, B., Mizar, S., & Briganti, R. (2013). A neural network for the prediction of wave reflection from coastal and harbor structures. Coastal Engineering., 80, 49–67.



- Zhang, N.C., Wang, L.Q., & Yu Y. X. (2005). Oblique irregular waves load on semicircular breakwater, *Coastal Engineering Journal*, 47, 183 –204.
- Zhou, K., & Yang, S. (2016). Exploring the uniform effect of FCM clustering : A data distribution perspective. *Knowledge Based systems* 96, 76–83.

## PUBLICATIONS

### **INTERNATIONAL JOURNAL PUBLICATIONS:**

- 1) **Kundapura, S.,** Hegde A. V., & Pinho, J.L.S. (2019). Below the data range prediction of soft computing wave reflection of semicircular breakwater. *Journal of Marine Science and Applications* 18(2) 167-175. <https://doi.org/10.1007/s11804-019-00088>
- 2) **Kundapura, S.,** & Hegde A. V. (2018). PSO-ANFIS hybrid approach for prediction of wave reflection coefficient for semicircular breakwater, Published online by Taylor and Francis, *ISH Journal of Hydraulic Engineering*. DOI: 10.1080/09715010.2018.1525688
- 3) **Kundapura, S.,** & Hegde, A. V. (2017). Current approaches of artificial intelligence in breakwaters- A Review, *Techno Press, Ocean Systems Engineering*, 7 (2) 75-87, DOI: <https://doi.org/10.12989/ose.2017.7.2.075>.

### **CONFERENCES**

- 1) **Kundapura, S.,** & Hegde, A.V., (2016). Applications of ANN in Breakwaters- A Review, 10<sup>th</sup> International symposium of Lowland Technologies, ISLT 2016.
- 2) **Kundapura, S.,** & Hegde, A.V., (2016). Application of ann in prediction of reflection coefficient for an emerged perforated semicircular breakwater, *Hydro 2016*, 21<sup>st</sup> International conference on hydraulics water resources and coastal engineering, CWPRS, Pune.
- 3) **Kundapura, S.,** & Hegde, A.V., (2017). Prediction of reflection coefficient below the data range for emerged perforated non-overtopping Semicircular Breakwater, *OSICON 17 Conference*, NCESS Thiruvananthapuram. (Poster).
- 4) **Kundapura, S.,** & Hegde, A.V., (2017). Soft computing wave reflection for a semicircular breakwater for below the data range of wave periods, *Suman Kundapura and Arkal Vittal Hegde, ICSOT–2017*, December, IIT Kharagpur.
- 5) **Kundapura, S.,** & Hegde, A.V., (2017). Anfis to predict the wave reflection coefficient for a semicircular breakwater” *Suman Kundapura and Arkal Vittal Hegde, Hydro-2017*, L D College of Engg., Ahmedabad.
- 6) **Kundapura, S.,** Hegde, A.V., & Wajerkar, A.V., (2019). Proceedings of the Fourth International Conference in Ocean Engineering (ICOE2018), *Lecture Notes in Civil Engineering* 23, Lecture Notes in Civil Engineering, Springer. [https://doi.org/10.1007/978-981-13-3134-3\\_21](https://doi.org/10.1007/978-981-13-3134-3_21) ICOE 2018, IIT, Madras.
- 7) **Kundapura, S.,** & Hegde, A.V., (2018). Extreme learning machines to predict the stability of semicircular breakwater, *NFiCE2018*, IIT Bombay, Paper I

8) **Kundapura, S.**, Rao S. & Hegde, A.V., (2019). Relative wave runup parameter prediction of emerged semicircular breakwater, ICRTICE-2019, Medi-caps University, Indore.

9) **Kundapura, S.**, Rao S. & Hegde, A.V., (2019). Stability parameter prediction of semicircular breakwater by using hybrid models, Hydro-2019, Osmania University, Hyderabad.

D: DJCE1234.

Mrs. SUMAN KUNDAPURA

#6-20/2, "Nidhi", Kodical cross road,  
Vivekananda Nagar,  
Mangaluru – 575006  
Karnataka, India  
Mobile: +91 9480225021  
E-mail: [sumankundapura@yahoo.com](mailto:sumankundapura@yahoo.com)



Life Member of Indian Society of Hydraulics, Reviewer of technical papers in journals and conferences, Students Co-ordinator in the NBA (National Board of Accreditation) accreditation process of M.Tech. program.

### **EDUCATION & CREDENTIALS**

M.Tech. (Hydraulics and water resources Engg.), NITK Surathkal, 2004  
B.E. (Civil Engg.), Visvesvaraya Technological University, Belgaum, 2002

### **PERSONAL DETAILS**

Date of Birth: 05-Oct-1980

Languages Known: English, Hindi, Kannada, Tulu and Tamil

Computing Skills: ArcGIS, MATLAB, AutoCAD, Microsoft Office Suite

ORCID: <http://orcid.org/0000-0003-0481-4223>